# Heterogeneous Oxidation of Alcohols

**By**

**Hamza Mounzer**

A thesis submitted to
The University of Birmingham
for the degree of
DOCTOR OF PHILOSOPHY

Department of Chemical Engineering
School of Engineering
The University of Birmingham
March 2009

*To My Mother,*
*In the Heavens…*

## Acknowledgements

I would like to express my deepest and sincerest gratitude to the following people and organisation for their support and assistance:

Dr Joe Wood for his patience, guidance and efforts in helping me throughout my research. Particular thanks must be extended to Prof. Mike Winterbottom and Prof E. Hugh Stitt for their support and advice.

My colleagues and friends in the Department of Chemical Engineering especially Dr Fabio Chiti, Mr Andrea Gabriele, Dr Andreas Tsoligkas, Dr James Bennett, Dr. Aman Dhir, Mr Gareth Thompson and Mr Nima Niknaf.

I also wish to express a debt of gratitude to Johnson Matthey for providing catalyst and all the helpful discussions I had with their personnel.

Finally I wish to personally thank my family for their indispensable support through the good times and the difficult ones, the support staff at the Department of Chemical Engineering and TOOL for the inspiration.

# ABSTRACT

The selective oxidation of alcohols is one of the most challenging reactions in green chemistry. While the current chemical industry uses organic and inorganic oxidants to produce carbonyl compounds, it is highly desirable to use a heterogeneous catalyst for the efficient oxidation of alcohols. The present research is focused on increasing the activity and selectivity towards the corresponding carbonyl of the heterogeneous oxidation for alcohols.

The low activity of 5 wt.%Pt-1 wt. %Bi/Carbon for the oxidation of 2-octanol was investigated in a 500ml stirred tank reactor. The fast reaction rate drops dramatically from 0.23 M/hr to 0.006 M/hr after 15 minutes reaction time when heptane was used as solvent. Different possible causes such as overoxidation, leaching and poisoning were examined. It was found that the loss of high conversion rate was due to product adsorption and hence, different solvents were investigated. A mixture of 16-18% v/v dioxane in heptane was able to effectively regenerate active sites and allow a constant reaction rate of 0.07M/hr. The effects of temperature and pressure were also studied. Gas-liquid, liquid-solid and internal mass transfer effects were determined experimentally and semi-empirically. Six different Langmuir-Hinshelwood rate models were examined

where a modified model based on Schuurman *et al.* (1992) was found to adequately describe the experimental data.

The novel 2.5%Au-2.5%Pd/titania catalyst was investigated for the oxidation of benzyl alcohol. Different parameters such as catalyst oxidation state, pressure and stirrer design were studied to increase the activity and selectivity of the catalyst. The selectivity was shown to be highly dependent on the oxygen concentration. Therefore, the pressure, temperature, catalyst treatment were optimised and the reactor configuration was re-designed to enhance oxygen transport to the catalyst. While the conversion rate was unaffected by the oxygen concentration, the catalyst pre-treatment significantly increased the reaction rate. Eventually, the use of a Rushton Turbine at 20 rps with a shower disc sparger and a treated catalyst allowed the selectivity to reach 93%. The reaction could be described with a Power Law model satisfactorily. Transition Metal Oxide catalysts such as $AgO/SiO_2$, $Fe_2O_3/SiO_2$, $CuO/SiO_2$ and $CuO/Al_2O_3$ were investigated as an alternative to the expensive noble metal based catalyst. However, it was shown that such catalysts are ineffective for the oxidation of different alcohols by studying the effects of different engineering parameters. The maximum conversion reached was 15% with calcined copper oxide catalyst for 1-octanol oxidation.

**Contents** **Page**

**List of figures** **Page**

**List of tables** **Page no**

# NOMENCLATURE

| | |
|---|---|
| $a_B$ | Gas-liquid interfacial area, $m^2$ |
| $a_p$ | External surface area of the catalyst particles per mass unit of catalyst, $m^2 / kg$ |
| $A_c$ | Cross sectional area $m^2$ or $nm^2$ |
| C | Concentration, M |
| C' | Constant |
| D | Diameter, m |
| $d_b$ | Bubble diameter, m |
| $d_p$ | Particle diameter, m |
| $D_{AB}$ | Diffusion coefficient, $m^2 / s$ |
| $D_m$ | Molecular diffusion coefficient, $m^2 / s$ |
| $D_{eff}$ | Effective diffusion coefficient, $m^2 / s$ |
| $E_A$ | Activation energy, kJ/mol |
| $E_d$ | Desorption energy, kJ/mol |
| F | Stochiometric Factor, dimensionless |
| g | Gravity constant, $m / s^2$ |
| $h_1, h_2$ | Height of the first impeller from the bottom and height of the liquid, m |
| $k_d$ | Desorption coefficient, $s^{-1}$ |
| $k_{SL}$ | Mass transfer coefficient from the bulk liquid to the external surface of the catalyst, m/s |
| $k_{GL}$ | Mass transfer coefficient from the gas to the liquid, m/s |
| $k_{\text{int}}$ | Mass transfer coefficient from the liquid film on the catalyst surface to the internal pores of the particle, m/s |
| $k$ | Specific reaction rate with internal mass transfer, $dm^3 / gcat.s$ or $m^3 / kgcat.s$ |

| | |
|---|---|
| $K_1, K_2 .. K_n$ | Rate equilibrium constant |
| $\overline{K}$ | Constant |
| L | Characteristic size of a catalyst particle |
| m | Mass, kg |
| M | Molecular weight, g/mol |
| $M_w$ | Wagner-Weisz-Wheeler modulus |
| N | Impeller speed, $s^{-1}$ |
| $N_A$ | Avogadro's Number |
| $N_P$ | Impeller power number |
| $N_b$ | Number of baffles |
| $N_s$ | Impeller speed for suspension of solid particles in unaerated liquid, rev/s |
| $N_{sg}$ | Impeller speed for suspension of solid particles in aerated liquid, rev/s |
| P | Power draw, $kg.m^2.s^{-3}$ |
| $P_{Air}$ | Air pressure, bars |
| $Q_{VG}$ | Vessel volume per minute flow, $m^3/s$ |
| $r_b$ | Resistance to gas absorption, s |
| $r_c$ | Resistance to transport to surface of catalyst particle, $gcat.s/dm^3$ or $kgcat.s/m^3$ |
| $r_r$ | Resistance to diffusion and reaction within the catalyst particle, $gcat.s/dm^3$ or $kgcat.s/m^3$ |
| $r_{cr}$ | Combined resistance to internal diffusion, reaction, and external diffusion, $gcat.s/dm^3$ or $kgcat.s/m^3$ |
| $r_d$ | Deactivation rate, M/(kg.s) |
| $r_V$ | Reaction rate per unit of volume of catalyst particles, $moles.m_{cat}^{-3}.s^{-1}$ |
| $R_A, R_B, R_C$ | Reaction rate, M/s |
| Re | Reynolds number, dimensionless |
| rps | Stirring speed, rev/s |

| | |
|---|---|
| S | Reactor configuration constant |
| Sc | Schmidt number, |
| Sh | Sherwood number |
| T | Temperature, K |
| T | Tank diameter, m |
| TPO | Temperature Programmed Oxidation |
| TPR | Temperature Programmed Reduction |
| $U_g$ | Superficial gas velocity, m/s |
| $U_t$ | Terminal velocity of bubble in free rise, m/s |
| V | Volume, l or $dm^3$ |
| $V_s$ | Adsorbed volume, ml |
| w | Catalyst loading, $dm^3 / g$ or $m^3 / kg$ |
| We | Weber number |
| X | Percentage of catalyst loading, dimensionless |

**Greek Symbols**

| | |
|---|---|
| $\delta, \varphi, \gamma$ | Parameters |
| $\varepsilon$ | Energy dissipated, $m^2 / s^3$ |
| $\phi$ | Thiele Modulus |
| $\eta$ | Effectiveness factor |
| $\mu$ | Viscosity, $kg.s^{-1}.m^{-1}$ |
| $\rho$ | Density, $kg / m^3$ or $g / dm^3$ |
| $\sigma$ | Surface tension, N/m |
| $\upsilon$ | Kinematic viscosity ($m^2$/s) |
| $\alpha$ | Rate of reaction on the deactivated catalyst divided by the rate on fresh catalyst. |

# I) INTRODUCTION AND BACKGROUND

## 1.1) The Emergence of Catalysis in the Chemical Industry

Before the appearance of industrial catalysts back in 1875, the chemical industry used to rely on increasing the pressure, temperature, reactant concentration, and residence time to increase production (Davis and Hettinger 1983). While these variables enhance the reaction rate, they consume a significant amount of power and capital to operate. Moreover, using harsh conditions to enhance reaction rates do not distinguish between the different possible reaction paths, which will eventually form unwanted side products. It becomes clear from the above that another variable must be taken into consideration, which ideally, would only enhance specifically the wanted reaction path from an otherwise difficult and unselective reaction. Thus, the attention turned into finding a selective catalyst, which by definition, would decrease the activation energy of the wanted reaction path and discriminate against other possible pathways. The optimum catalyst would also be separable from the reaction mixture and recyclable for economic purposes.

The first catalytic processes used are centuries old involving enzymes to manufacture wine and dairy products (Heineman 1981). The earliest commercial catalyst was platinum supported on Vanadia to produce sulphuric acid from sulphur oxide in 1875 by Peregrin Philips (British Patent No. 6096, 1831). Over the twentieth century industry became increasingly reliant on the use of catalysts for the production of a range of manufactured products. The economy based on catalysts was estimated to be worth 10 trillion dollars per year in 1988 (Farrauto and Bartholemew 1988). The petroleum division is the most dependent on catalysts for different processes such as cracking, reforming and hydrotreating. The chemical production division includes organic synthesis, hydrogenation, oxidation and polymerisation amongst others. Finally, catalysts are increasingly used to protect the environment by breaking down green house gases from industrial and automotive exhausts such as NO, $N_2O$ and CO with Platinum Group Metal (PGM) based catalysts.

However, catalysts are not the only novel way to increase the efficiency and profits in the chemical industry. Sometimes, it is not the reaction which limits the production rate but the transport of reactants between different phases (Fogler 2001). This is especially true for gas-liquid-solid systems. In this case, the attention is focused on the reactor type and configuration to maximise the mass transfer of substrates. One example is the trickle bed using a cocurrent downflow of gas and liquid into a packed reactor (Miller and Kaibel 2004). Stirred Tank Reactors (STR), which constitute 50 % of reactors in the chemical production, can be more effectively designed to improve the transport of a reactant if it limits the reaction (Kresta, Edward PL *et al.* 2004).

## 1.2) Green Chemistry and Alcohol Oxidation

With an increase in chemical consumption and needs, industrial processes expanded considerably throughout the 20$^{th}$ century. However, governmental regulations, such as the Environmental Protection Act 1990-UK, were introduced as well to control the subsequent damage inflicted upon the environment. Industrial liquid wastes have destroyed natural habitats and the gaseous exhaust contributes significantly to global warming and acid rain (Cheremisinoff, Rosenfeld *et al.* 2008). Therefore, over the last 20 years interest in solving pollution problems within the chemical industry has grown significantly. Structured catalysts such as the monolith for example are widely used to break down green house gases emitted from automobiles. The monolith corresponds to a support with a number of small straight and parallel channels coated with a catalyst. Nonetheless, this type of innovation should be extended to benefit the chemical industry as well. For example, the replacement of the refrigerant chlorofluorocarbons with ammonia in-vapour compression systems minimised the damage on the ozone layer.

The production of ketones and aldehyde in industry occurs via alcohol oxidation. This process involves the stochiometric addition of an inorganic oxidant such as chromate, or organic oxidant such as dimethyl sulfoxide DMSO (Cainelli and Cardillo 1984; Dimitratos, Villa *et al.* 2006). These processes produce considerable amounts of toxic wastes, and the poor selectivity of the reaction creates by-products which decreases the profits. Therefore, heterogeneous catalysts for the alcohol oxidation to carbonyl compounds are attracting interest from industry and academics alike (Kluytmans, Markusse *et al.* 2000; Besson and Gallezot 2003; Muzart 2003). Unlike stochiometric

oxidants that produce chemical wastes, heterogeneous catalysis can effectively use molecular oxygen to produce only water as side-products, and can be operated under mild temperature and pressure conditions. From a cost-efficiency point of view, supported catalysts have an advantage over homogeneous catalysts by being easily recoverable and they can be used in continuous flow regimes (Kreutzer, Kapteijn *et al.* 2005).

The heterogeneous oxidation of alcohols with noble metals has been exponentially improved since it was first studied 150 years ago (Wieland 1921; Mallat and Baiker 1994). However, before the industry can apply heterogeneous catalysts on a large scale for the production of carbonyl compounds and invest in new processes, it is crucial to investigate and optimise the catalytic oxidation of alcohols.

### 1.3) Aims of this Thesis

While the literature is very rich in studies of oxidation for different kinds of alcohols, catalysts and reaction conditions, there is still room to further understand and improve the efficiency of promising catalysts. 5 wt. %Pt-1 wt. %Bi/Carbon shows a high potential for the oxidation of alcohols and is a leading catalyst in terms of selectivity during reactions. However, before it can be introduced for large scale uses, its versatility for the effective oxidation of different alcohols should be established. The oxidation of 2-octanol has shown mediocre results with different catalysts including 5%Pt-1%Bi/Carbon. Thus, this work aims to investigate the low activity and improve the oxidation of 2-octanol with 5%Pt-1%Bi/Carbon. In particular, to understand how the

selection of suitable solvent mixtures can be used to control the adsorption equilibrium at the catalyst surface and thus prevent the strong adsorption of products from blocking the active sites.

Furthermore, a recent catalyst has been developed (Landon, Collier *et al.* 2002; Hutchings 2008) composed of 2.5 wt.%Au-2.5 wt.%Pd/titania. This novel catalyst showed promising results for the oxidation of different alcohols in terms of activity and selectivity. However, most of the work published on this catalyst was done in small scale reactor volumes with an emphasis on the chemistry of this particular catalyst. No examination on the engineering parameters on this systems has been published which underlines the importance of carrying a detailed study on the different engineering effects. Therefore, a thorough study was undertaken to optimise the oxidation of benzyl alcohol with 2.5%Au-2.5%Pd in a medium scale reactor, paying particular attention to the reactor design and catalyst treatment. Ultimately, the effects investigated also improve the understanding of the chemistry of the catalytic oxidation of benzyl alcohol with 2.5%Au-2.5%Pd.

Finally, an attempt was undertaken to oxidise alcohols with Transition Metal Oxides (TMO) since the previous catalysts investigated were constituted with noble metals. TMO are significantly cheaper and more abundant than PGM. While TMO catalysts are used for gas phase oxidation, their successful application for liquid phase oxidation would have a significant impact on the economy and industrial processes. Hence, TMO catalysts based on copper oxide, iron oxide and silver oxide supported on alumina and silica were investigated for the oxidation of primary, secondary and aromatic alcohols.

In summary, the aims can be presented as followed:

1. *Oxidation of 2-octanol with 5%Pt-1%Bi/Carbon.* The investigation of the low oxidation rate of 2-octanol with this catalyst. Research into finding an effective solution to increase the reaction rate.
2. *Oxidation of Benzyl Alcohol with 2.5%Au-2.5%Pd.* The investigation into optimising the reaction rate and selectivity of the oxidation of benzyl alcohol with 2.5%Au-2.5%Pd by studying the STR configuration, support effects and catalyst treatment.
3. *Oxidation of* 1-*octanol, 2-pentanol and benzyl alcohol with TMO catalysts.* A study with unconventional catalyst to try to get the best possible conversion.
4. *Catalyst characterisation.* Catalyst characterisation with XRD, TPR and Chemisorption

## 1.4) Scope of the Thesis

A brief introduction was presented above on the importance of the heterogeneous oxidation of alcohols and the necessity to further understand and improve the catalytic processes. A literature survey will then be presented to clarify in details all aspects of the heterogeneous oxidation of alcohols and to report the most important findings published in the literature in Chapter 2. Following the literature survey, the experimental setup, equipment and analysis tools used in this work will be described in Chapter 3. The subsequent chapters explain thoroughly the findings of this work while discussing the results, and comparing them with the literature before the final conclusion chapter to summarise this thesis. Supplementary information and data are incorporated in the Appendices.

# II) LITERATURE REVIEW

This chapter concerns the work published in the literature on the heterogeneous oxidation of alcohols using noble metals. Different aspects of the catalytic oxidation are discussed such as the mechanisms, catalyst properties, the engineering parameters and the kinetics that could be adjusted to optimise such processes in industry. The main focus will be on platinum-bismuth and gold-palladium catalysts since they are the centre of the current work and are of academic and industrial interest. The designs and characteristics of the stirred tank are also described in order to provide the relevant background to the optimisation of the reactor configuration used in this study. Finally, a discussion of the kinetic modelling of the alcohol oxidation will be presented.

## 2.1) Oxidation Mechanism on Noble Metals

The partial oxidation of alcohols involves the loss of hydrogen to form the corresponding carbonyl compound. Secondary alcohols form ketones while primary alcohols form aldehydes before becoming carboxylic acids with further oxidation. A loss

of a carbon dioxide molecule will occur in more forcing oxidation conditions. In order to determine the mechanism of alcohol oxidation and the Rate Determining Step (RDS), researchers have tried to oxidise isotopically labelled alcohols (DiCosimo and Whitesides 1989).


**Figure 2.1)** Proposed mechanism for the oxidation of alcohol (Van den Tillaart, Kuster *et al.* 1994).

The dissociation mechanism happens when the alcohol adsorbs on the metal by forming an alkoxide or the conjugate base of an alcohol, and hydrogen occupying two active sites. On the other hand, it is also suggested that the alcohol can be adsorbed associatively as a whole molecule on the catalyst surface and then will undergo dehydrogenation (Schuurman, Kuster *et al.* 1992). The adsorbed alcohol or alkoxide then may react with a free active site * in an acidic medium, an adsorbed oxygen O* if there is a high oxygen surface coverage, and/or an adsorbed hydroxyl OH* in an alkaline medium to abstract the $\alpha - H$ from the reactant (Mallat and Baiker 1994). The alcohol was proposed to undergo the following path in a basic medium (Dijkgraaf, Rijk *et al.* 1988):

I) $$R - CH_2OH_{ads} + OH^- \longleftrightarrow R - CH_2O^-_{ads} + H_2O$$

II) $$R - CH_2O^-_{ads} + * \longrightarrow R - CHO_{ads} + H^-_{ads}$$

III) $$H^-_{ads} + O_{ads} \longrightarrow OH^-_{ads} + *$$

However, it was later rejected since deprotonation of a weak acid in alkaline medium is unlikely (Mallat and Baiker 1994; Gangwal, van der Schaaf *et al.* 2005). The following mechanism was suggested:

I) $R-CH_2OH_{ads}+* \longleftrightarrow R-CH_2O_{ads}+H_{ads}$

II) $R-CH_2O_{ads}+* \longrightarrow R-CHO_{ads}+H_{ads}$

III) $\frac{1}{2}O_2+* \rightarrow O_{ads}$

IV) $2H_{ads}+O_{ads} \longrightarrow H_2O+3*,$

where the first reaction is fast and the second one is the Rate Determining Step, or RDS. An adsorbed oxygen $O_{ads}$ or adsorbed hydroxyl $OH_{ads}$ can replace the active site * depending on the oxygen coverage and pH.

In electrochemical studies, Kluytmans *et al.* (2000) suggested that the catalyst acts as a short-circuited cell where the alcohol dehydrogenates on the surface which causes the desorption of $H^+$ and $OH^-$ from $H_{ads}$ and $OH_{ads}$.

I) $\frac{1}{2}O_2+* \rightarrow O_{ads}$

II) $R-CH_2OH_{ads}+O* \longleftrightarrow R-CH_2O_{ads}+OH_{ads}$

III) $R-CH_2O_{ads} \longrightarrow R-CHO_{ads}+H^++e^-$

IV) $e^-+OH_{ads} \longrightarrow OH^-+*$

V) $H^++OH^- \longrightarrow H_2O$

Consequently, the ketone formation (III) and the hydroxyl reduction (IV) may happen at different sites on the catalyst while electrons are transported by conduction and the proton by diffusion (V) guided by Fick's first law. It becomes apparent that there is no agreement on the mechanism of the alcohol oxidation (Keresszegi, Ferri *et al.* 2005). The oxidation may depend on the nature of the adsorbed species, the pH of the solution, the oxygen coverage and the metal oxidation state (Gallezot 1997).

Since C-C bonds are difficult to break under mild reaction conditions, the oxidation of secondary alcohols yield ketones and the carbon chain is preserved (Mallat and Baiker 1994). However, primary alcohols are oxidized to aldehyde and can further undergo catalysis to yield carboxylic acids. A high pH or an aqueous media increases considerably the carboxylic acid yield unless the hydroxyl function is adjacent to a C=C bond or an aromatic ring that stabilize the carbonyl group (Muzart 2003). The selectivity of an oxidation is strongly affected by the reaction conditions, nature and promotion of the catalyst and by the solvent as will be discussed in the corresponding sub-chapters.

## 2.2) Oxidation Catalysts

This section will deal firstly with the active noble metals such as Au, Au-Pd, Pd and Pt. The importance of promoters will then be examined before discussing the oxygen adsorption. The physical characteristics of the catalyst and support will then be studied before considering the main reasons of catalyst deactivation.

### 2.2.1) Noble Metals

Noble metals constitute some of the few elements that are efficient in oxidising alcohols heterogeneously under the Sabatier principle. Catalysts containing palladium, platinum or gold give promising results in terms of activity and selectivity when used to oxidise alcohols (Ebitani, Ji *et al.* 2004). Specific examples of oxidation activity with these metals are discussed below.

#### 2.2.1.1) Au and Au-Pd catalyst

Gold was always thought to be an ineffective catalyst due to its chemical inertness. It was only in the early 1980's that Hutchings and Haruta discovered that gold is a very valuable catalyst for acetylene hydro-chlorination and low temperature CO oxidation (Hutchings 1985; Hutchings and Haruta 2005). Their pioneering work set in motion numerous studies on improving catalysis by gold. The discovery that gold can be a catalyst for alcohol oxidation was only made in the late 1990's (Prati and Rossi 1998). It was established that, unlike Pt/C and Pd/C that can oxidise alcohol independently of the solution pH, a base was necessary for activity with Au/C (Hutchings 2008). Indeed, the base would allow the abstraction of hydrogen from the alcohol to create an alkoxide (Carrettin, McMorn *et al.* 2003). It was also shown that the selectivity of the highly functional glycerol with Au/C is directly dependent on the concentration of base where a NaOH/glycerol ratio of 4 and metal particle size of 20nm gave the best results (Porta and Prati 2004). This underlines a fundamental difference in oxidation mechanism between these noble metals. In a solution with neutral pH, a metal oxide support can allow gold to be an active catalyst (Enache, Knight *et al.* 2005) as will be explained later on. The

conversion rate of gold is also strongly dependent on the metal particle size, where nano-crystalline gold requires less base to achieve similar activity (Christensen, Betina *et al.* 2006). Nano-particles or a high support surface area ensure a high contact between the gold and the support, which in turn enhances the interaction between the noble metal and the metal oxide support (Demirel, Kern *et al.* 2007). Indeed, large gold particles are unable to chemisorb reactant molecules unless the particles are small enough to be deficient in the complete metal coordination character (Bond and Thompson 1999).

At the start of the 21st century, it was established that the alloying of gold with palladium increases the activity of hydrogen oxidation to yield hydrogen peroxide (Landon, Collier *et al.* 2002; Hutchings and Haruta 2005; Edwards, Landon *et al.* 2007). Therefore, the investigation of Au-Pd catalysts for alcohol oxidation started. An early trial was the comparison of monometallic Au, Pd and Pt with bimetallic Au-Pd and Au-Pt (Dimitratos, Porta *et al.* 2005). In the absence of a metal oxide support or a base that can abstract a hydride from the alcohol to initiate the oxidation, gold is almost unable to oxidise alcohols. On the other hand, while Pd and Pt are effective oxidation catalyst, they are readily deactivated by overoxidation (Mallat and Baiker 1994). It was discovered that Au-Pd and Au-Pt alloys were resistant to overoxidation during the oxidation of D-Sorbitol (Dimitratos, Porta *et al.* 2005). Gold, being almost inert to oxygen corrosion, was partly protecting the Pd and Pt from overoxidation by limiting the exposure of Pd and Pt to oxygen (Schwank 1985; Dimitratos, Villa *et al.* 2006). However, the complete effect of adding gold upon the reaction mechanism is still not entirely understood. Dimitratos *et al.* (2006) reported that adding gold to platinum decreases the activity of benzyl alcohol oxidation but when added to palladium it is increased. The explanation of

this observation was attributed to two catalyst properties. First, a geometric effect between gold and the second noble metal causes intra-atomic bond length or lattice constants changes which ultimately affects the electronic structure of the alloyed particle and prevents the ensemble effect. The Au atoms can also isolate palladium monomers which increases activity, stability and the selectivity by preventing the breaking of C-C bonds and the over-oxidation of the same molecule (Prati, Villa *et al.* 2007; Wang, Villa *et al.* 2008). Secondly, electronic interactions appear between the two different metals. Hence, the bonding energies of substrate on alloyed particles are affected. The gold protects the catalyst from overoxidation since the binding energy of oxygen on palladium decreases when the latter is surrounded with gold (Prati, Villa *et al.* 2007).

Imaging techniques such as scanning transmission electron microscopy combined with x-ray photoelectron spectroscopy were performed by Enache *et al.* (2006). The results showed that the gold-palladium catalysts have a gold core in a palladium shell conformation on metal oxide supports suggesting that gold interacts electronically with palladium. However, this shape was not observed by Dimitratos *et al.* (2006) or Hutchings (2008) when the bimetallic catalyst was prepared on carbon supports. Hence, it was deduced that the core/shell structure does not play a significant role in the enhanced activity of the catalyst (Wang, Villa *et al.* 2008). In order to have a positive effect of the bi-metal, the geometric and electronic properties must work synergistically. Recently, another attribute was revealed; the identity of the substrate also plays an important role in the synergy of Au and Pd/Pt bi-metals (Prati, Villa *et al.* 2007). In basic conditions, poly-functional alcohols such as glycerol were more active with Au-Pt than Au-Pd while with aliphatic octanol, the contrary was observed. Au-Pd catalyst was

particularly studied for the benzyl alcohol oxidation due to the high activity of the latter and the different possible mechanistic pathways (Enache, Edwards *et al.* 2006). Benzyl alcohol oxidation may undergo the following steps:

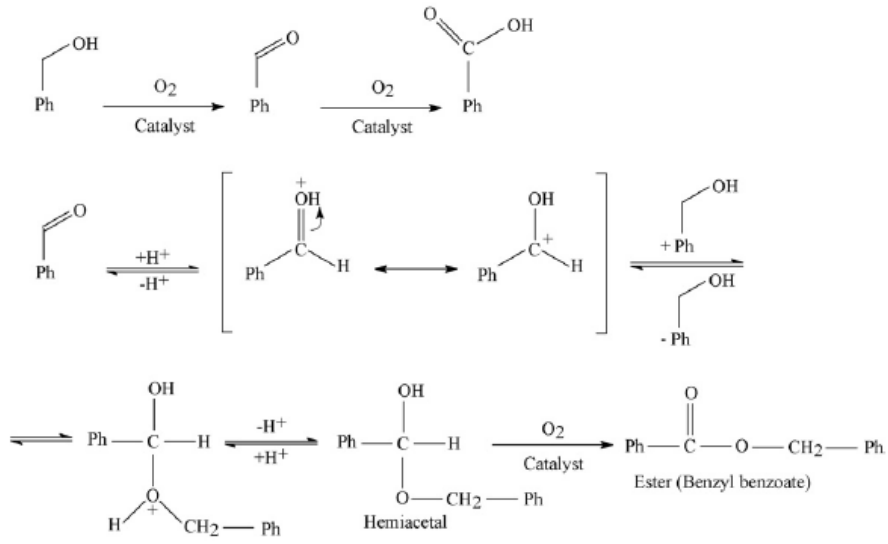


Scheme 1.

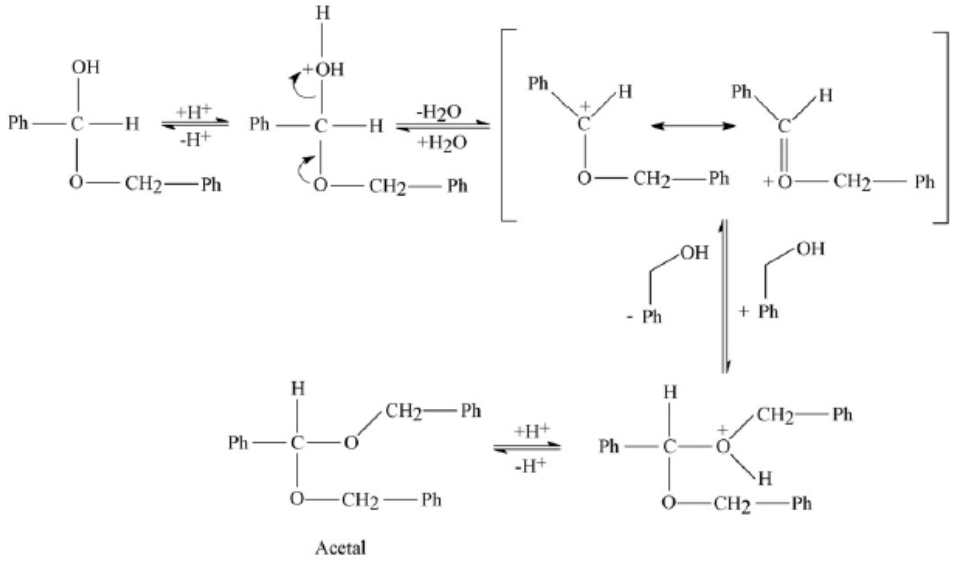


Scheme 2.

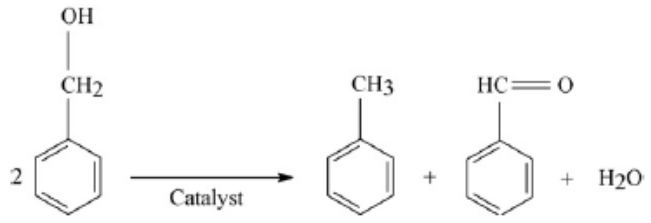


Scheme 3.

**Figure 2.2)** Benzyl alcohol oxidation. (Adapted from Enache *et al.* 2007).

Different supports were investigated for the Au-Pd catalyst including alumina, silica, titania, carbon, iron oxide and different zeolites such as ZSM-5, $\beta$ and Y types (Enache, Edwards *et al.* 2006). The outcome of the benzyl alcohol oxidation was strongly dependant on the support. Acidic supports such as iron oxide and alumina gave respectively 66% and 87% selectivity for the benzyl alcohol oxidation while titania gave 92%. Titania support had the highest conversion/selectivity ratio. Different Au:Pd ratios were investigated as well, ranging from 5%Au/titania without any palladium to 5% Pd/titania without gold (Enache, Barker *et al.* 2007). Mono-gold on titania gave a negligible amount of conversion. Conversely, palladium catalyst gave a selectivity of 70%. The best results were obtained using 2.5% Au-2.5% Pd/titania where the selectivity was 90%.

2.2.1.2) Palladium and platinum

The use of heterogeneous palladium has been investigated for the last 60 years and this metal is one of the most commonly used heterogeneous catalysts in academia and industry (Muzart 2003). Pd differs from other metal catalysts such as Pt, Rh, Ru, Ni, or Cu through the following characteristics (Blaser, Indolese *et al.* 2001):

- Pd catalysts can be easily tuned with the addition of organic and inorganic modifiers to alter the catalyst behaviour.
- Palladium shows low activity for the hydrogenation of aliphatic ketones and aldehyde and almost no activity at low temperature for aromatic rings.

- Pd has the highest activity for the hydrogenolysis reactions and the saturation of double bonds in conjugation with aromatic rings.

The ability of platinum to oxidise alcohols with molecular oxygen was discovered one and a half centuries ago (Mallat and Baiker 1994). Similarly to palladium, platinum has a high affinity to adsorb hydrogen which allows it to dehydrogenate alcohol to yield the corresponding carbonyl. However, platinum and palladium have a different catalytic behaviour even for the same substrate. For instance, benzoic acid adsorbs irreversibly on platinum but reversibly on palladium, as was shown by online mass spectroscopy (Souto, Rodríguez *et al.* 2000). Also the oxidation of $SO_2$ to $SO_3$ can occur on both Pd and Pt, however $SO_3$ deactivates only Pd (Kent 2007).

The activity and selectivity of platinum and palladium catalysts are strongly dependent on the metal particle size, nature of support, reaction medium and substrate which underlines the importance of investigating the effects of these conditions (Gallezot 1997). The main challenge is to maintain the selectivity towards the carbonyl intermediate without producing by-products or deactivating the catalyst. A novel way of achieving this goal is with the help of promoters.

### 2.2.2) The role of promoters.

The effect of adding promoters was a major step forward for the heterogeneous oxidation of alcohols since it dramatically affected the performance of the catalyst and its life-cycle (Mondelli, Ferri *et al.* 2007). While adding "non-noble" metals such as bismuth, lead and tin to Platinum Group Metals (PGM) affects the activity and increases

considerably the selectivity of the reaction, the promoter role was not entirely understood. Mallat *et al.* (1995) suggested 3 major possible roles for bismuth promoter:

1. Bismuth adatoms have a geometric effect and act as site blockers which change the orientation of the adsorbing alcohol. This phenomenon was witnessed for the oxidation of glycerol (Kimura, Tsuto *et al.* 1993). Also, adatoms prevent the presence of a large active metal surface, responsible for the "ensemble effect", which causes C-C bond cleavage that decreases selectivity (Pinxt, Kuster *et al.* 2000; Wenkin, Ruiz *et al.* 2002).
2. Since bismuth is a non-noble metal, it is much more likely to adsorb oxygen than the PGM (Mallat, Bodnar *et al.* 1993; Mallat, Bodnar *et al.* 1995). Therefore it creates a new active centre on the catalyst that contributes to the oxidation of alcohol by supplying the required oxidising species for the reaction. Gallezot (1997), proposed the following mechanism for the oxidation of glucose:

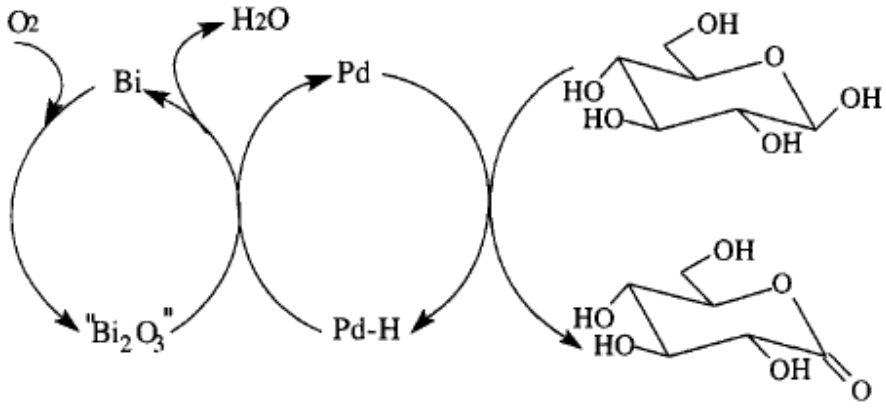


**Figure 2.3)** Glucose oxidation with Pd-Bi

3. Bismuth metal increases the selectivity and activity by preventing the adsorption of hydrogen by-product (and other substrates) via occupying active sites on PGM which will avert the hydrogen from reacting to yield unwanted by products. (Parsons and VanderNoot 1988; Mallat, Bodnar *et al.* 1993; Wenkin, Ruiz *et al.* 2002).

Keresszegi *et al.* (2004) investigated the effect of adding bismuth to platinum for the oxidation of phenylethanol. The presence of bismuth increases the conversion from 30% to 80%. The selectivity towards acetophenone was increases as well from 70% to 95%. Also, Keresszegi *et al.* (2004) used a simple technique to evaluate the role of bismuth on activity by comparing the alcohol dehydrogenation with argon and air for promoted and unpromoted catalysts. It was found that the bismuth led to an increased selectivity in the presence of air but had no effect in argon. Therefore, it was deduced that bismuth increases the oxygen transfer to remove the by-products and hence creates available active sites. Bismuth is therefore also used to protect the PGM catalyst from "over-oxidation" which happens when the alcohol is unable to reduce the oxygen coverage on the metal surface resulting in the deactivation of the catalyst (Gallezot 1997). However, Wenkin *et al.* (2002) have suggested that the bismuth may have a homogenous role by leaching and forming complexes with substrate that facilitates the dehydrogenation step. This was shown by adding a solution of bismuth to the successful oxidation of glucose. Conversely Keresszegi *et al.* (2003) showed that bismuth is in metallic form by insitu XAS studies that proved the presence of bismuth during the oxidation of phenylethanol.

2.2.3) Oxygen adsorption

One of the roles of the noble metal in heterogeneous catalysis is to activate the gaseous reactant. Oxygen can be adsorbed in three ways (Gangwal, van der Schaaf *et al.* 2005):

1. Physisorption: Weak adsorption, i.e. Van der Waals forces
2. Chemisorption: Strong and reversible adsorption, i.e. Covalent bonds
3. Corrosion: Strong and irreversible sub-layer penetration of oxygen in the metal.

On Pt (111), oxygen adsorbs associatively at temperatures below 120K and dissociatively at temperature between 150K and 500K. Corrosion happens at temperature above 500K which causes sub-surface platinum oxide. However, for liquid phase oxidation occurring at temperature between 293K and 353K, oxygen adsorbs atomically (Lewis and Gomer 1968). The adsorption mechanism is as follows:

I) $O_2 + * \longleftrightarrow O_{2-ads}$ Associative adsorption

II) $O_{2-ads} + * \longleftrightarrow 2O_{ads}$ Dissociation

*Pressure effects and over-oxidation*

The oxygen solubility in solution is proportional to the oxygen partial pressure according to Henry's law. While the presence of oxygen is vital to remove adsorbed hydrogen and other by-products for the regeneration of free sites, a high oxygen coverage will decrease the reaction rate (Keresszegi, Bürgi *et al.* 2002). Working at low oxygen partial pressure prevents the catalyst from being over-oxidized, although the adsorbed

hydrogen formed from alcohol dehydrogenation may react then with an other substrate to generate unwanted by-product instead of being oxidised to form water (Hardacre, Mullan *et al.* 2005). Keresszegi *et al.* (2005) suggested that the oxidation of primary alcohols such as 1-octanol and benzyl alcohol can yield CO by decarbonylation which deactivates the catalyst. The reaction rate can then be dramatically enhanced by the introduction of oxygen which removes adsorbed carbon monoxide. On the other hand, working at high oxygen partial pressure tends to deactivate the catalyst by oxidizing the metal and occupying the active sites (Kimura, Kimura *et al.* 1993). Overoxidation is widely considered as a major reason for catalyst deactivation (Mallat and Baiker 1994; Gallezot 1997; Markusse, Kuster *et al.* 2001). A catalyst is overoxidized or covered with oxygen when the catalyst potential is higher than 0.8V vs the Reversible Hydrogen Electrode (RHE). The catalyst is reduced or covered with hydrogen/CO when the potential is lower than 0.4V vs. RHE (Markusse, Kuster *et al.* 2001). The optimum catalyst potential then lies between 0.4 and 0.8V vs. RHE as illustrated in Figure 2.4). Extensive modelling work on overoxidation can be found in the following references (Gangwal *et al.* 2002; Gangwal *et al.* 2004; Gangwal *et al.* 2005b).

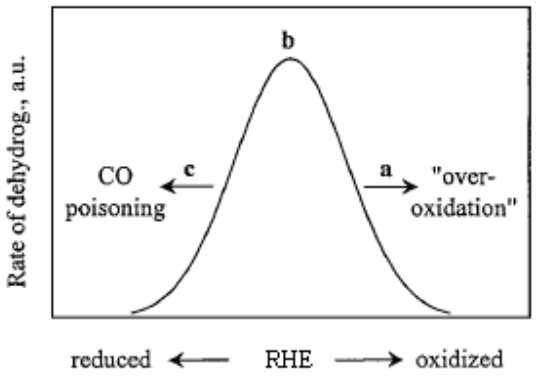


**Figure 2.4)** Illustration on the catalyst state. Adapted from Keresszegi *et al.* 2002

Kluytmans *et al.* (2000) and Markusse *et al.* (2001) found that stopping the oxygen flow during the reaction in case of overoxidation allows the alcohol to reduce the oxidised Pt catalyst, therefore reactivating it. Another way of overcoming poisoning as well as overoxidation is the addition of promoters. As it was previously explained, the addition of non-noble metals such as bismuth controls the oxygen supply to the noble metal and prevents the formation of adsorbed hydrogen and carbon monoxide (Mondelli, Ferri *et al.* 2007). Therefore an optimum oxygen concentration exists that is high enough to oxidise adsorbed hydrogen and by-products without overoxidizing the catalyst. Many researchers have suggested working in the oxygen mass transfer limited regime to prevent any overoxidation since working in a kinetic regime results in rapid catalyst deactivation (Gangwal, van Wachem *et al.* 2002; Keresszegi, Grunwaldt *et al.* 2004; Keresszegi, Mallat *et al.* 2004; Hardacre, Mullan *et al.* 2005). The selectivity towards the partially oxidised intermediate of the reaction is also dependant on the oxygen concentration. While ketones and carboxylic acids are resistant to further oxidation in mild conditions, aldehyde can easily be oxidised again to carboxylic acids in oxygen rich system, aqueous or alkaline medium (Mallat and Baiker 1994).

### 2.2.4) Catalyst Preparation

Catalysts are most commonly prepared using an impregnation or adsorption methods (Bamwenda, Tsubota *et al.* 1997; Winterbottom and King 1999) and are summarised from Farrauto and Bartholemew (1988).

*Impregnation*

The impregnation technique consists of dissolving the salt of the active metal in a solvent volume equal to the pores volume of the dried support. The solution is then added drop-wise to the support until all of the solvent is absorbed by the pores of the carrier. This method guarantees that the desired amount of active metal is present on the catalyst when the solvent is evaporated. The drying rate affects the deposition of the metal inside the pores. A high temperature causes the active metal to settle at the mouth of the pores while a low temperature causes the metal to occupy the bottom of the pore. This is because at higher temperatures the liquid evaporates from the solution before there is sufficient time for the metal to be transported in to the pores. A moderate temperature causes a more uniform pore occupation of active metal. Another relevant issue is the control of access of reacting molecules to active centres on the catalyst. Molecular sieves for instance are very selective catalysts by discriminating against compounds that are bigger than their regular pore size. In this case it might be desirable to have the active sites inside the catalyst pores to prevent unwanted reaction at the pore mouth. Zeolites are an example of a molecular sieve. The $Ni/Al_2O_3$ catalyst for hydrogenation is usually prepared with the impregnation method. The main disadvantage of the impregnation method is the possibility of a heterogeneous deposition of active metal within the pores of the support. A more uniformly distribution of active metal can be achieved with the adsorption method.

*Adsorption*

The adsorption method, or ion exchange, consists of substituting a cation or anion of the support with the ionic form of the active metal. Thus, this technique is strongly influenced by the number of available adsorption sites on the support, concentration of ions, the pH and the adsorption strength (Farrauto and Bartholemew 1988). However, this method allows the formation of a variety of metal particle sizes, loadings, shapes and surface area (Bamwenda, Tsubota *et al.* 1997). This process is very effective with the use of zeolites, such as ZSM-5 or Y-type faujasite since they exchange ions efficiently. While only low loadings can be achieved with this method, it is appropriate when expensive active metals are used such as platinum or gold on silica. There are obviously many other catalyst preparation processes such as precipitation or chemical reduction and their methods can be found in Farrauto and Bartholemew (1988). Catalysts can be characterised using XRD, TEM and Chemisorption and these methods are reviewed in Chapter 3: Experimental Methods.

2.2.5) Metal Particle Size, Loading and Distribution

Depending on the objective of the experiment the catalyst can either be treated under a flow of inert gas like nitrogen or argon to remove adsorbed molecules on the catalyst or be reduced by a flow of hydrogen. Control of metal deposition on the support is achieved by adjusting the quantity of support, pH, time of crystallization, calcination procedure and concentrations of metal ions in solution (Bamwenda, Tsubota *et al.* 1997). The metal particle size of a supported catalyst plays an important role in the activity and selectivity of the reaction as well as on the catalyst behaviour. The use of small Pd

particle (<2 nm) for the oxidation of glucose results in over-oxidation deactivation due to the higher oxygen affinity of small particles (Besson and Gallezot 2003; Gangwal, Schaaf *et al.* 2004). On the other hand the use of large metal particles lowers the intrinsic activity of the catalyst since the total exposed metal surface area decreases compared to a catalyst with similar metal loading and smaller metal particle size (Gallezot 1997). It becomes obvious that catalysts with similar metal identity but different metal particle size behave differently. The use of highly dispersed Pd nano-cluster (0.13nm) on alumina for allylic alcohols oxidation results in Turn Over Number (TON) per mole of Pd ten fold higher than ten times bigger particle size (1.3nm) (Hackett, Brydson R.M *et al.* 2007). On the other hand, by increasing the metal loading and cluster size on the catalyst the yield was increased although at the expense of a dramatically reduced TON. The same increase of activity with a decrease of cluster size using a gold catalyst was reported for the benzyl alcohol oxidation (Dimitratos, Lopez-Sanchez *et al.* 2007). In terms of selectivity, a catalyst with a higher metal surface area can be expected to over-oxidize the intermediate formed and hence might decrease the selectivity. For example, it was deduced that a gold catalyst with a larger metal surface area was considerably less selective for the glycerol oxidation since an intermediate formed had more chance of being over-oxidized into an unwanted by-product (Porta and Prati 2004).

### 2.2.6) Catalyst supports

Precious metals are supported to increase their dispersion, stability and the active surface area even to a higher degree than ground bulk metal (Hills, Nashner *et al.* 1999; Abad, Corma *et al.* 2008). Therefore, in the development of a novel catalyst, much

research and trials are performed to find the most appropriate support since it will influence the metal particle size, structure, charge and form the specific active sites at the metal–support boundary (Qu, Huang *et al.* 2005). Supports can be classified in two categories: metal oxides and organic based supports.

*Metal oxide supports*

A wide range of inorganic supports exist for different catalyst preparations including zeolites (Srinivas, Radha Rani *et al.* 2001), hydrotalcites (Dimitratos, Villa *et al.* 2006), washcoated ceramic foams (Twigg and Richardson 2002). However only unstructured supports will be reviewed. The common metal oxides used are alumina $Al_2O_3$, iron oxide $Fe_2O_3$, silica $SiO_2$, titania $TiO_2$ and ceria $CeO_2$. Depending on the method of preparation, the surface area and pore sizes may vary considerably. However, a high surface area (>100 $m^2/g$) and highly porous supports (~1-5 nm pore diameter) are usually used for commercial catalyst in order to maximise the dispersion of the expensive, active metal (Vayenas, Bebelis *et al.* 2001).

The support can act as a Lewis acid affecting the conversion and selectivity by accepting a pair of electrons. The potential of a support to act as Lewis acid can subsequently affect the conversion and selectivity. Strong Lewis acids such as alumina and iron oxide may have $Al^{3+}$ and $Fe^{3+}$ ions in their structure which exhibit strong affinities to oxidise substrates which usually show a higher activity at an expense of selectivity. These supports were investigated using gold and gold-palladium mixtures for the oxidation of benzyl alcohol showing a loss of selectivity compared to titania and

silica as was mentioned in 2.2.1.1 (Enache, Knight *et al.* 2005; Enache, Edwards *et al.* 2006). Supports using alkaline earth metals such as magnesium oxide were shown to be active as well since platinum had a higher tendency to form small metal particles on the support (Jia, Jing *et al.* 1994).

The support may play a direct role in the catalysis other than dispersing the active metal. In the case of gold based catalysts, it is the lattice oxygen of the support that participates in the oxidation while gaseous oxygen will replenish the vacancy created in the absence of basic conditions (Vayenas, Bebelis *et al.* 2001). The following mechanism was proposed when ceria is used as support (Abad, Concepción; *et al.* 2005):

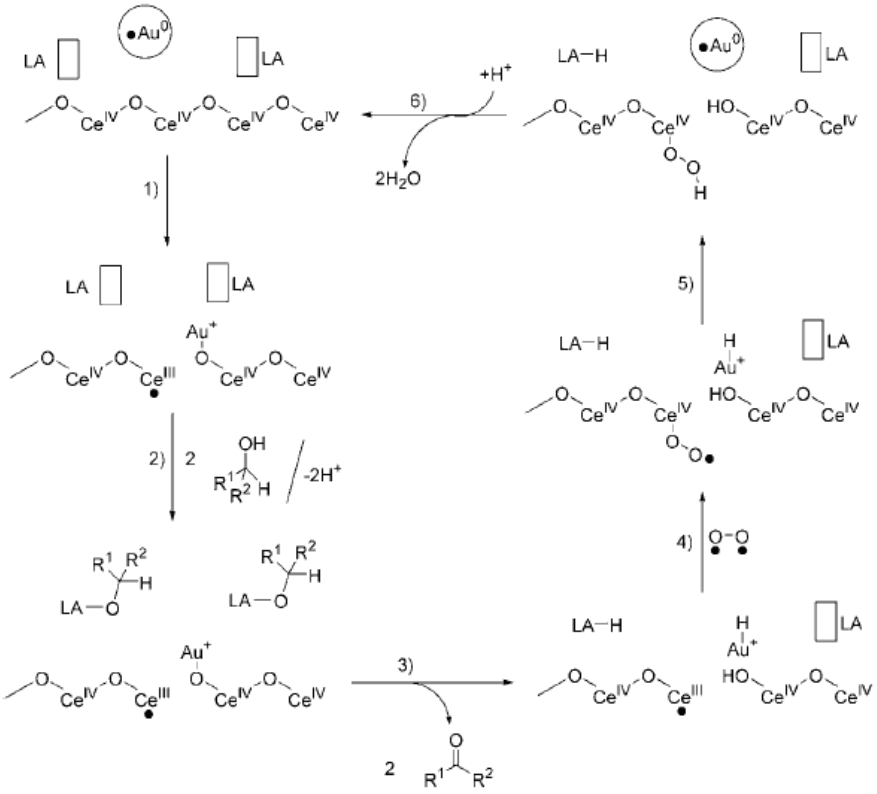


**Figure 2.5)** Alcohol oxidation with Au/Ceria catalyst

Figure 2.5) shows that the oxidation of alcohol happens on the gold-support boundary. The Lewis Acid (LA) sites and the lattice oxygen are indispensable in the oxidation of the alcohol which explains the considerable difference in activity between different supports (Enache, Knight *et al.* 2005).

*Carbon based supports*

Carbon based supports like graphite and activated charcoal, are widely used as supports. Typically, carbon can be activated following two methods: chemical and physical activation (Auer, Freund *et al.* 1998). The chemical preparation involves the addition of activating agents such as $H_3PO_4$ or $ZnCl_2$ to raw organic material and increasing the temperature up to 1073 K. The physical preparation involves the heating of pre-carbonized material in absence of air or under steam at 1073 K. The activation of carbon creates a considerable number of pores and hence increases substantially its surface area. While graphite has an average surface area of 10-50 $m^2/g$, the surface area of activated carbon can reach 800-1200 $m^2/g$ (Auer, Freund *et al.* 1998). Also, depending on the precursor from which the carbonisation was prepared, different morphologies will be expected. Figure 2.6) shows an SEM picture of activated carbons prepared with different precursors.

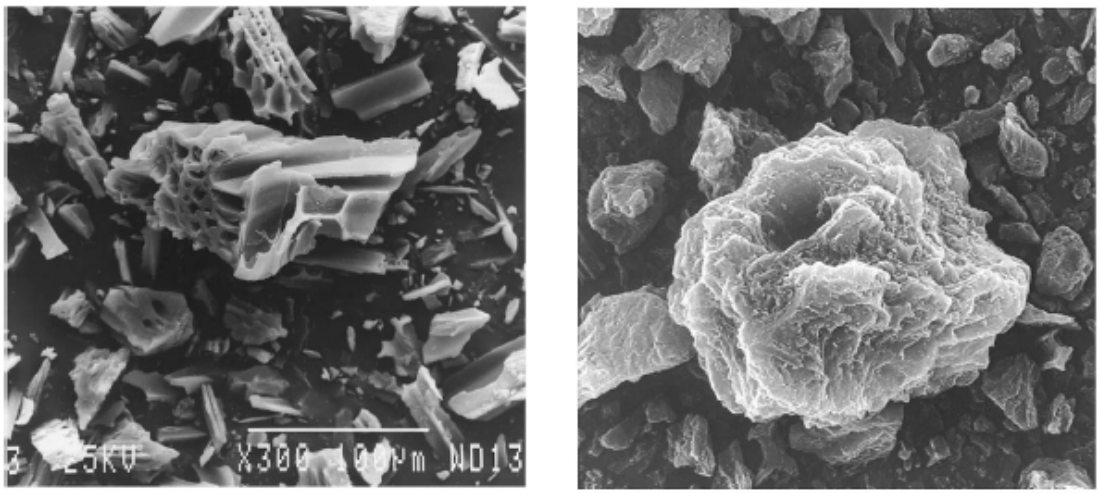


**Figure 2.6)** Scanning Electron Microscopy on activated carbon with 450 and 1000 times magnification respectively made by a) wood, b) peat (adapted from Auer *et al.* 1998)

A carbon support offers many advantages such as stability in acidic and basic mediums unlike alumina and silica for example, and it can be burnt in case of catalyst deactivation to easily recover the metals (Prati, Villa *et al.* 2007). Therefore, carbon supports have been widely used for oxidation processes with precious metals (Lee A, J.J *et al.* 2000; Pinxt, Kuster *et al.* 2000). Unlike metal oxides, carbon supports are electronically inert but extremely conductive causing a different conversion activity for a similar process especially for the case of gold (Dimitratos, Lopez-Sanchez *et al.* 2007). Abad *et al.* (2008) showed that for the benzyl alcohol oxidation with similar sized supported gold particles on carbon and metal oxides, the chemical nature of the supports affected the activity and selectivity of the catalysis. Indeed, gold supported on ceria gave a conversion of 45% for cinnamyl alcohol while on carbon support the conversion was 15% for the same substrate and conditions.

### 2.2.7) Catalyst Deactivation

Catalyst deactivation is a major reason that delays the application of PGM catalyst in the fine chemical industry (Markusse, Kuster *et al.* 2001). It becomes crucial to identify the reasons that cause such deactivation and investigate any possible solutions. Mallat and Baiker (1994), Gallezot (1997) and Vleeming *et al.* (1997) have enumerated different deactivation causes:

1. Overoxidation: Strongly adsorbed oxygen on the catalyst surface.
2. Poisoning: Substrate adsorption on the active sites
3. Metal leaching/ Particle agglomeration: Metal leaching is defined as the loss of active metal during the catalysis in the solution. After leaching occurs, a metal ion may be re-deposited on another metal particle causing, an increase in particle size through agglomeration which decreases the efficiency.
4. Fouling/coking: The blockage of active sites by deposition of species such as carbon.

#### 2.2.7.1) Overoxidation

As was previously discussed in section 2.2.3), overoxidation occurs at high oxygen coverage or a catalyst potential higher than 0.8V vs. RHE for platinum (Markusse, Kuster *et al.* 2001). The catalyst activity can be restored by allowing the catalyst to be reduced or by interrupting the oxygen flow (Dirkx and van der Baan 1981; Nicoletti and Whitesides 1989; Bronnimann, Bodnar *et al.* 1994) or can be enhanced with the addition of promoters as was previously discussed in section 2.2.2).

2.2.7.2) Poisoning

Poisoning is the strong chemisorption of compounds or impurities on catalytic active site. A principal example is the presence of $H_2S$ in feeds for the steam reforming of CO on nickel based catalysts. The formation of $Ni_3S_2$ is thus irreversible and renders the catalyst inert (Smith, Xia *et al.*; Alvarez and Ancheyta 2008). In the case of alcohol oxidation, strongly adsorbed substrate is referred to as chemical poisoning and can occur due to alcohol, carbonyl or by-product bonding to the metal. The adsorbed molecule may dissociate and bond chemically to the metal surface. Therefore, poisoning is highly dependent on the identity of the substrate. Carboxylic acids (Kluytmans, Markusse *et al.* 2000), ketones (Nicoletti and Whitesides 1989; Vleeming, Kuster *et al.* 1997), and even alcohols (Mallat and Baiker 1994) may deactivate the catalyst by strong adsorption. Similarly to the rate of adsorption, the rate of desorption is expected to be follow an Arrhenius-like form, $k_d = Ae^{-E_d/RT}$, where typical energies for desorption are 100kJ/mol (Atkins 2002). It is crucial to have the rate of product desorption faster than the rate of reactant adsorption in order to regenerate active sites. While substrate can physisorb and/or chemisorb, it is only the latter that inhibits the active sites due to the strong bonding with the metal.

Poisonous substrates can be classified into two categories: Molecules containing the CO group and non-oxygenated hydrocarbons. Carbon monoxide or carbonyl compounds can be re-oxidised to form carbon dioxide at high catalyst electro-potential while hydrocarbons can be hydrogenated to break the RC-M (carbon-metal bond) and form RC-H in order to prevent deactivation. Primary alcohols exhibit more CO poisoning than secondary alcohols and as the carbon chain length increases, the carbonyl

poisoning decreases (Parsons and VanderNoot 1988; Leung and Weaver 1990). For instance, the oxidation of methanol or propanol deactivates the catalyst with a decrease in the potential of the latter up to 0.5V vs. RHE (Pastor, Wasmus *et al.* 1993) which means the catalyst has a high coverage of CO. The oxidation of benzyl alcohol decreases the potential down to 0.3V vs. RHE (Leung and Weaver 1990) since non-oxygenated rings such as benzene adsorbed strongly on the catalyst, lowering the potential. The best example for chemical poisoning comes from the oxidation of glucose with platinum (Popovic, Markovic *et al.* 1991; Popovic, Tripkovic *et al.* 1992). The intermediates gluconic acid, gluconate and smaller fragments strongly bound on the Pt surface which deactivates the catalyst as can be illustrated in Figure 2.7) (Bae, Xing *et al.* 1990).

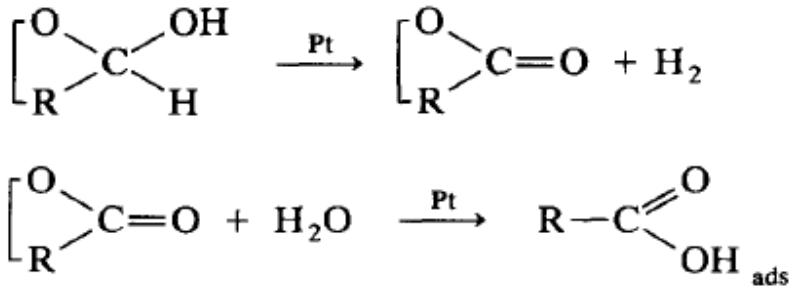


**Figure 2.7)** Gluconic acid poisoning on platinum (Popovic, Tripkovic *et al.* 1992)

Poisonous substrates can also be created by possible side reactions which lead to decreases in selectivity towards the intermediate carbonyl as well. Overoxidation of an aldehyde molecule creates carboxylic acids which strongly adsorb on the surface (Nicoletti and Whitesides 1989). Other reported side reactions are polymerization and aldol condensation in strongly basic or acidic solution (Tsujino, Ohigashi *et al.* 1992). Selectivity is also affected if the adsorbed hydrogen is not removed from the metal surface since hydrogenation may occur, thus forming different by-products (Hardacre,

Mullan *et al.* 2005). In an anaerobic basic medium, fructose was oxidised into gluconate with platinum, and the adsorbed hydrogen hydrogenated the fructose into mannitol and sorbitol (Gallezot 1997).

2.2.7.3) Metal leaching/ Particle agglomeration

There are different causes for the loss of metal particles in solution, the sintering of active metal or the sintering of the support. The common deactivation cause is thermal sintering where a high temperature causes the support to collapse (Farrauto and Bartholemew 1988). However, thermal deactivation is not a common phenomenon in liquid phase oxidation due to the lower temperature used.

The presence of certain species, such as anions and carbohydrates, can enhance the loss of the active metal into the solution (Vleeming, Kuster *et al.* 1997). Schuurman *et al.* (1992) reported the loss of activity for the oxidation of alpha-D-glucopyranoside due to re-deposition of platinum ions, which is known as the Ostwald effect. The Ostwald ripening points toward small crystallites which tend to increase in size to bring the surface to volume condition to a favourable low free energy state (Kent 2007). The literature on this type of deactivation is scarce since catalysts might lose their efficiency by leaching or agglomeration only after many runs (Vleeming, Kuster *et al.* 1997). While poisoning and overoxidation are reversible processes, leaching and agglomeration are irreversible and may render the catalyst completely useless (Mallat and Baiker 1994).

2.2.7.4) Fouling/coking

While poisoning is the selective bonding of a substrate to the active metal, fouling is the mechanical random or non-selective deposition of species unto the catalyst surface. The most common example is coking or carbon deposit of oil cracking in porous catalysts that blocks active sites. The most common cause of coking is the decomposition at temperature higher than 473K (Farrauto and Bartholemew 1988). The catalyst can be regenerated by controlled combustion of the coke while preventing a high temperature peak in order not to cause any sintering of the catalyst. Therefore, in liquid phase oxidation coking is rarely a cause of catalyst deactivation. The major catalyst deactivation causes can be summarised in Figure 2.8).

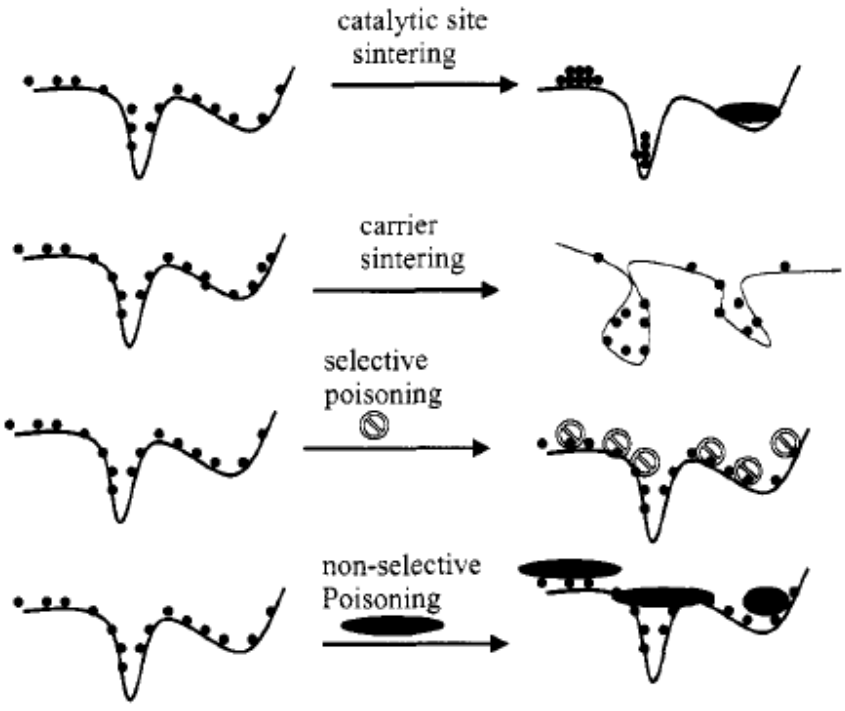


**Figure 2.8)** Different deactivation mechanism (Kent 2007).

2.2.8) Reaction Kinetics with Deactivated Catalyst

Catalyst deactivation is an inevitable phenomenon. However, being able to predict the deactivation by modelling allows the appropriate design, in labs or industry, of processes. Such improved designs greatly increase the commercial application of a catalyst, its lifetime expectancy and the use of the appropriate reactor (Farrauto and Bartholemew 1988). Therefore, a mathematical symbol was introduced in the kinetics of catalytic reactions called $\alpha$, which is the activity function or the rate of reaction on the deactivated catalyst divided by the rate on fresh catalyst (Butt 1980). When the activity function occurs separately from the concentration function $f(C)$ of the reaction, the deactivation rate is given by (Levenspiel 1972):

$$-r_d = \frac{-d\alpha}{dt} = k_d f(C)\eta_d \alpha^d , \qquad \text{Eq. 2.2.8.1}$$

$f(C)$ is the function of concentration of reactants and products, $\eta_d$ is the effectiveness factor for deactivated processes and d is the corresponding order of deactivation of $\alpha$ (Froment 1980; Butt 1982).

However, Eq. 2.2.8.1 assumes that the activity will eventually decrease to zero. In some deactivation cases such as poisoning or sintering, the catalyst is still active. Therefore, a constant, C', was introduced in the general reaction kinetic form with deactivated catalysts (Fuentes 1985).

$$-r_d = \frac{-d\alpha}{dt} = k_d f(C)_d \eta_d \alpha^d + \mathrm{C}', \qquad \text{Eq. 2.2.8.2}$$

In this case, the deactivation is included in the concentration function as well $f(C)_d$. Finally, by modelling and predicting the catalyst deactivation, it allows the delay of

activity loss which is always better than attempting to regenerate the catalyst (Kent 2007).

## 2.3) Solvent Effects

The choice of solvent influences certain processes depending on many of its characteristics (Rajadhyaksha and Karwa 1986). Firstly, the gaseous reactant should be soluble enough in the medium in order not to slow the reaction. Secondly, both liquid and gaseous reactants should have a high diffusivity coefficient in the given solvent to be transported to the catalyst particle. Thirdly, solvents have characteristic macroscopic and structural effects. Macroscopic effects are the physical properties of bulk solvent such as dielectric constants and dipole moments. The dielectric constant is the ratio of the quantity of stored electrical energy to the permittivity of air when a potential is applied. The dielectric constants and dipole moments strongly influence the transition state containing charges. Solvents having a high dielectric constant enhance the dissociation of a bond to form charges while solvents with a low dielectric constant tend to neutralise charged species by forming bonds (Carey and Sundberg 2007). However, a solvent interaction with solute and catalyst cannot be predicted based solely on macroscopic properties since the solvent molecule structure also plays a considerable intermolecular role that has been difficult to investigate.

Solvents may be classified into two categories: non-polar and polar. Non-polar solvents have a low dipole moment and dielectric contrary to polar solvents. Polar

solvents can be further divided between protic, which forms hydrogen bonds and aprotic polar which do not form hydrogen bonds. Non-polar solvents such as heptane, toluene, and p-xylene are often used due to their inertness and higher oxygen solubility than alcohols (Mallat and Baiker 1994; Keresszegi, Mallat *et al.* 2004). Another advantage of apolar solvents is their lack of interaction toward catalysts. Different solvents including polar and non-polar have been tested for alcohol oxidation (Kawabata, Shinozuka *et al.* 2005). It was deduced that reactions performed in non-polar solvents such as toluene tend to have higher reaction rate since polar solvents such as acetonitrile would compete with reactants to adsorb on active metallic sites, hence lowering the reaction rate.

If the solvent has a low dipole moment and dielectric constant it becomes hydrophobic and could have detrimental effects on conversion. One of the by-products of oxidation with molecular oxygen is water which is produced in equimolar amounts with the carbonyl product. However, water can strongly adsorb on noble metals and on metal oxide supports such as alumina, titania and silica via H-bonding thus blocking active sites from reactants. Keresszegi *et al.* (2004) used a water surfactant to remove adsorbed water on Pt/Alumina in order to proceed with the alcohol conversion since the hydrophobic toluene and cyclohexane were unable to remove adsorbed water. Gallezot, (1997) substituted the silica and titania supported platinum with carbon support due to the excessive H-bonding of glyoxal hydrogen-bonded to the hydroxyl groups of the oxide supports. Therefore, in order to achieve a satisfactory reaction rate, products should be miscible enough in solvents to be removed from the catalyst surface while reactants should not have to compete for metal site adsorption.

The ideal solvent for green chemistry would be water since it is the least toxic. However water has many limitations such as the insolubility with organic compounds, low oxygen solubility and due to its high polarity, water may strongly adsorb on the catalyst. Mallat and Baiker (1994) suggested the use of water-detergent systems that are more environmentally friendly than organic solvents and are as efficient, such as dodecylbenzenesulfonic acid sodium salt.

Solvents may also help tune or determine the production distribution of a certain reaction. When a substrate can undergo different reactions pathways resulting in different possible products, the solvent can favour one path over the other. For example, the use of a dioxane solvent leads to the production of benzaldehyde from the benzyl alcohol oxidation. On the other hand, dioxane/water mixtures led to the production of benzoic acid (Donze, Korovchenko *et al.* 2007; Korovchenko, Donze *et al.* 2007). Hence, depending on the nature and polarity of a solvent, one product may be more favoured than another. Consequently the solvent choice then becomes crucial where the most desirable characteristics are: Reactant solubility and diffusion, inertness toward the catalyst and a balance in the interaction with reactants/products (Rajadhyaksha and Karwa 1986). Table 2.1) shows a few examples of solvents used in the literature for alcohol oxidations.

| Author | Solvent | X($O_2$)at 298K and 1 bar ($\times 10^{-4}$)[b] | Dielectric Constant | Alcohol | % S (Selectivity) at %C (Conversion) | Catalyst used | Comments |
|---|---|---|---|---|---|---|---|
| (Ebitani, Ji *et al.* 2004) | Benzotrifluoride[a] | — | — | 2,2-dimethyl-1-propanol | 64%S at 100%C | Ru /CeO2/CoO | The efficiency of a solvent varies with the nature of the substrate |
| | | | | 1-Octanol | 97%S at 100%C | | |
| (Jia, Jing *et al.* 1994) | Diethyl Carbonate (basic) | — | — | Cyclohexanol | 99%S at 66%C | Pt/MgO | Alkaline medium increases the reaction rate |
| | Heptane | 22 | 1.9 | | 100%S at 29%C | | |
| (Hardacre, Mullan *et al.* 2005) | Toluene | 9.2 | 2.4 | cinnamyl alcohol | 88%S at 100%C | 5% Pd/Alumina | The higher selectivity in the ionic liquid is due to a lower reaction rate. |
| | Ionic liquid (1-butyl-3-methyl-imidazolium bis(trifluoromethylsulphonyl)imide) | — | ~ 40 | | 96%S at 100%C | | |
| (Donze, Korovchenko *et al.* 2007) | Dioxane | 5.3 | 2.2 | Benzyl Alcohol | 95% Benzaldehyde at 95%C | 1.95% Pt/C | Solvent determines the product and reaction rate. |
| | 50% Dioxane/Water | — | — | | 98% Benzoic acid at 95%C | | |

**Table 2.1)** Examples of different solvents used. [a]) Selectivity towards the carboxylic acid. [b]) Battino *et al.* (1983)

## 2.4) Temperature Effects on the Oxidation

At high temperatures, the reaction rate of liquid phase alcohol oxidation increases according to the Arrhenius equation. The minimum kinetic energy that reactants must have to be oxidised, or the activation energy, depends strongly on temperature (Perry 1997). This dependence is strongly manifested if the reaction is carried out in the kinetic regime. Sometimes, the formation of hot spots in trickle beds may result in a heterogeneous product distribution (Kresta, Edward PL *et al.* 2004). In the mass transfer regime, a variation of temperature does not result in a significant change of the reaction rate (Winterbottom and King 1999; Fogler 2001). In addition, a temperature increase may result in C-C bond rupture. CO molecules and $C_xH_y$ by-products may form and strongly adsorb on the active sites, decreasing selectivity and causing catalyst deactivation by strong adsorption (Colmati, Antolini *et al.* 2006; Tokarev, Murzina *et al.* 2006). In this case a strong oxygen flow is required to oxidise CO and a hydrogen flow to remove bonded hydrocarbon chains. Conversely, low temperature reactions have lower reaction rates and may deactivate the catalyst by strong substrate adsorption (Mallat and Baiker 1994). The temperature effects on oxidation vary depending on the nature of the substrate. Molecules such as carbohydrates are more sensitive to temperature effects in terms of degradation and poisoning effects on the catalyst. The oxidation of D-glucose exhibited a slower rate at high temperature since it transformed D-glucose into D-fructose which adsorbed on the platinum catalyst (Yei, Beden *et al.* 1988). Typical temperatures for liquid phase oxidation are below 373K and usually between 310K and 350K (Gallezot 1997).

## 2.5) Stirred Tank Reactors

### 2.5.1) Reactor Design

Stirred Tanks Reactors (STR) are commonly used in industry for medium scale chemical productions and when processes require uniform temperature and concentration which makes them suitable for fast reaction rates (Perry 1997). The application of stirred tanks represents around 50% of the world chemical production (Kresta, Edward PL *et al.* 2004). Efficient reactant mixing is highly desirable when mass transfer is limiting the production and to increase production profit.

Uneconomical mixing may occur for example when the stirrer is incapable of lifting the solid particles from the bottom of the vessel. It is advised to use down-pumping impellers in this case to push the particles away from the reactor base. Flooding may happen when gas at high velocity is supplied under an impeller at low stirring speed. Then the gas is not dispersed effectively and the reactants don't mix well. In three phase systems, it is desirable to have the solids suspended and the gas well dispersed while avoiding flooding. Therefore, there are key parameters to be considered when designing an STR:

1. Reactor geometry
2. Impeller types
3. Baffles
4. Gas spargers

2.5.1.1) Reactor Geometry

A conventional STR is usually shaped cylindrically although square shaped or horizontally orientated STR's exist as well to prevent gross vortexing of the solution (Kresta, Edward PL *et al.* 2004). The bottom may be flat or slightly concave. The location of inlets and outlets depend on the type of batch process. For slow reaction processes the feed inlet may be positioned on top of the reactor between the walls and the shaft. For fast reaction processes, the feed inlet tip should discharge the chemicals in a highly turbulent region to allow maximum mixing while keeping an appropriate nozzle size to prevent back-mixing. For dead end reactions in which gas is only supplied to replenish that used up by the reaction, the outlet may be located on the side or bottom of the reactor as long as it is not blocked by the presence of solids. This configuration can be used when the transport of the gaseous reactant is not limiting the reaction or to prevent its loss. For continuous operation it is advised that the outlet is located far from the inlet to prevent any loss of reactants. This configuration can be used to enhance the gas to liquid mass transfer by enhancing the gas distribution in the vessel with appropriate gas spargers and impellers. Gas spargers are usually rings with a number of spaced holes just underneath the impeller. A steel mesh can also be used on the tip of the inlet pipe to generate micro-bubbles (Nienow 1998; Kresta, Edward PL *et al.* 2004). A major challenge lies in designing a stirred tank with an optimum mixing configuration. One parameter to determine the mixing efficiency is the maximum turbulence energy dissipation rate per unit mass $\varepsilon_{\max}$ (Gabriele, Nienow *et al.*). The energy dissipation rate evaluates the degree of bubble break-up and coalescence, chemical reaction and segregation (Sheng, Meng *et al.* 2000). Zhou and Kresta (1996) have evaluated the

impact of different reactor configurations in order to determine the effects of baffles number $N_b$, clearance C, impeller diameter D and C/D ratio on $\varepsilon_{\max}$ with various impellers on a typical stirred tank as is illustrated in Figure 2.9).

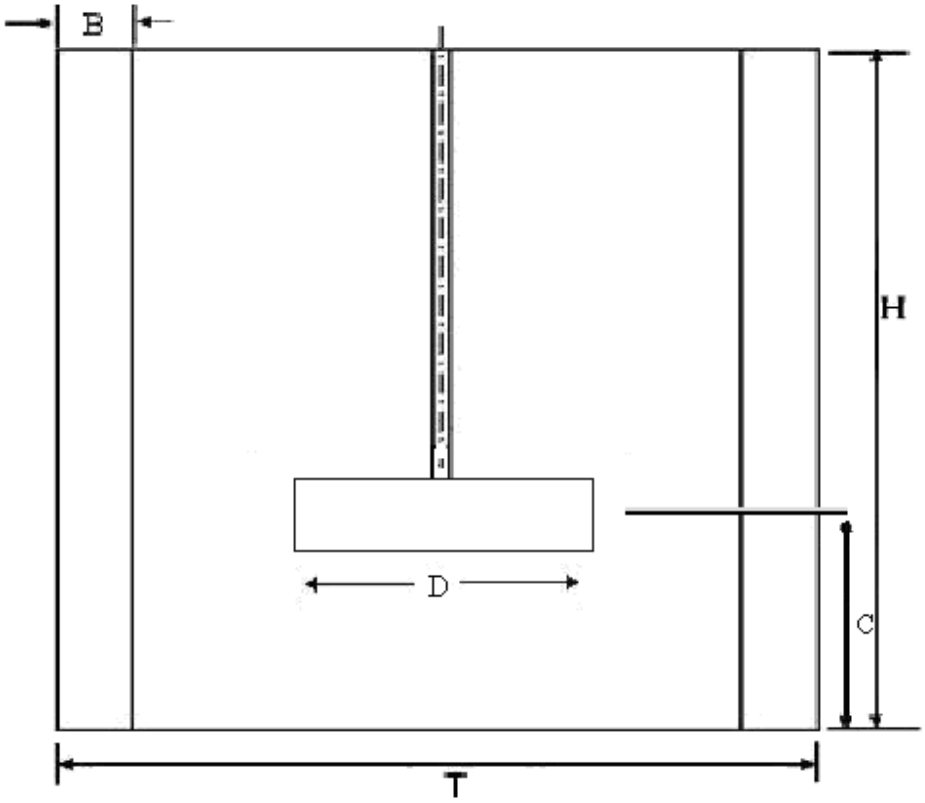


**Figure 2.9)** STR dimension nomenclature

The value of $\varepsilon_{\max}$ was determined using laser Doppler velocimetry to evaluate the mean and fluctuating velocity near the impeller with $\varepsilon_{\max} = \frac{A v^3}{L}$ where A=1 and L=D/10 (Wu and Patterson 1989; Zhou and Kresta 1996). A large variety of impellers exist for commercial uses. The optimal reactor configurations for the Rushton Turbine (RT),

Pitched Blade Turbine (PBT), hydrofoil turbine (A310) and High-Efficiency turbine (HE3) in order to maximise $\varepsilon_{max}$ are be summarised in Table 2.2).

| Impellers | $N_b$ | C | D | C/D | $N_P$ |
|---|---|---|---|---|---|
| RT-4 | 4 | T/4 | T/2 | 1/2 | 4.4 |
| PBT-4 | 4 | T/2 | T/2 | 1 | 1.27 |
| A310-3 | 4 | T/2 | 0.550T | ~1 | 0.3 |
| HE3 | 2 | T/2 | T/2 | 1 | 0.3 |

**Table 2.2)** Optimum reactor configuration to create the highest $\varepsilon_{max}$ in solid-liquid systems (Zhou and Kresta 1996)

2.5.1.2) Impeller types

Some commonly used impellers are illustrated in Figure 2.10).

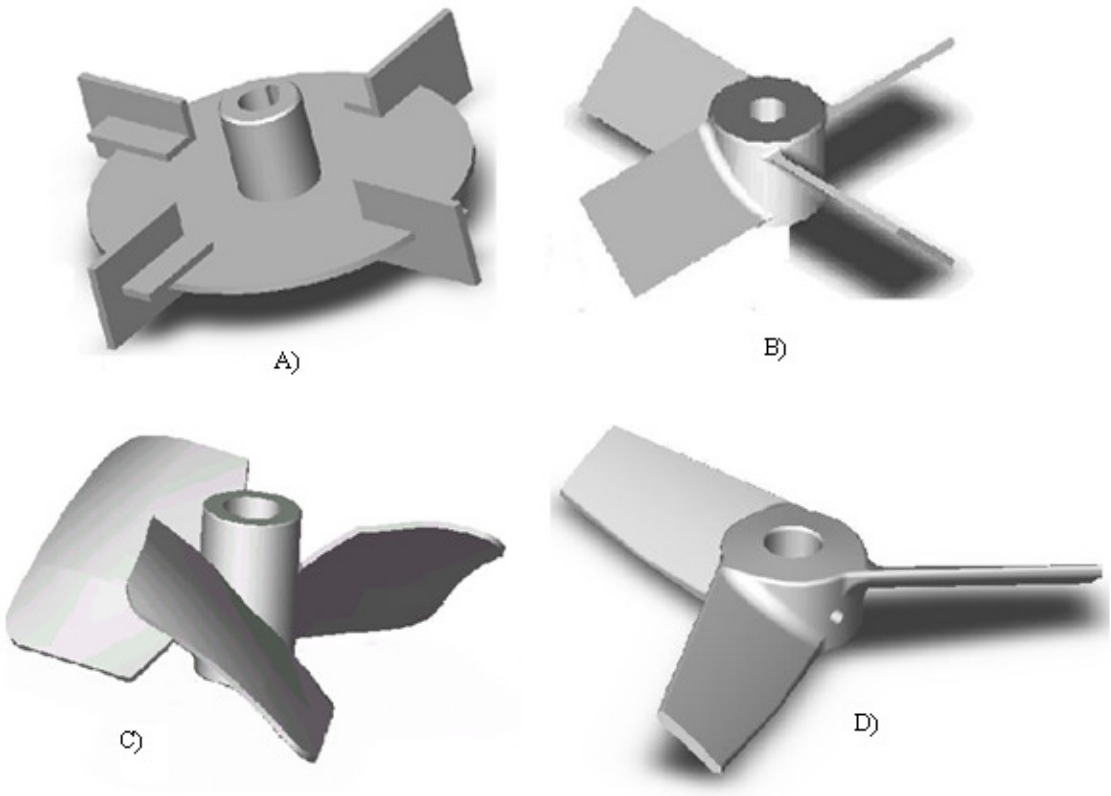


**Figure 2.10)** Impeller variety. *A) Rushton Turbine; B) Pitched Blade Turbine; C) A320 Turbine; D) A310 Turbine*

Depending on the type of process, the appropriate impeller should be used. For example, different stirrers may be selected for single phase, gas-liquid or gas-liquid-solid

operations. Impellers can be characterized by the power number and flow patterns (Kresta, Edward PL *et al.* 2004). The power used by an impeller is defined by:

$$P = N_P \rho_L N^3 D^5 \qquad \text{Eq. 2.5.1.2.1}$$

The power number $N_P$ is a dimensionless number relating the resistance force to the inertia force. It depends on the impeller type and the Reynolds number. The Reynolds number is defined as:

$$\mathrm{Re} = \frac{\rho_L N D^2}{\mu} \qquad \text{Eq. 2.5.1.2.2}$$

When Re<10 the flow is laminar and when Re>$10^4$ it is turbulent. Between these two values the flow is in a transitional state. $N_P$ is constant in a turbulent regime. The energy dissipated by the impeller is:

$$\varepsilon = \frac{N_P \rho_L N^3 D^5}{m} \qquad \text{Eq. 2.5.1.2.3}$$

Using the energy dissipated, the Reynolds number can be calculated from the following formula:

$$\mathrm{Re} = \left( \frac{\varepsilon D^4}{\nu^3} \right)^{1/3} \qquad \text{Eq. 2.5.1.2.4}$$

The position and size of the impeller in the reactor has a large effect on the efficiency of mixing and recommendations of the most suitable designs for different applications may be found in Kresta *et al.* (2004).

Impellers are also characterised by the flow type they generate as can be illustrated in Figure 2.11).

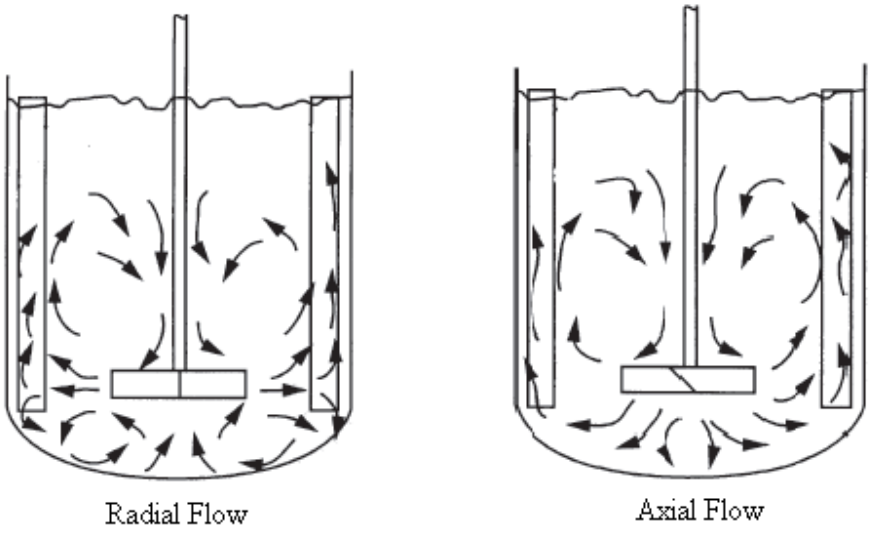


**Figure 2.11)** Radial and Axial Flow. (Kresta, Edward PL *et al.* 2004)

An RT impeller generates a radial flow with two circulating loops, above and below the impeller while a PBT produces an axial flow. However, at high stirring speed, large D or high viscosity liquids, the PBT will generate a radial flow as will be demonstrated in Figure 2.12) (Kresta, Edward PL *et al.* 2004; Fishwick, Winterbottom *et al.* 2005).

In three phase stirred tanks and gas-liquid systems, the use of downward pumping, or PBT-D, when the gas is sparged under the impeller creates instable flow patterns (Nienow 1998; Nienow and Bujalski 2002) and may flood easily especially for D/T<1/2 (Chapman, Nienow *et al.* 1983). In order to reduce the flooding tendency, a 6 blade turbine can be used instead of 4 blades and a 0.8D sparger. An increase in the impeller speed also reduces the flooding by gas break up. Upward pumping, or PBT-U,

however, disperses gas very well and is energy efficient (Chapman, Nienow *et al.* 1983). Fishwick *et al.* (2005) have used Positron Emission Particle Tracking (PEPT) technique to further to evaluate the effects of gassing on a PBT-D and PBT-U. The PEPT technique uses a pair of gamma-rays detector to track the position of a single radioactively labelled particle. It can thus be used to determine velocity fields and particle trajectories in opaque process equipment. Figure 2.12) demonstrates the results.

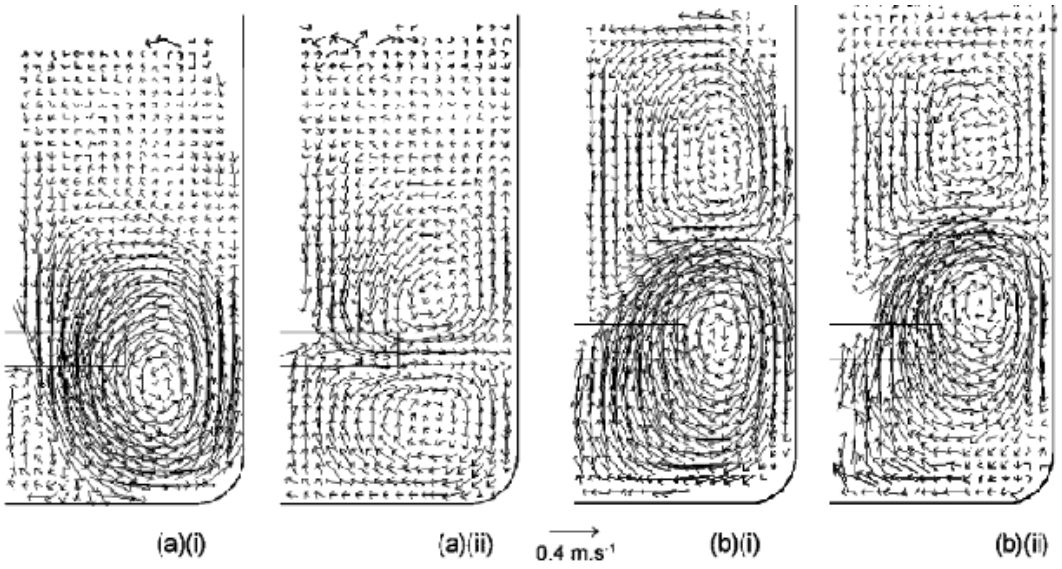


**Figure 2.12)** PEPT measurements of the mean radial-axial velocity vector plots for: a) PBT-D and b) PBT-U when i) un-gassed and ii) gassed at 1.5vvm (Fishwick, Winterbottom *et al.* 2005).

Figure 2.1 2) a(i), a(ii) clearly shows how the introduction of gas disturbs the magnitude as well as the pattern of the flow for the PBT-D. On the other hand, the flow created by the PBT-U is barely affected upon gas introduction in Figure 2.1 2) b(i), b(ii). Bujalski *et al.* (1990) have shown that a PBT-U can achieve similar gas-liquid mass transfer

coefficient as an RT with comparable power input. The PBT-U can also achieve a high gas hold-up comparable to the one produced by the RT (Aubin, Le Sauze *et al.* 2004).

2.5.1.3) Baffles

Baffles are used in a turbulent or transitional flow regime and rarely in Laminar flow of viscous systems. Baffles prevent the liquid in the reactor from just swirling around ineffectively and allow top-bottom mixing. Since the baffles increase the drag in the system, the power draw increases as well. The width of baffles is usually 8-10% of the tank diameter (Kresta, Edward PL *et al.* 2004). Having $N_b$>8 and B/T>0.2 interrupts the mixing, while 4< $N_b$ <8 increases the mixing efficiency (Lu, Wu *et al.* 1997).

2.5.1.4) Gas Spargers

A well-designed gas sparger will increase the gas-liquid mass transfer by decreasing bubble sizes, increasing the number of bubbles produced (increasing the gas-liquid interface area) and allowing a more homogenous distribution of bubbles throughout the reactor. The bubble development depends on the gas flow rate, pore size distribution and the physical characteristics of the liquid phase (Kazakis, Mouza *et al.* 2008). Gases are usually introduced in the tank via a shower disc plate that should be around 0.8 times the size of the impeller (Bujalski, Nienow *et al.* 1990). Other techniques involve the use of porous ceramic distributors, or steel mesh.

2.5.2) Advantages and Disadvantages of the STR

The use of the STR is mainly in the fine chemical and pharmaceutical industry where flexibility in product recipe and ease of cleanliness are essential. The STR has many advantages over other three-phase reactors, such as trickle bed reactors (TBR) or packed bed bubble column (PBBC) (Chaudhari and Ramachandran 1980):

1. The STR allows the use of any particle size. Therefore, in case internal mass diffusion limits a certain reaction, the catalyst can be further crushed into fine particles to increase the effectiveness factor. While within a packed reactor such as a trickle bed decreasing the particle size will considerably increase the pressure drop, hence the cost of operation.
2. Similarly to mass transfer coefficients, heat transfer coefficients are higher as well avoiding the creation of hot spots as is the case with TBR for instance. Throughout the reactor the temperature is uniform and relatively easy to control.
3. All the external surface of the catalyst is exposed to the reaction medium in STR while in TBR some of the catalyst may not be wet from the liquid flow which decreases the efficiency per unit of catalyst in the packing.
4. The STR provides an easy maintenance and cleaning procedure which is valuable in industrial processes.

However the STR has some limitations as well (Chaudhari and Ramachandran 1980; Fogler 2001).

1. STR has the lowest reactant conversion per unit of reactor volume compared to other three phase reactors. Hence the requirement to build large reactors for high production.
2. Loss of catalyst may occur due to particle attrition which may require a further filtration step.
3. The cost for mechanical agitation may be substantial

**2.6) External Mass Transfer**

In a three phase slurry reactor where the catalyst is a solid and the reactants are gaseous and liquid, it is crucial to transport the reactants past the interface walls and onto the catalyst surface. This means that the oxygen has to first diffuse from the gaseous phase to the liquid phase and then to the catalyst particle, while the liquid alcohol has to diffuse through the liquid-catalyst thin film. These diffusion steps can be considered as resistances which may decrease the concentration of the substrate as it passes from one phase to another depending on the mass transfer coefficients and the superficial area of contact (Fogler 2001). Figure 2.13) shows the 3 main steps of the material transport consisting of gas-liquid mass transfer, liquid-solid mass transfer and internal diffusion and reaction on the catalyst.

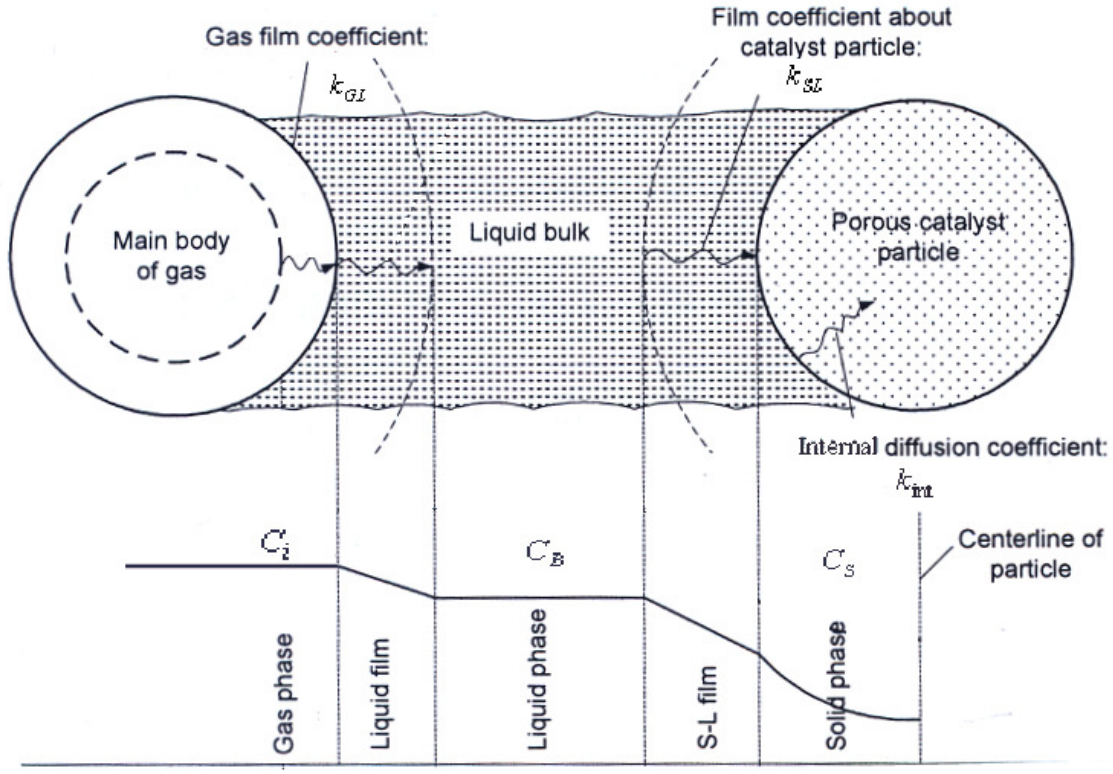


**Figure 2.13)** Gas concentration profile under mass transfer resistances (Monteiro 2005).

The first step of mass transport in the above figure is the oxygen incorporation into the liquid phase. The rate of oxygen absorption in the organic solvent depends on the gas bubble superficial area $a_b$, the mass transfer coefficient $k_{GL}$ and the oxygen concentration difference between gas bubble and the liquid bulk $(C_i - C_B)$. Hence for first or pseudo-first order reactions, the absorption rate is:

$$R_A = k_{GL} a_B (C_i - C_B) \qquad \text{Eq. 2.6.1}$$

The second step of mass transport in Figure 2.9 is the reactant transport onto the catalyst surface. The rate of reactant transport depends similarly on the external specific surface area of the particles $a_P$, the mass transfer coefficient $k_{SL}$, the catalyst loading $w$ and the reactant concentration difference between the liquid bulk and the catalyst surface $(C_B - C_S)$. Thus the transport rate is:

$$R_B = k_{SL} a_P w (C_B - C_S) \qquad \text{Eq. 2.6.2}$$

The last step consists of internal diffusion of the reactant within the catalyst particle and the surface reaction. The rate of internal diffusion and reaction depends on the catalyst loading $w$, the specific reaction rate $k_{\text{int}}$, the reactant concentration on the catalyst surface $C_S$ and the internal effectiveness factor $\eta$. Therefore the internal diffusion and surface reaction rate is:

$$R_C = k_{\text{int}} \eta C_S w \qquad \text{Eq. 2.6.3}$$

At steady state, all three mass transfer rates are equal, consequently $R_A = R_B = R_C$. The components of these three equations can be rearranged to give:

$$\frac{C_i}{R_A} = \frac{1}{k_{GL} a_b} + \frac{1}{w}\left(\frac{1}{k_{SL} a_p} + \frac{1}{k\eta}\right) \qquad \text{Eq. 2.6.4}$$

By plotting $\frac{C_i}{R_A}$ vs. $\frac{1}{w}$, which parameters can be experimentally measured for a pseudo-first order reaction, the following resistances can be established from the resulting straight line as can be seen Figure 2.14):

$Intercept = r_b = \frac{1}{k_{GL}a_b}$: Resistance to gas absorption

$Slope = r_c + r_r = \frac{1}{k_{SL}a_P} + \frac{1}{\eta k}$: Resistance to liquid-solid mass transfer and internal diffusion with surface reaction respectively.

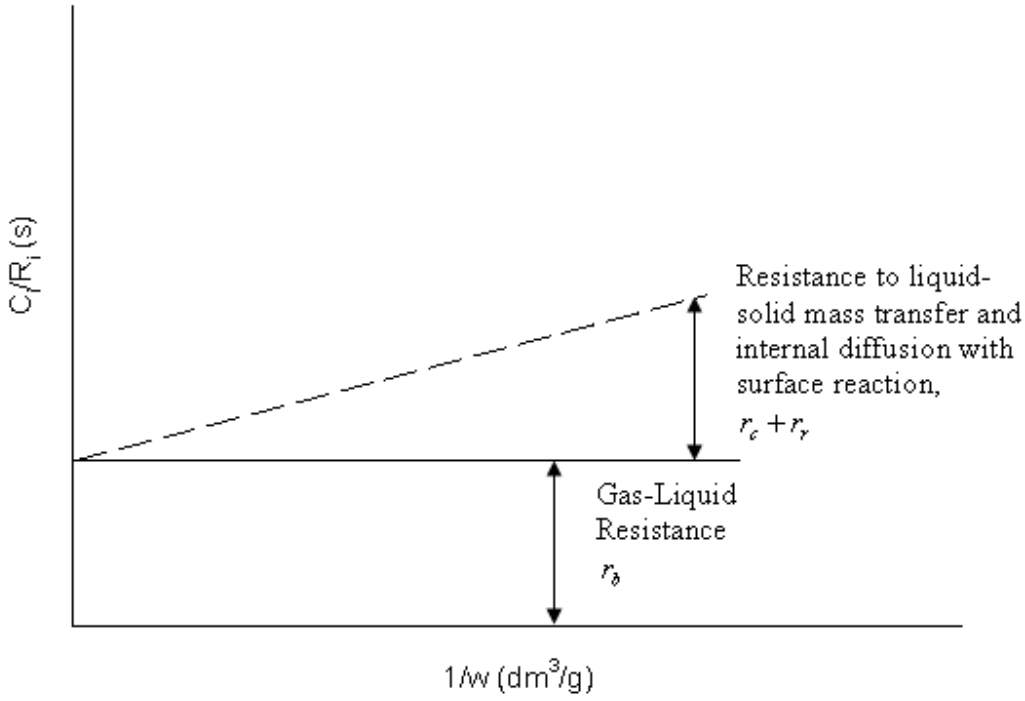


**Figure 2.14)** Plot to determine the mass transfer resistances

2.6.1) Gas-Liquid Mass Transfer

Oxygen has a very low solubility in organic liquids (Battino, Rettich *et al.* 1983). It can be expected that the oxygen concentration will be much less in the solution than in the gas phase. The resistance to gas absorption can be determined experimentally by equation 2.6.4 and Figure 2.14 or by an appropriate semi-empirical formula. Empirical gas-liquid mass transfer correlations have been thoroughly investigated for different conditions for STR in the literature (Table 2.1). Some formulas are dependant on the Reynolds number like the one proposed by Yagi and Yoshida (1975) while Van't Riet (1979) supposed that $k_{GL}a_b$ is dependant on the power draw, gas superficial velocity and the liquid volume. Chaudhari *et al.* (1987) proposed correlations for dead-end batches that are evidently not dependant on the gas superficial velocity (Litmans, Kukurechenko *et al.* 1972). It is therefore crucial when applying a semi-empirical equation to remain within the limitations and conditions set for such formulas in order to have valid results. Kawase *et al.* (1997) developed an equation to determine gas-liquid mass transfer that takes into effect the presence of solid particles and whether or not the liquid is Newtonian. A survey of the different correlations can be found in literature (Ramachandran and Chaudhari 1983).

| Correlation | Author |
|---|---|
| $\frac{k_{GL}a_b D^2}{D_{AB}} = 0.06\,\mathrm{Re}^{1.5}\left(\frac{DN^2}{g}\right)^{0.19} Sc^{0.5}\left(\frac{\mu_L\mu_G}{\sigma_L}\right)^{0.6}\left(\frac{ND}{u_G}\right)^{0.32}$ | (Yagi and Yoshida 1975) |
| $k_{GL}a_b = K\left(\frac{P}{V}\right)^{\varphi} u_G^{\xi}$ | (Van't Riet 1979) |
| $k_{GL}a_b = 1.48\times10^{-3} N^{2.18}\left(\frac{V_G}{V_L}\right)^{1.88}\left(\frac{D}{T}\right)^{2.16}\left(\frac{h_1}{h_2}\right)^{1.16}$ <br> $V_G/V_L > 1,\ h_1/h_2 > 0.3,\ N > 8.33s^{-1},\ D/T > 0.5$ | (Chaudhari, Gholap *et al.* 1987) |
| $k_{GL}a_b = C'\sqrt{D_{AB}}\,\frac{\overline{\rho}_l^{3/5}\,\varepsilon^{(9+4n)/10(1+n)}}{\left(\overline{K}/\overline{\rho}_l\right)^{1/2(1+n)}\sigma^{3/5}}\left(\frac{U_g}{U_t}\right)^{1/2}\left(\frac{\overline{\mu}_a}{\overline{\mu}_w}\right)^{-0.25}$ | (Kawase, K; *et al.* 1997) |
| $k_{GL} = 1366 d_b^{1.376}\left(\frac{D_{AB}u_b}{d_b\pi}\right)^{0.5}$ | (Miller 1974) |
| $k_{GL} = 0.42\left(\frac{(\rho_L-\rho_G)gu_L}{\rho_L^2}\right)^{1/3} Sc^{-0.5}$ | (Calderbank and Moo-Young 1961) |

**Table 2.3)** Semi-empirical correlations for $k_{GL}a_b$

2.6.2) Liquid-Solid Mass Transfer

In three phase systems two limiting mass transfer cases may occur: the transport of the dissolved gaseous reactant and the transport of the liquid reactant. However the liquid reactant concentration far exceeds the oxygen solubility in organic media. Subsequently it is the mass transport of oxygen that is expected to be limiting the reaction. Equation 2.6.4 cannot determine directly $k_{SL}a_p$ since the slope of the

corresponding plot includes the internal mass transfer and surface reaction resistances as well. However there are many semi-empirical formulae that can be used to estimate $k_{SL}a_p$. Frossling (1938) developed a correlation based on the Reynolds and Schmidt number and there have been since many variations of the same formula but valid at different conditions such as the range of the Reynolds and Schmidt number for a given system (Fogler 2001). Frossling's correlation evaluates the Sherwood number:

$$Sh = 2 + \alpha \mathrm{Re}_s^{\delta} Sc^{\gamma}, \qquad \text{Eq. 2.6.5}$$

where $\alpha$, $\delta$ and $\gamma$ are variables that have been estimated for different conditions, impellers by many researchers.

Kluytmans *et al.* (2000) suggested using similar correlations to evaluate liquid-solid mass transfer coefficients. However, Kushalkar and Pangarkar (1994) developed a different equation from the Frossling form that takes into account the effect of gas sparging in three phases systems similar to the work presented in this work and has the following form:

$$k_{SL} = 1.19 \times 10^{-3} \left( \frac{N}{N_{sg}} \right)^{1.15} (Sc)^{-0.47}, \qquad \text{Eq. 2.6.6}$$

where $N_{sg}$ is the critical impeller speed for suspension of solid particle in aerated liquid and is a function of $N_s$, which is the critical impeller speed for suspension of solid particle in unaerated liquid. It is crucial to have the solid particle suspended in the reactor to allow the use of the whole catalyst surface and to have uniform mixing which will affect $k_{SL}$ in return. Although downward pumping impellers are recommended for

solid-liquid two phase system in order to disperse the sinking catalyst, this configuration will have a negative effect on the gas-liquid mass transfer and is therefore not advised for three phase reactors. For upward pumping in three phase stirred tanks, the critical impeller speed for suspension of solid particle in aerated liquid $N_{sg}$, can be determined by (Bujalski, Konno *et al.* 1998):

$$N_{sg} = N_S \left(1 + Q_{VG}\right)^{0.11} \qquad \text{Eq. 2.6.7}$$

$Q_{VG}$ is the vessel volume per minute flow. $N_S$ is the critical speed for the suspension of solid particles in non-aerated liquid and can be determined by the following correlation:

$$N_S = \frac{S\upsilon^{0.1} d_p^{0.2} (g\Delta\rho / \rho_L)^{0.45} X^{0.13}}{D^{0.85}} \quad \text{(Zwietering 1958).} \qquad \text{Eq. 2.6.8}$$

It has been shown that when the solid-liquid mass transfer is limiting the reaction rate, increasing N above $N_{sg}$ does not improve the conversion since the particles are already covered in liquid (Nienow and Bujalski 2002). A survey of the different correlations can be found in Table 2.4).

| Correlation | Conditions | Author |
|---|---|---|
| $Sh = 2 + 0.60\,\mathrm{Re}^{0.5}\,Sc^{1/3}$ | $\mathrm{Re} < 10^4$<br>$0.6 < Sc^{1/3} < 400$ | (Fogler 2001) |
| $Sh = 2 + 0.52\,\mathrm{Re}^{0.52}\,Sc^{1/3}$ | $420 < Sc^{1/3} < 1.3\times10^5$ | (Armenante and Kirwan 1989) |
| $Sh = 2 + 0.4\,\mathrm{Re}^{1/4}\,Sc^{1/3}$ | Micro-particles | (Kluytmans, Markusse *et al.* 2000) |
| $k_{SL} = 1.19\times10^{-3}\left(\frac{N}{N_{sg}}\right)^{1.15}(Sc)^{-0.47}$ | Three phase system | (Kushalkar and Pangarkar 1994) |
| $\frac{k_{SL}d_p}{D_m} = 2 + 0.47\left(\frac{d_p^{4/3}e^{1/3}\rho_L}{\mu_L}\right)^{0.62}\left(\frac{D}{T}\right)^{0.17}\left(\frac{\mu_L}{\rho_L D_m}\right)^{0.}$ | $0.07 < \mathrm{Re} < 10^4$<br>$267 < Sc^{1/3} < 35000$ | (Levins and Glastonbury 1972) |

**Table 2.4)** Semi-empirical correlations for $k_{SL}$

## 2.7) Internal Mass Transfer

When a support is coated with an active metal, the catalytic sites will be distributed on the particle surface as well as on the porous walls (Fogler 2001). The reactant has to be transported inside the pores to reach the active sites in order to use the catalyst efficiently. It then becomes crucial to determine if the reaction rate is limited because of internal reactant diffusion. A concentration gradient will be the driving force transporting the corresponding reactant inside the particle. If internal mass transfer is

important the substrates will react before reaching the end of the pores while if the internal mass transfer is negligible no concentration gradient will exist throughout the catalyst. Hence the substrate will be transported inside the catalyst through molecular diffusion (liquid-solid systems) and pore walls collision by the Knudsen diffusivity (solid-gas systems). There is no Knudsen diffusion for liquids, since the mean free paths in liquids are smaller than pore diameters (Petersen 1965; Perry 1997; Levenspiel 1999) as can be illustrated Figure 2.15)

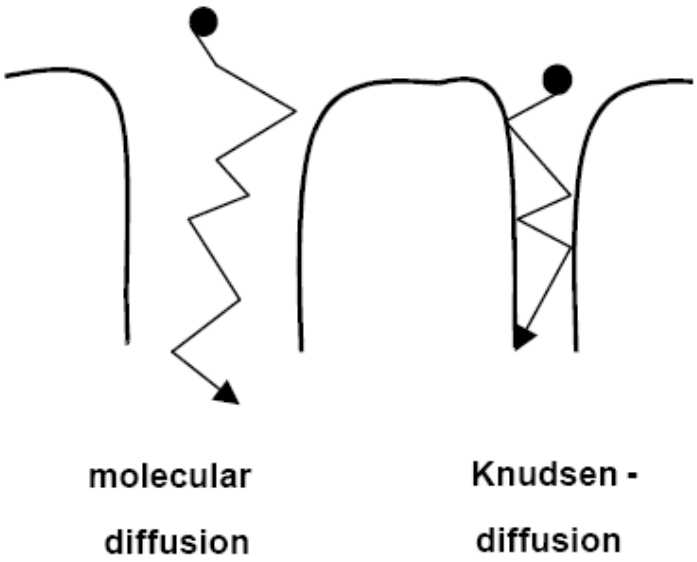


**Figure 2.15)** Different types of diffusion.

*Effectiveness factor, Thiele Modulus and Wagner-Weisz-Wheeler Modulus*

In order to evaluate the outcome of internal mass transfer, the effectiveness factor and the Thiele Modulus can be determined and they are defined as:

$$\eta = \frac{actual\ mean\ reaction\ rate}{reaction\ rate\ if\ \ all\ actives\ sites\ were\ on\ the\ surface}$$ Effectiveness Factor

$$\phi^2 = \frac{surface\ reaction\ rate}{diffusion\ rate}$$ Thiele modulus

The effectiveness factor is a function of the Thiele modulus which is dependant on the catalyst shape, size and reactant concentration on the surface. Many researchers have investigated the properties of different catalyst shape for many reaction orders. When the particles are small, the reactants are highly diffusive or the reaction is too slow, the Thiele modulus is close to zero since the diffusion rate tends be very high and the reaction is intrinsically limited. The effectiveness factor then approaches 1. On the other hand if the particles are large, reactants slowly diffuse and the reaction is much faster than the diffusion rate, the Thiele modulus is very high and the reaction is diffusion limited. The effectiveness factor then approaches zero. A problem that arises from the determination of the Thiele modulus is that the observable experimental reaction rate does not correspond to the surface reaction rate only but to both the diffusion and surface reaction rate (Levenspiel 1999). Therefore in order to evaluate the internal mass transfer effects another parameter was introduced which is the Wagner-Weisz-Wheeler modulus $M_W$.

$$M_W = \frac{Observed\ reaction\ rate}{diffusion\ rate} = \eta\phi^2$$

The Weisz-Prater criterion can determine if the reaction is intrinsically limited or diffusion rate limited for an nth order reaction (Petersen 1965; Perry 1997; Fogler 2001).

$$M_W = L^2 \frac{(-r_V / C_A)_{\exp}}{D_{eff}} \left( \frac{n+1}{2} \right) < 0.15 \text{ Diffusion free regime} \qquad \text{Eq. 2.7.1}$$

$$M_W = L^2 \frac{(-r_V / C_A)_{\exp}}{D_{eff}} \left( \frac{n+1}{2} \right) > 0.4 \text{ Diffusion limited regime} \qquad \text{Eq. 2.7.2}$$

Where $L$ is the characteristic size of a catalyst particle, $r_V$ is the observed reaction rate per unit of volume of catalyst particles, $C_A$ is the initial concentration of reactants and $D_{eff}$ is the effective diffusivity (Weisz and Prater 1954).

## 2.8) Reaction Modelling and Kinetics

Heterogeneous catalysts provide an alternative reaction path with lower activation energy (Atkins 2002). The catalyst activates the reactants which increases the reaction rate (Gangwal, van der Schaaf *et al.* 2005). It is of crucial importance to extract kinetic data and establish a model able to describe the reaction rate and products under different conditions. This allows scale up for an industrial use of a certain process. A common approach towards experimental data fitting is the power law model which provides the activation energy and the order of reaction of different substrates. The power law model has the following form:

$$R = kC_a^{\alpha} C_B^{\beta} ... C_i^n , \qquad \text{Eq. 2.8.1}$$

Where $C$ is the concentration of different substrate defined by a, b and $i$ with $\alpha, \beta$ and n being the reaction order for the corresponding substrates. The power law model is simple, fits easily the experimental data and has been recommended (Weller 1956).

However, the power-law model does not take into account different mechanistic steps or the existence of intermediates. Therefore, another model is used, the Langmuir-Hinshelwood (L-H) rate expression, to describe the mechanism and kinetics of a reaction based on different assumptions. The L-H model presumes that substrates (reactant and/or products) adsorb on the surface of the catalyst under the following assumptions (Perry 1997; Levenspiel 1999):

1) An active site can be occupied by only one molecule. A monolayer is a catalyst surface covered with adsorbate.
2) The energy of adsorption is the same on all active sites.
3) An adsorbed molecule does not affect the adsorption of a neighbouring molecule.

Obviously, these assumptions over-simplify the reaction mechanism since multi-layers, different active sites and various adsorption energies on the same catalyst have been reported (Satterfield 1991; Kapteijn, Marin *et al.* 1999; Atkins 2002). Nonetheless, L-H models are helpful in discriminating between different proposed mechanisms and even predicting reaction rates (Boudart 1972) and will hence be used to model reaction rate in this work

Since there is no agreement on the mechanism of the alcohol oxidation there are different proposed rate laws (Mallat and Baiker 1994). Schuurman *et al.* (1992) assumed that the oxidation of alpha-D-glucoside on Pt/C is based on reversible adsorption of oxygen and associative adsorption of alcohol. The surface reaction happens between the adsorbed alcohol and oxygen.

I) $R-CH_2OH + * \xleftrightarrow{K_1} R-CH_2OH_{ads}$

II) $O_2 + 2* \xleftrightarrow{K_2} 2O_{ads}$

III) $R-CH_2OH_{ads} + O_{ads} \xrightarrow{k_3} R-CHO + H_2O + 2*$

$$R = \frac{k_3 K_1 [A](K_2[O_2])^{0.5}}{(1 + K_1[A] + (K_2[O_2])^{0.5})^2}, \qquad \text{Eq. 2.8.2}$$

*A* is the alcohol substrate, *P* is the ketone product and * denotes an active site on the catalyst. $K_1 = k_1 / k_{-1}$ and $K_2 = k_2 / k_{-2}$ are the equilibrium constants for the forward and reverse reactions of step I) and II) respectively. Step III) is irreversible with $k_3$ as the rate constant.

On the other hand, van den Tillaart *et al.* (1994) proposed a different mechanism for the oxidation of ethanol with Pt/C based on an irreversible adsorption of oxygen and a reversible dissociative adsorption of alcohol. The surface reaction happens between an alkoxide and adsorbed oxygen.

I) $R-CH_2OH + 2* \xleftrightarrow{K_1} R-CH_2O_{ads} + H_{ads}$

II) $O_2 + 2* \xrightarrow{k_2} 2O_{ads}$

III) $R-CH_2O_{ads} + O_{ads} \xrightarrow{k_3} R-CHO + OH_{ads} + *$

IV) $H_{ads} + OH_{ads} \xrightarrow{k_4} H_2O + 2*$

$$R = \frac{2k_2[O_2]}{(1 + \frac{2k_2[O_2]}{k_3\sqrt{K_1[A]}} + 2\sqrt{K_1[A]})^2} \qquad \text{Eq. 2.8.3}$$

In electrochemistry Markusse *et al.* (2001) proposed a kinetic model to describe the kinetics of alpha-glucopyranoside based on the electro-potential of the catalyst:

$$E = \frac{RT}{2F}\ln\left(\frac{k_2[O] + k_{ox}[O_{ads}][*]}{2k_3[A][*]}\right) \qquad \text{Eq. 2.8.4}$$

Where $[O_{ads}]$ is the surface coverage of oxide (which causes deactivation) and [*] are the concentration of available sites. Therefore, based on the pH, oxygen coverage, reactant identity, different rate laws will describe more adequately different oxidation reactions (Gallezot 1997).

*Summary*

In this chapter a review on the oxidation mechanism with noble metals was given together with a physical and chemical description of the catalysts used. The deactivation causes, solvent and temperature effects were also investigated. The mass transfer explanation and the optimisation of stirred tanks were presented as well before examining the kinetics of the oxidation mechanism. This chapter will serve as a foundation and references for the following experimental and results chapters.

# III) EXPERIMENTAL AND ANALYTICAL METHODS

This chapter describes the experimental setup used for the alcohol oxidation investigation. Firstly, the materials used, the experimental rig and procedures are described. Secondly, the analytical method used to quantify and identify samples taken during a reaction is explained. Finally, the catalyst characterisation methods are detailed where the results can be found in the corresponding chapters.

## 3.1) Chemicals, Gases and Catalysts

The subsequent commercial chemicals were used as received without further purification: n-Heptane (99%, Acros), 1,4-Dioxane (≥99%, Acros), 2-Octanol (>97%, Alfa Aesar), 1-Octanol (>98%, Alfa Aesar), p-Xylene ( 99%, Acros), 2-pentanol ( 99%, Acros), DMSO (>99%, Fisher), Benzyl Alcohol (>99%, Acros) and Benzaldehyde (>99%, Acros).

Air (>99.9%), 40% oxygen Enriched Air, hydrogen (>99.9%) and helium (>99.9%) were all supplied by BOC Gases. Helium was further purified using a moisture, hydrocarbon and oxygen trap when it was used as a carrier in the GC.

## 3.2) Experimental Setup

### 3.2.1) Baskerville Reactor

All reactions were performed in a Baskerville autoclave reactor except when the experiments consist of analysing kinetic parameters where a smaller lab scale setup was used to prevent any interference from mass transfer limitations. The Baskerville reactor is a 500ml autoclave shaped cylindrically that is fitted in a heating coil. It is equipped with 4 baffles, while the impeller and gas purging pipe can be unscrewed and changed to alternative designs in order to study different hydrodynamic regimes. A 4 blade up-pumping impeller and a 4 blade Rushton turbine were manufactured to study the effect of different mixing patterns on the reaction rate and selectivity of the oxidation and are illustrated in Figure 3.1).

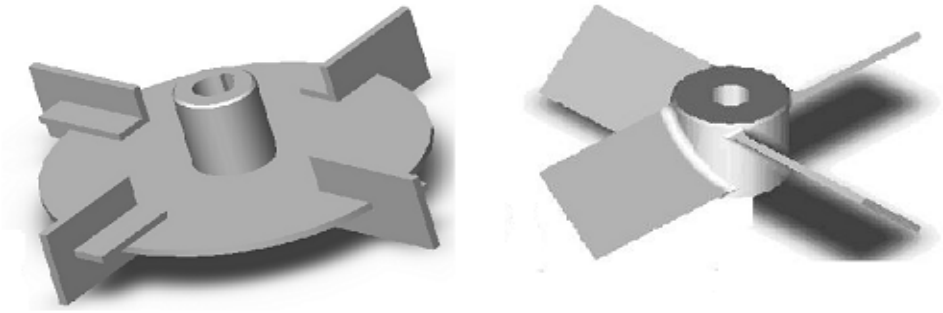

**Figure 3.1)** Rushton Turbine and Pitched Blade Turbine. *Impeller diameter of 4.0cm, height of blades of 1.0cm and width of 1.5cm.*

The temperature was monitored digitally with the help of a thermocouple inserted into the solution through the reactor. As to the gas purging system, initially a simple pipe was produced to bubble gas just under the impeller. Later, a disk shower head with 21 holes was manufactured as well to produce more bubble with smaller surface area in order to increase gas-liquid mass transfer. The recommended disc sparger diameter is 0.8 times the impeller diameter which is 3.2 cm in this work with the holes equally spaced as is illustrated in Figure 3.2).

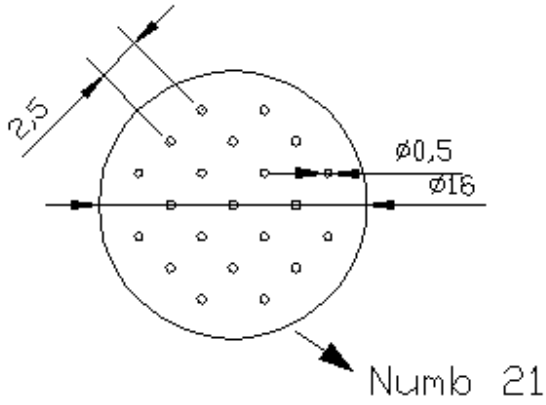


**Figure 3.2)** Disc Sparger Design. $\phi$ *Represent the radii*; *Dimensions are in millimetres; 21 holes present; Sparger thickness is 5mm.*

The reactor vessel is illustrated in Figure 3.3). The maximum operating pressure of the reactor is 150 bars while the maximum temperature is 623K. The reactor is also equipped with a safety bursting disk that can withstand up to 20 bars at 393K. After each experiment, the reactor is allowed to cool down to minimise the amount of vapour and is then drained through a sieve to re-collect the catalyst while the liquid chemicals are stored in waste drums prior to professional disposal.

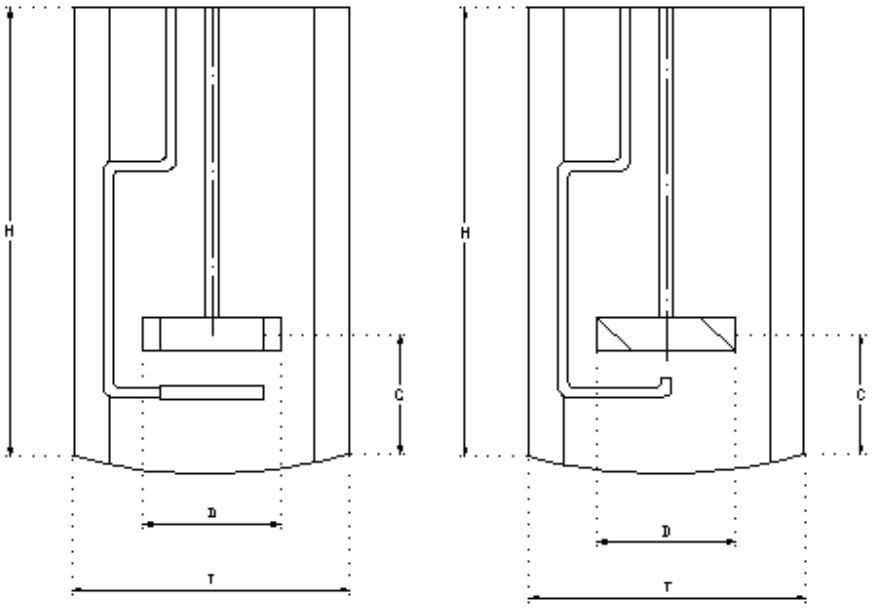


| Characteristics | Dimensions (cm) |
|---|---|
| D | 4.0 |
| T | 8.0 |
| C | 3.0 |
| H | 13.0 |

**Figure 3.3)** Reactor vessel and dimensions.

3.2.2) Experimental Procedure

All experiments were performed according to the following method. The liquid solution (300 ml) was added into the reactor and heated to the suitable temperature. Once the desired temperature was achieved, the catalyst was added before sealing the reactor and pressurising the system. The reaction began when the stirring was applied and the gas started to flow. GC analysis was performed before the stirring was applied to verify whether there was any conversion in the absence of stirring to ensure that the method had not caused pre-conversion of reactants prior to starting the stirrer. Since no conversion whatsoever could be detected, it was safe to assume that there is no conversion until stirring is applied. Table 3.1) illustrates the range of different variables tested for the different catalysts studied.

| Catalyst | Substrates | Solvents | Pressure | Use of Enriched Air | Temperature | 50% w/w $H_2O_2$ addition effect |
|---|---|---|---|---|---|---|
| 5%Pt-1%Bi | Benzyl Alcohol, 1-Octanol, 2-Octanol | DMSO, Heptane, Dioxane, p-Xylene | 1-4 Bar | No | 323-353K | No |
| 2.5%Au-2.5%Pd | Benzyl Alcohol, 2-Octanol | Solvent free | 1-7 Bar | Yes | 343-393K | No |
| 5%CuO 5%AgO 5%$Fe_2O_3$ | Benzyl Alcohol, 1-Octanol, 2-Pentanol | Heptane, Octane, Decane | 1-8 Bar | No | 303-430K | Yes |

**Table 3.1)** Parameters investigated and varied for different catalysts in the Baskerville Reactor.

Figure 3.4) shows the flow diagram of the experimental unit used in this work. The gas flow was measured using an Alltech Digital Flow Meter on the venting valve V2. The work with the Pt-Bi/carbon and metal oxides catalysts (Chapter 4 and 7) was done using the PBT-U and single orifice pipe for the gas sparging while the RT, PBT, single orifice pipe and disc shower head were investigated for the Au-Pd/titania work (Chapter 5). Before analysing the constituents of the reaction mixture in the reactor, 4ml of the solution were flushed out to clean the sampling valve V1 from any earlier sample contaminants and discarded. Then, 2.5ml are taken and filtered through single use $0.7\mu m$ Chromacol filters to remove any catalyst particle that could block the GC column once the solution is injected into it.

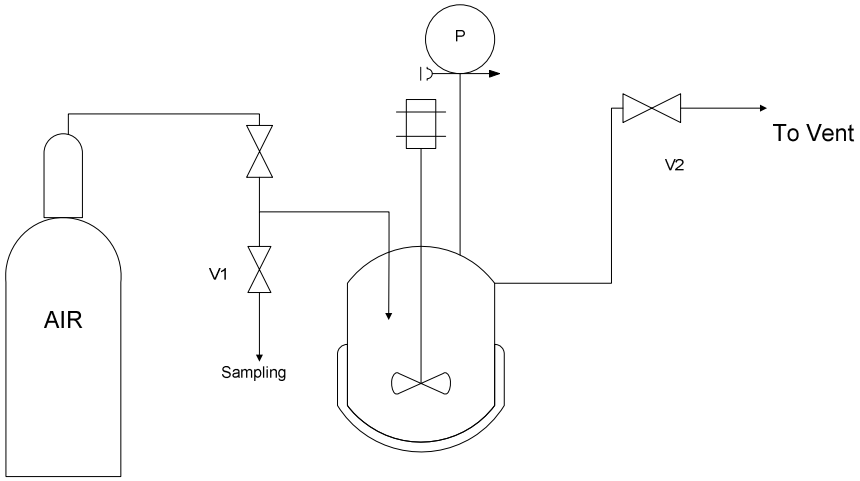


**Figure 3.4)** Experimental setup. *V1: Sampling valve; V2: Venting Valve; P: Pressure Gauge with bursting valve.*

3.2.3) Laboratory Scale Setup

The laboratory scale setup consists of a 100ml three necked round bottom flask on a heating and stirring plate. A magnetic stirrer was inserted inside the flask to stir the solution. A high efficiency Graham condenser was placed on the vertical opening of the flask while a mercury thermometer and a plastic air pipe were installed on the remaining openings. The air stream from a cylinder was controlled with the help of a flow meter to 200ml/min.

3.2.4) Laboratory Scale Procedure

The main use of a lab scale rig was to study kinetic parameters of oxidation reactions with minimum interference of mass transfer limitations. Hence, all reactions were performed at high stirring and high bubbling where any further increase of stirring or air flow makes no difference to the reaction rate. This setup was mostly used for the 5%Pt-1%Bi catalyst where 30ml of solution was used with 0.15g of catalyst. This setup is also useful to test different catalysts when their quantity is scarce.

## 3.3) Quantitative and Qualitative Analytical Methods

All samples taken from experiments were analysed using a Perkin-Elmer 8700 Gas Chromatography equipped with a Flame Ionization Detector (FID). The FID uses hydrogen and air to partially burn the organic constituents that are carried by helium through a retention column. This will produce ionic sub-compounds that are detectable

by the FID and the resulting signal is proportional to the quantity injected into the GC. Known chemical standards can be injected in the GC to determine the corresponding retention time, which allows the identification of the compounds from experimental samples. Moreover, by injecting a substrate at different concentrations, a calibration plot between the signal versus the substrate concentration can be established which permits the quantifications of the substrate concentrations in the experimental samples. Hence, by choosing appropriate conditions that allows different substrate to elute at different times and by calibrating the GC, the qualitative and quantitative analysis of chemicals can be established. In case peaks with different retention times than the standards appear in the chromatogram, then these by-products are unknowns that can be identified using a Mass Spectrometry.

The GC was equipped with a CP-Wax capillary column that is made from polyethylene glycol. This very polar column would ensure that the apolar solvent would elute first since the alcohol reactant and ketone products have polar affinities. The following conditions were used to analyse different substances.

| | Parameters | Octanol | Benzyl Alcohol |
|---|---|---|---|
| **Gases and Flow rate** | Carrier Gas | Helium | |
| | Flow rate | 35.0 ml/min | |
| **Injector** | Temperature | 523K | |
| | Injection Volume | 1.0 $\mu L$ | 0.1 $\mu L$ |
| **Detector** | Temperature | 523K | |
| | Range | 10 | |
| **Oven Conditions** | Equilibrium Time | 1.0 min | |
| | Isothermal temperature and time | 373K for 10min | 403K for 9 min |
| | Ramp Rate | 10K/min | 30K/min |
| | $2^{nd}$ Isothermal temperature and time | 448K for 5 min | 473K for 9 min |
| | GC Column | 50m x 0.32 mm (1.2 $\mu m$) CP-Wax 52B | |

**Table 3.2)** GC conditions for the analysis of octanol and benzyl alcohol oxidation.

## 3.4) Catalyst Characterisation

### 3.4.1) Chemisorption

The chemisorption technique uses the principle of molecular adsorption on catalyst sites to retrieve information on metal dispersion, active surface area and size of

crystallites. The adsorption of a compound depends on the temperature, pressure, surface energy distribution and the surface area. For instance, the Temperature Programmed Reduction (TPR) consists of applying a temperature ramp under a flow of a reducing gas such as hydrogen. The gas stream is analysed with a Temperature Conductor Detector (TCD) which monitors the constituents of the stream. TPR allows the determination of the temperature at which the solid reduces and the different oxidative states of the catalyst. For example, an amorphous metal oxide might show different desorption peaks under the TPR since different structural phases are reduced at different temperature. The Temperature Programmed Oxidation (TPO) works in a similar manner although an oxidative gas is used such as oxygen with helium. The TPO is very effective in measuring the amount of carbon deposits or coking on a catalyst.

Pulse Chemisorption is used to determine the active surface area and percent metal dispersion. This characterisation technique involves the purging, in known specific doses or pulses, a binding or analytical gas onto a cleaned catalyst sample until the surface is saturated and no more adsorption can occur. The gas flow is monitored by the TCD and when few consecutive pulses contain the same amount of initially administrated gas, the catalyst surface is said to be saturated, i.e. a monolayer is formed on the catalyst surface. Usually the first few pulses show no or some analytical gas since most of it is bonds on the metal. The active metal surface area can be determined from the amount of gas adsorbed and from the molecular area of the adsorbed species. When the amount of metal incorporated on a catalyst is known, the metal dispersion can then be determined by the ratio of the number of active metal atoms to the total number of metal atoms in the

catalyst material. Figure 3.5) shows the Micromeritics Autochem II 2920 used for TPR and Pulse Chemisorption in this work.

**Figure 3.5)** Micromeritics Autochem II 2920.

For the Pt-Bi catalyst, the analytical gas used was carbon monoxide which binds associatively on platinum. The 1.27g sample catalyst was first purged with helium to remove any adsorbate at 363K for 10 minutes. The temperature was then lowered to 315K and the pulsing of carbon monoxide in a helium carrier flow of 50ml/min started. Figure 3.6) depicts the TCD response to successive and consistent in volume of carbon monoxide pulses.

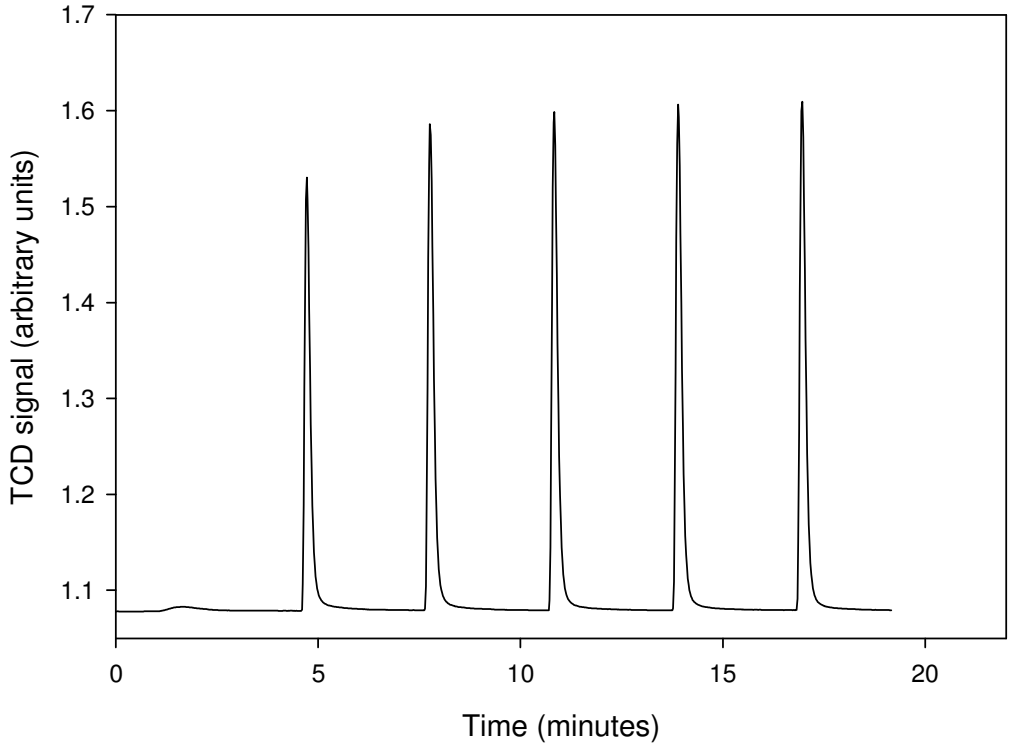


**Figure 3.6)** Pulse Chemisorption graph for the 5%Pt-1%Bi/Carbon.

The area of each peak can be integrated to determine the volume it represents. The first dose is almost completely adsorbed on the catalyst. The following doses show little and then no adsorption on the catalyst. Hence, the adsorbed volume on the catalyst can be determined by subtracting the total amount of volume injected and the total amount of volume detected. The data in Table 3.3) show the parameters used for the evaluation of Pulse Chemisorption data.

| Element | % Sample atomic weight | Stochiometric factor, F | Atomic cross-sectional area, $A_c$ (nm²) | Atomic weight | Cumulative Volume, $V_s$ (mL at STP) | Temperature (K) |
|---|---|---|---|---|---|---|
| Platinum | 5.0 | 1.0 | 0.08 | 195.08 | 0.3837 | 315 |

**Table 3.3**) Pulse Chemisorption data.

With the use of the data in Table 3.3), the percent metal dispersion (%D), metallic surface area and Active Particle Size can be determined from the following equations calculated by the software of the Micromeritics Autochem II 2920.

$$\%Dispersion = \left( \frac{V_s F}{22414 \times (\%loading) \times m} \right) M \qquad \text{Eq. 3.4.1}$$

$$Metallic\ Surface\ Area = \left( \frac{V_s}{22414m} \right) F A_c N_A \qquad \text{Eq. 3.4.2}$$

$$Active\ Particle\ Diameter = \left( \frac{6M}{\rho N_A A_c} \right) \text{ or,} \qquad \text{Eq. 3.4.3}$$

$Active\ Particle\ Diameter = 110/(\%D)$ for platinum (Farrauto and Bartholemew 1988)

The chemisorption is not recommended to be used for bimetallic catalyst samples such as Au-Pd/Titania since different metals have different binding energies and stochiometric factors for an analytical gas. However, for the Pt-Bi catalyst, the bismuth

does not bind to CO which allows the use of the Chemisorption technique (Hayden 1997).

### 3.4.2) X-Ray Diffraction (XRD)

The XRD is used to characterise the bulk of a crystal structure by diffraction of an X-ray beam as a function of the angle of the incident beam. The atomic planes of a crystal cause an incident beam of X-rays to be refracted at specific angles. This allows the identification of the structure when compared to a database of XRD patterns and the particle size from the width of the peaks. The XRD was performed in the Department of Chemistry at the University of Birmingham using a Siemens D5005 diffractometer with a monochromatic high intensity CuK$\alpha$ radiation with an angle varied between 10 and 140 degrees at a setting of 40kV and 40mA.

### 3.4.3) Scanning Electron Microscopy with Energy Dispersive X-ray (SEM-EDX)

The SEM focuses a scanning electron beam on a sample. The interaction between the electron and the atoms results in different beam emissions. Backscattering and a lower energy reflection allows the generation of a topographic image of the sample. The EDX bombards the compound with X-ray exciting the atom which in return emits a characteristic beam upon relaxation allowing its identification. The SEM-EDX was also performed in the Department of Chemistry at the University of Birmingham using a JEOL 1200CX2 with an accelerating voltage of 80keV.

# IV) HETEROGENEOUS OXIDATION OF 2-OCTANOL ON 5%Pt-1%Bi/CARBON

The 5%Pt-1%Bi/Carbon catalyst for the selective oxidation of alcohols has been intensely studied in the literature and is classified as one of the most efficient catalyst for such processes (Mallat, Bodnar *et al.* 1995; Kluytmans, Markusse *et al.* 2000; Lee A, J.J *et al.* 2000; Pinxt, Kuster *et al.* 2000). Conversely, limitations of this catalyst such as the deactivation, low oxidation activity and apolar medium poisoning of the catalyst have been reported by Keresszegi *et al.* (2004b) where they needed to work in a water-surfactant system to be able to oxidize aliphatic alcohols especially 2-octanol. Dimitratos *et al.* (2006) also reported a very low activity for the oxidation of octanol whether they tried supported platinum, palladium or gold where the maximum conversion in an organic solvent was 8% with 5% platinum. By working in an aqueous solvent they were able to increase conversion up to 45% but at the expense of selectivity towards the ketone since 34% of the products were carboxylic acids. This underlines the importance of finding the appropriate reaction conditions to keep a good balance between conversion

and selectivity. Therefore the aim of the work presented in this chapter is to investigate the reasons why this catalyst shows lower activity for 2-octanol oxidation compared with other alcohols, such as benzyl alcohol, and try to improve the catalyst life-time by preventing any deactivation.

An initial preliminary experiment was performed with a typical solvent such as heptane to demonstrate the low conversion with the platinum catalyst. The cause was then examined and a solution was investigated. The effect of various parameters such as temperature, solvent choice, pressure, initial alcohol concentration and catalyst loading were studied. A Langmuir-Hinshelwood model was investigated as well. The catalyst was characterized using CO pulse chemisorption.

### 4.1. Oxidation of 2-Octanol on 5%Pt-1%Bi/carbon in heptane.

Results are first reported for the reference experiment in order to provide a comparison with other data sets presented later in this chapter. The aim of the work was to optimise the experimental conditions so as to improve conversion of 2-octanol and yield of 2-octanone.

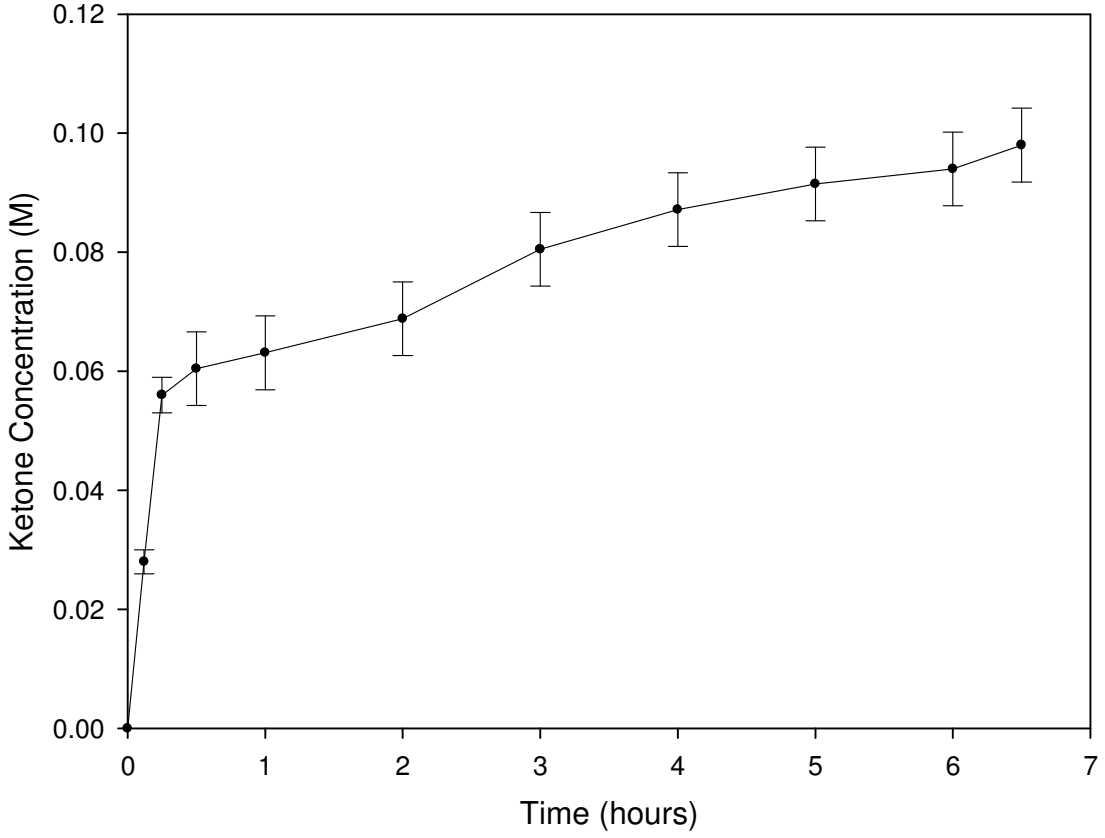


**Figure 4.1a)** Reference reaction: conversion of 2-Octanol versus time. *Reproduced 3 times. Reaction conditions: T=343.15 K;* $P_{Air}$ *=1 Bar;* $C_i$ *=0.248M; 3g cat; rps=22.5* $s^{-1}$ *; Flow=0.680L/min.*

By examining Figure 4.1a) it can be observed that there are two regimes during the alcohol oxidation. The first regime, where the catalyst is very active and the conversion reaches over 22% in 15 minutes and the second regime where the reaction rate dramatically decreases afterwards. Hence one of the aims of this work is to understand the reason why the reaction rates drops and if there can be a solution to keep the catalyst active for a prolonged period. Extending the catalyst lifetime would be essential for industrial production.

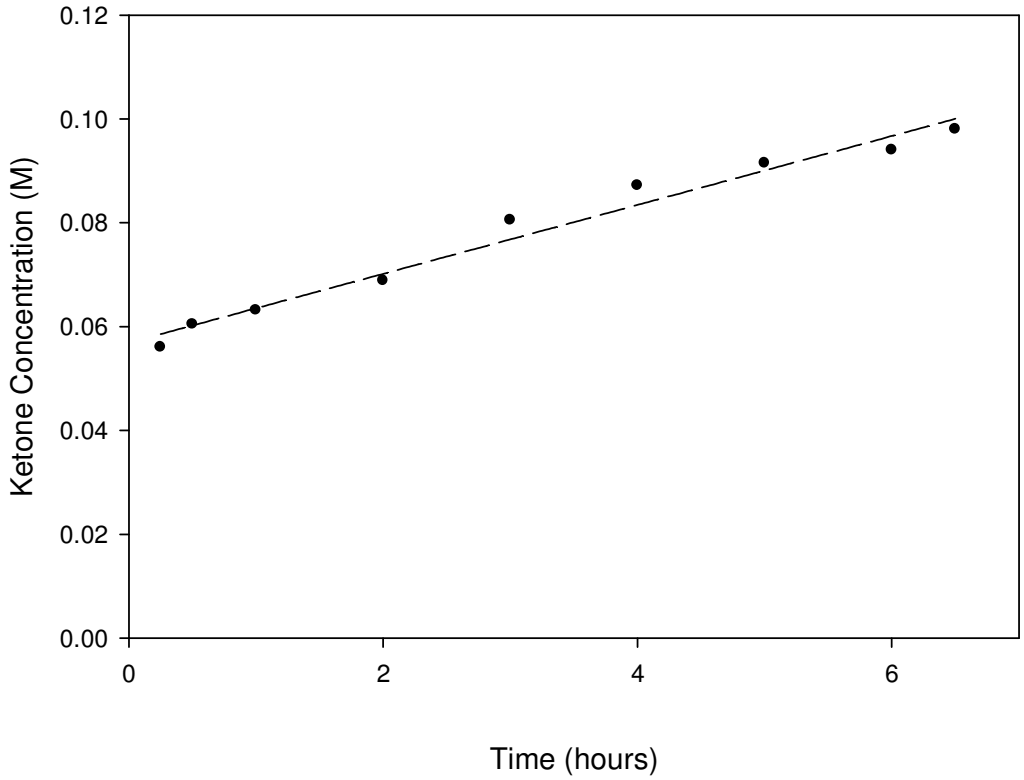


**Figure 4.1b)** 2nd Regime of the reference reaction- *Reaction conditions: T=343.15 K;* $P_{Air}$ *=1 Bar;* $C_i$ *=0.248M; 3g cat; rps=22.5* $s^{-1}$ *Flow=0.680L/min.*

Figure 4.1b) shows a straight line regressed to the data of the second rate regime. From the slope of the line the reaction rate was calculated to be 0.0065M/hr. This value is considerably lower than the initial reaction rate of 0.23M/hr corresponding to the initial fifteen minutes of the first regime.

## 4.2 Deactivation Causes

In order to determine which of the plausible 3 main reasons of catalyst deactivation, as described by Kluytmans *et al.* (2000), a series of testing experiments was undertaken. Possible causes of deactivation are a) noble metal over-oxidation, b) metal leaching/agglomeration and c) catalyst poisoning.

### 4.2.1) Noble metal over-oxidation

The investigation of the over-oxidation hypothesis consists of studying the effect of the air flow and reactor pressure on the catalyst performance. By limiting the amount of oxygen that can be adsorbed on the metal, the catalyst should last longer by avoiding over-oxidation even if it is at the expense of a slower reaction rate. Therefore, air was introduced to the reactor at atmospheric pressure and a flow of 500 ml/min for a duration of 5 minutes at intervals of 30 minutes. Kluytmans *et al* (2000) used a related periodic sparging method for his system for the oxidation of methyl-glucoside and were able to regenerate the initial reaction rate since his catalyst was being over-oxidized.

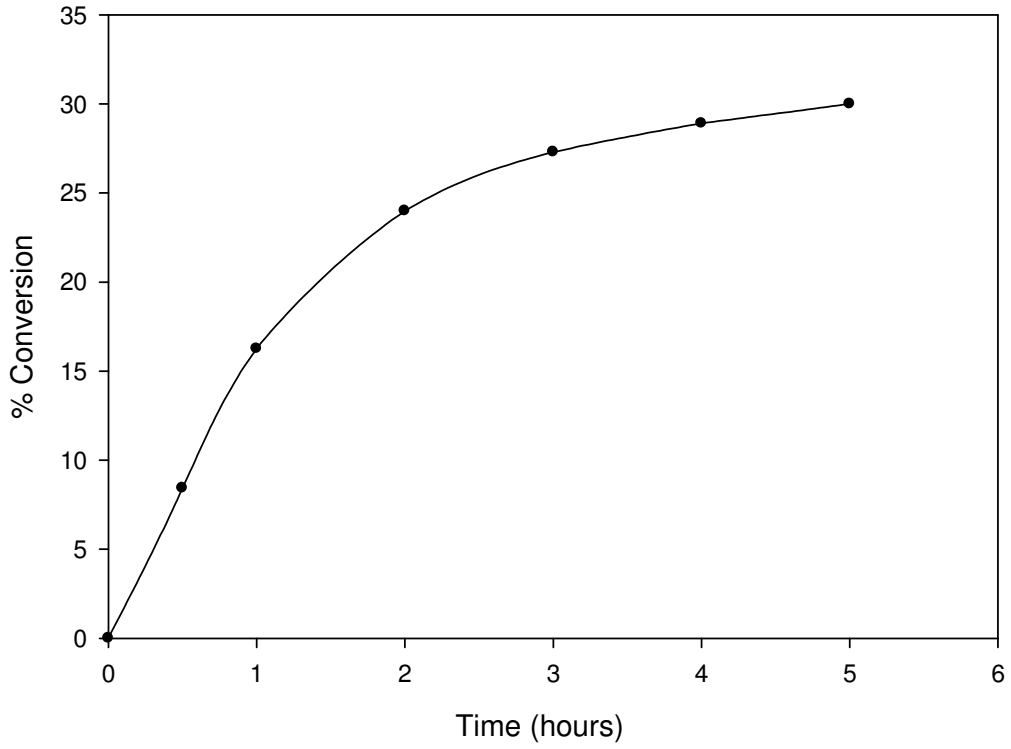


**Figure 4.2)** – Interrupted Flow: Conversion when purging air every 30 minutes for 5 minutes. *Reaction conditions: T=343.15 K;* $P_{Air}$ *=1 Bar;* $C_i$ *=0.248M; 3g cat; rps=22.5* $s^{-1}$

In this case, by interrupting the flow of air, the conversion appears to be slower than the continuous air flow reaction of the reference reaction as can be seen in Figure 4.2) and after two hours starts trailing which is a sign of catalyst deactivation.

4.2.2) Noble metal leaching/agglomeration

Catalyst that has been previously used, recovered and recycled should show a different behaviour to fresh catalyst if leaching or agglomeration of platinum particles occurs during the reaction. Therefore, used catalyst was prepared for recycling by

washing with acetone before mixing in a 1 M NaOH alkaline solution at 333K. The alkaline solution was replaced by water at the same temperature, and then hydrogen was bubbled through the flask to reduce the catalyst (Mallat and Baiker 1994). The conversion profile shows no difference compared with the one for a fresh catalyst which suggests that platinum leaching/agglomeration does not occur during this reaction.

4.2.3) Catalyst poisoning

The final likely cause of deactivation is catalyst poisoning. This occurrence may be due to strong adsorption of the reactant, product, an unwanted by-product or CO (Bond 1962; Clark and Rhodes 2000). Since the selectivity of the studied reaction is 100% at the working conditions the most likely adsorbent is either the alcohol or the ketone. The alcohol reacts on the surface of the catalyst to become a ketone which then can slow the reaction rate by desorbing gradually. The most straight forward way to verify that the ketone is in fact strongly adsorbing onto the catalyst is to immerse the catalyst in ketone and then use it without washing in an experimental reaction. If the conversion profile is still the same as the fresh catalyst this indicates that the ketone is not deactivating the catalyst. Figure 4.3) shows the conversion profile when the catalyst has first been immersed in ketone prior to the experiment.

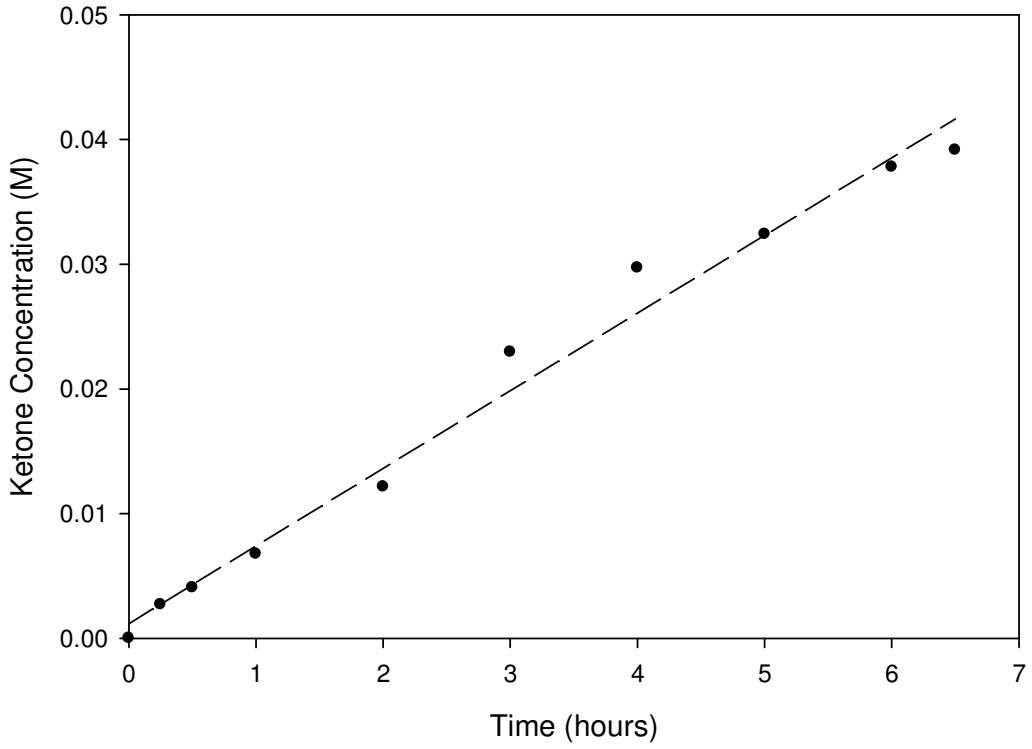


**Figure 4.3)** – Ketone Addition: Conversion when the catalyst is initially immersed for 15 minutes in 2-octanone. *Reaction conditions: T=343.15 K;* $P_{Air}$ *=1 Bar;* $C_i$ *=0.248M; 3g cat; rps=22.5* $s^{-1}$

Comparing to the reference reaction profile of Figure 4.1a), the reaction rate in Figure 4.3) is a reasonably straight line passing though the origin which does not display the two distinct regimes observed in the initial experiment. Moreover, the rate of conversion is almost identical to that of the second regime of the reference reaction profile. The observed reaction rate of 0.0062M/hr is similar to the second regime of the reference reaction (0.0065M/hr). Therefore, it was deduced that the presence of, or more precisely the slow rate of desorption of ketone from the catalyst surface is limiting the rate of conversion. Conversely the surface reaction is relatively fast during the initial

stage of the reaction since there is little or no ketone present to occupy the active sites of the catalyst as is demonstrated in Figure 4.1a). It is only when a significant amount of ketone is formed that the reaction rate dramatically changes to become constant. This is supported by the fact that when the catalyst was immersed in ketone its active sites became saturated with 2-octanone and this eliminated the fast initial reaction since there were no available active sites left for the alcohol to adsorb.

## 4.3 Measurement of quantity of adsorbed ketone.

Since 2-octanone is adsorbing onto the metal surface slowing the reaction rate it is necessary to have an estimate of the amount required to saturate a given amount of catalyst. Consequently, the evaluation of this value was performed in a lab scale setup.

### 4.3.1) Laboratory scale experimental setup

The lab scale setup consists of a 100ml three-necked round bottom flask positioned in contact with a heating and stirring plate. A magnetic stirrer was inserted inside the flask to stir the solution. A high efficiency Graham condenser was placed on the vertical opening of the flask while a mercury thermometer and a plastic air pipe were installed on the remaining openings. The air stream from a cylinder was controlled by a flow meter at a set-point of 200ml/min.

4.3.2) Octanone adsorption quantification

2-octanone was added every 10 minutes to a solution of 30mL of heptane and 0.3g of catalyst before a sample was taken for analysis in the lab scale experiment. The quantity of ketone on the catalyst surface was calculated from the difference between the known added amount of ketone and the concentration in the solution.

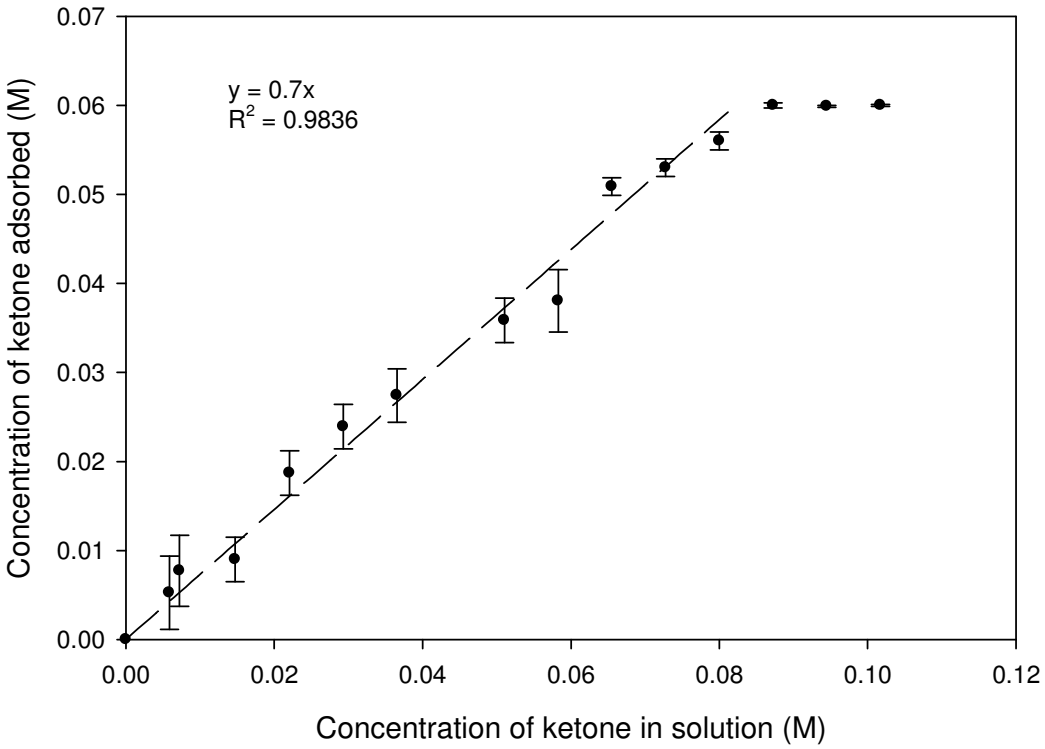


**Figure 4.4)** Saturation amount of ketone adsorbed on Pt-Bi/Carbon. *Reaction conditions: T=343.15 K; $P_{Air}$ =1 Bar; $C_i$ =0.248M; 0.3g cat.*

Figure 4.4) shows that the catalyst can adsorb a maximum ketone amount of 0.006moles/gram of catalyst. This result is surprising since it means that there is more ketone adsorbed than there is metal in the catalyst ($1.38\times10^{-4}$moles/gram), which may

suggest the ketone is adsorbed on the carbon support as well or that many layers are forming on the metal. The slope represents the adsorption constant, $K_4$, before saturation.

After samples are taken from the autoclave reactions, the concentrations of ketone and alcohol left in the solution were compared with the initial concentration added to the experiment. The difference in concentration from the mass balance gave the concentration of alcohol and ketone adsorbed on the catalyst surface. Different catalyst loadings were tested to validate the proportionality between the quantity of adsorbed 2-octanone and amount of catalyst. Figures 4.5a-c) show the ketone concentration in solution and adsorbed on the catalyst for different catalyst loadings.

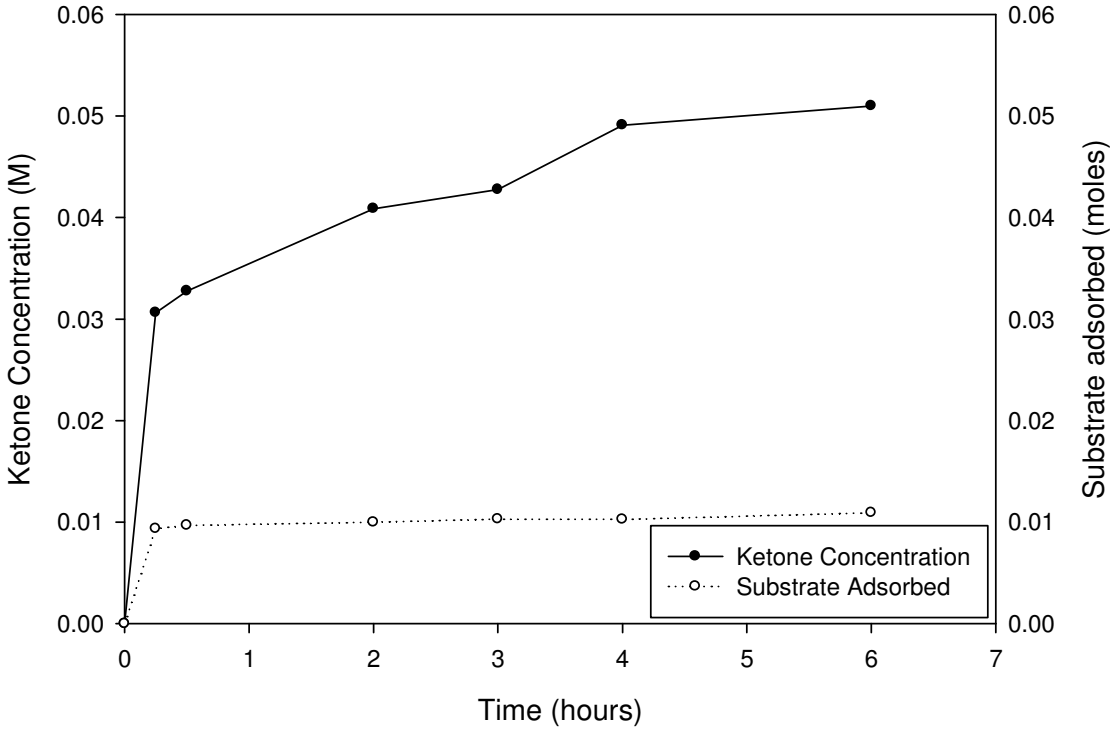


**Figure 4.5a)** 1.5g Pt-Bi/Carbon *Reaction conditions: T=343.15 K;* $P_{Air}$ *=1 Bar;* $C_i$ *=0.248M; 3g cat; rps=22.5* $s^{-1}$ *Flow=0.680L/min; solution volume=300mL*

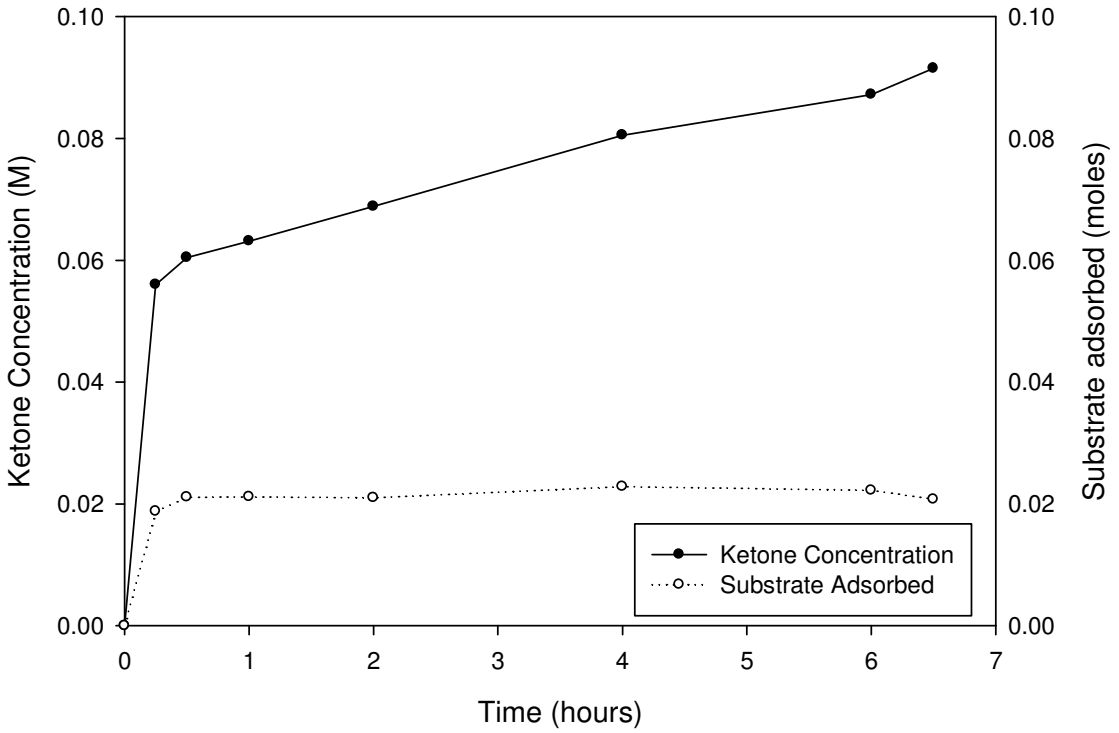


**Figure 4.5b)** 3.0g Pt-Bi/Carbon

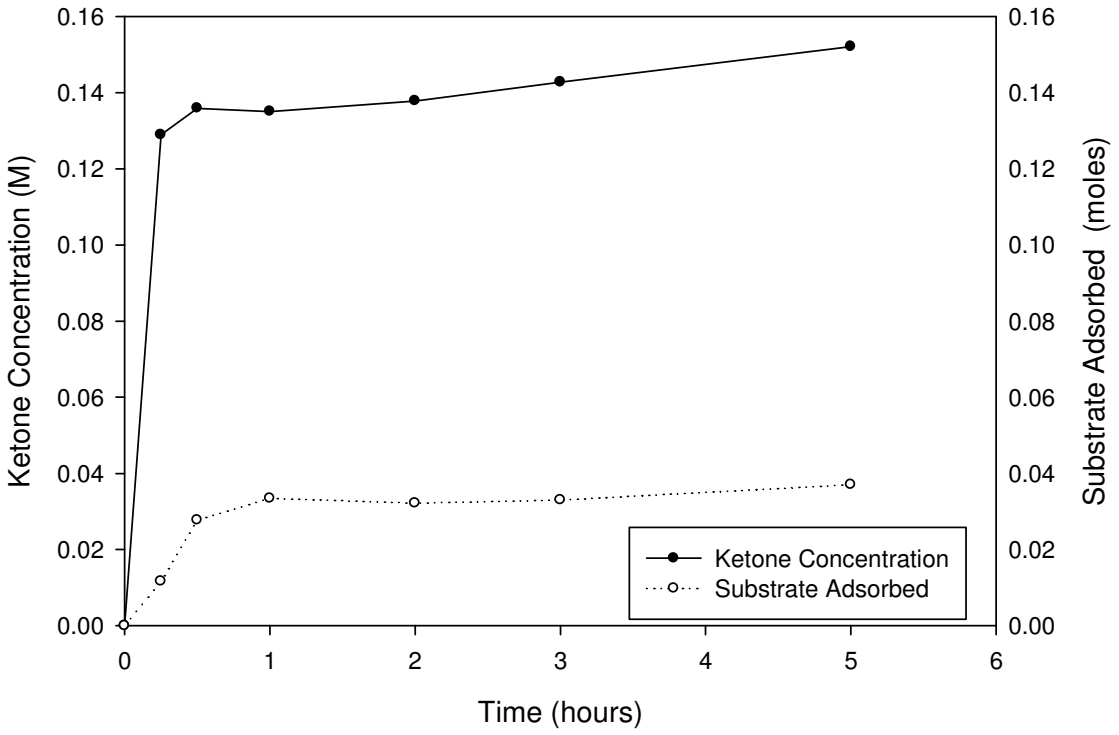


**Figure 4.5 c)** 6.0g Pt-Bi/Carbon

**Figures 4.5a-c)** Adsorption on different catalyst loading. *Reaction conditions: T=343.15 K;* $P_{Air}$ *=1 Bar;* $C_i$ *=0.248M; 3g cat; rps=22.5* $s^{-1}$ *Flow=0.680L/min; solution volume=300mL*

From the above figures it can be noticed that the reaction is very active at the beginning of the experiment where product adsorption is still low. As the catalyst loading is doubled, the amount of product adsorbed on the catalyst is doubled as well. Although increasing the quantity of catalyst appears to increase the conversion to ketone, the quantity adsorbed on the catalyst also increases. This would require the catalyst to be washed after the reaction and the collection of product adsorbed making the use of the catalyst uneconomical. It should be stressed that the amount adsorbed corresponds to this

specific batch of catalyst and depends on the method of preparation, water content, metal dispersion etc. Therefore each catalyst batch will adsorb a different amount of substrate. In order to evaluate the role of the support, a 5%Pt-1%Bi/$Al_2O_3$ was also tried with similar conditions as the one used in Figure 4.1a). Like with the carbon support, a deactivation was manifested after 15 minutes which eliminates the support effects in this case. Hence, a solvent was sought with a greater solubility of 2-octanone to reduce the amount of ketone adsorption upon the catalyst surface, which will enhance the ketone desorption and readily generate more available active sites.

## 4.4 Solvent effects

The aim of the work became focussed on finding a suitable solvent in which the ketone would be more soluble to allow a better desorption and a longer activity of the catalyst. The solvents that were considered beside heptane are p-xylene, DMSO and dioxane since they do not have a C=O group that would bind to platinum nor OH groups that can be oxidised and have an appropriate boiling point and vary in polarity.

### 4.4.1) DMSO

DMSO is very polar and has a higher dipole moment than water. However, the conversion was negligible even after 6 hours of reaction since the reactant did not adsorb on the surface making this solvent inappropriate. When the catalyst was added to this solvent it bonds strongly to it (Zelenay and Sobkowski 1984). DMSO binds even more

than the ketone on the catalyst given that when a lab scale reaction similar to the one shown in Figure 4.4) was performed and ketone is added and measured in the solution there was no ketone adsorption whatsoever on the catalyst.

### 4.4.2) P-xylene

The reaction profiles still showed two distinctive reaction regimes where the first one corresponds to 17% conversion after 15 minutes and then the reaction slows down abruptly and becomes constant as is shown in Table 4.1). Replacing heptane with p-xylene that contains a conjugated ring did in fact decrease the performance of the reaction without eliminating the ketone desorption effect. The lower reaction rate might be due to the lower oxygen solubility in p-xylene (Battino, Rettich *et al.* 1983).

### 4.4.3) Dioxane

Oxygen has a very low solubility in dioxane (Battino, Rettich *et al.* 1983). This can partly explain why the oxidation of 2-octanol is slow in it. Another reason is that the ketone was not removed from the catalyst surface since the slower reaction rate of the second regime corresponding to ketone adsorption was exhibited as well.

| Solvent | $O_2$ ($\times 10^{-4}$) fraction solubility at 298K[a] | Dielectric Constant at 298K | Dipole moment at 298K (D) | Initial reaction rate (M/hr) | Comments |
|---|---|---|---|---|---|
| *DMSO* | 1.5 | 47.2 | 3.96 | 0.005 | -No substrate adsorption |
| *P-Xylene* | 9.2 | 2.2 | 0.0 | 0.18 | -Substrate adsorbs |
| *Heptane* | 22 | 1.9 | 0.0 | 0.23 | -Substrate adsorbs |
| *Dioxane* | 5.3 | 2.2 | 0.45 | 0.027 | -Substrate adsorbs |

**Table 4.1** – Solvent characteristics and effects on initial reaction rates. [a] Battino, R *et al.* (1983). *Reaction conditions: T=343.15 K;* $P_{Air}$ *=1 Bar;* $C_i$ *=0.248M; 3g cat; rps=22.5* $s^{-1}$ *Flow=0.680L/min.*

4.4.4) Dioxane/heptane

The reactions carried out in DMSO, p-xylene and dioxane show that neither polar nor non-polar solvents were able to remove effectively the substrates from the catalyst surface. 2-Octanone has a long carbon chain giving it a lipophilic character but at the same time the C=O bond exhibits polar properties responsible for the bonding to the metal. Therefore different mixtures of dioxane and heptane were tried as solvents (Korovchenko, Donze *et al.* 2007). Donze *et al* (2007) found that changing the solvent made it possible to tune the product distribution and modify the rate of reaction of benzyl alcohol oxidation using dioxane and dioxane/water mixtures.

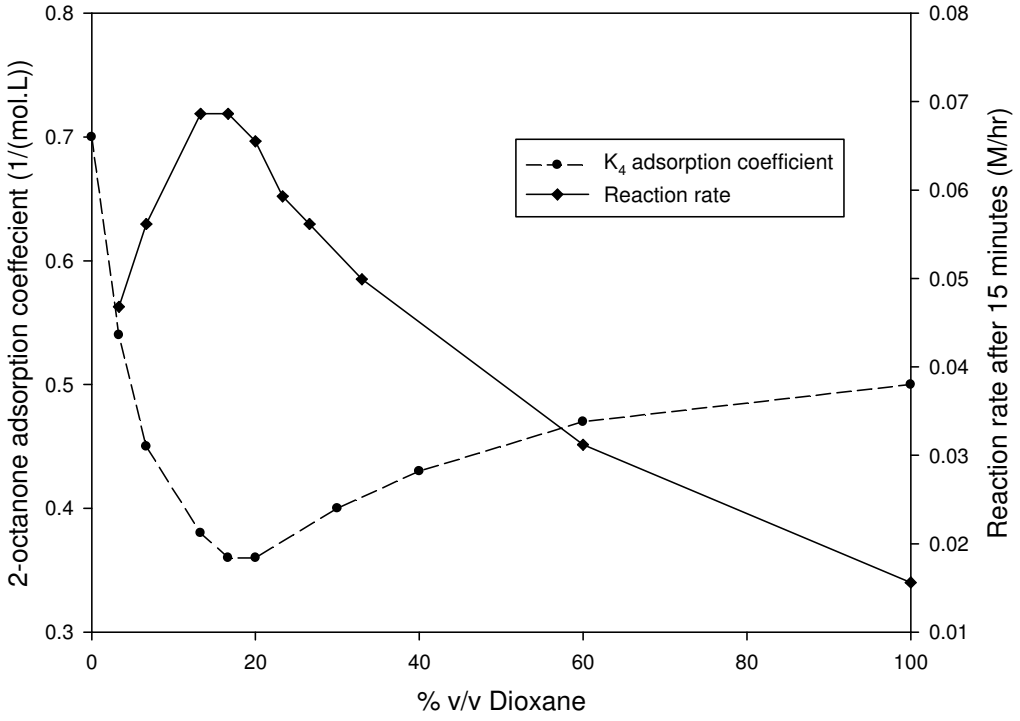


**Figure 4.6)** Effects of solvent composition upon reaction rate and ketone adsorption coefficient. *Reaction conditions: T=343.15 K;* $P_{Air}$ *=1 Bar;* $C_i$ *=0.248M; 0.3g cat.*

Figure 4.6) shows that the reaction rate passes through a maximum at 16-18% v/v dioxane. This corresponds to a minimum in the adsorption coefficient of ketone, $K_{4,}$ which can be calculated from the slope in a similar way to that in Figure 4.4) before saturation of the catalyst. The maximum reaction rate occurs when the lowest amount of ketone is adsorbed on the surface of the catalyst, such that the catalyst surface can allow adsorption of octanol reactant. However it should be stressed that the oxygen solubility will also change with the different dioxane concentration and that also affects the reaction rate. On the other hand, the change in oxygen solubility cannot explain the difference in reaction rates throughout the different solvent compositions, since a change of pressure

has no similar impact as will be discussed later in Section 4.7. This shows how the solvent can affect the reaction in different ways other than the gaseous reactant solubility in it but also by the interaction with the liquid reactant and product. Bond (1962) also suggested that there is an inverse relationship between catalytic activity and the bonding strength of the reactants.

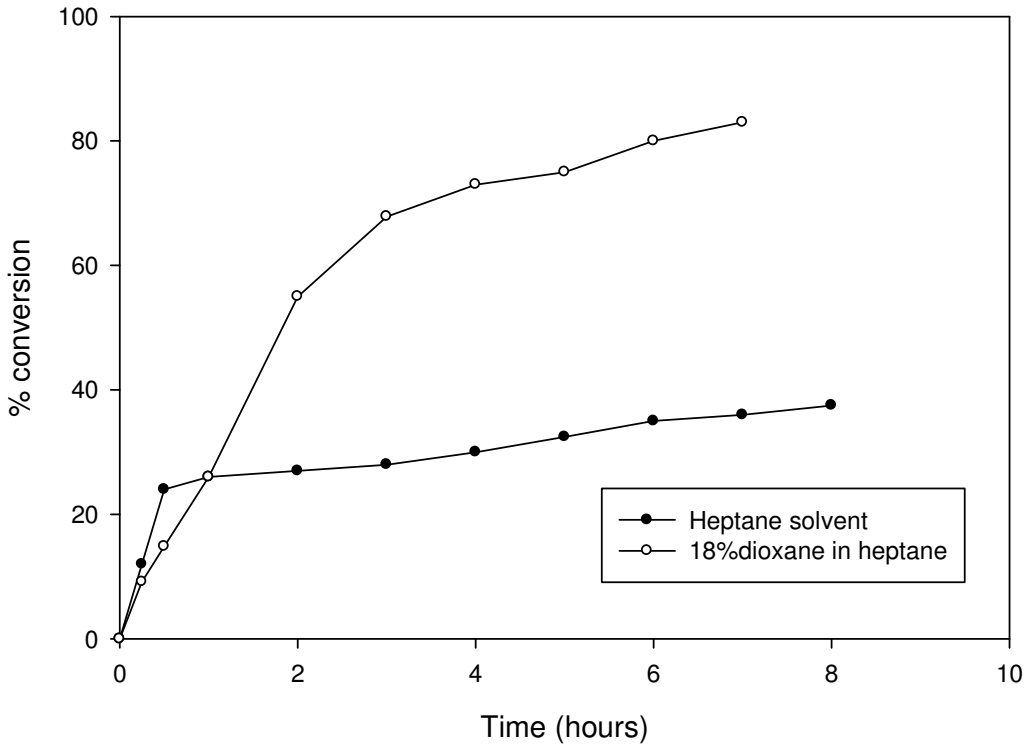


**Figure 4.7)** Conversion of 2-octanol in heptane and in dioxane-heptane mixture. *Reaction conditions: T=343.15 K;* $P_{Air}$ *=1 Bar;* $C_i$ *=0.248M; rps=22.5* $s^{-1}$

Referring to Figure 4.7), the initial lower conversion rate of the solvent mixture can be explained by the lower adsorption coefficient of the substrate on the catalyst due to its better solubility in the solvent mixture. But since the product adsorbs less strongly

in the dioxane/heptane mixture on the catalyst, the rate of conversion does not slow down contrary to what happens in the heptane solvent. Hardacre *et al.* (2005) found that the use of an ionic liquid organic solvent such as 1-butyl-3-methyl-imidazolium *bis*-(trifluoromethylsulphonyl) imide for the oxidation of cinnamyl alcohol decreases the activity compared to toluene although the selectivity increases. The oxidation had a lower activity rate in the ionic organic solvent which explains why the selectivity was higher than in toluene since an oxidized molecule did not undergo further oxidation. This is an example of how the selectivity (or catalyst longevity in this work) can be enhanced whilst decreasing the initial reaction rate.

| Solvent / Reactant | Heptane | | 18% v/v Dioxane-Heptane | |
|---|---|---|---|---|
| | Initial reaction rate (M/hr) | Reaction rate after 15 min (M/hr) | Initial reaction rate (M/hr) | Reaction rate after 15 min (M/hr) |
| 2-Octanol | 0.23 | 0.0062 | 0.07 | 0.07 |
| 1-Octanol | 0.25 | 0.0065 | 0.08 | 0.08 |
| Benzyl alcohol* | 1.0 | 1.0 | 0.8 | 0.8 |

**Table 4.2)** Solvent effects on initial rate for different alcohols. *Reaction conditions: T=343.15 K;* $P_{Air}$ *=1 Bar; rps=22.5* $s^{-1}$*; 3g catalyst;* $C_i$ *=0.248M; * Solvent free.*

Table 4.2) shows the effects of using 18% v/v dioxane-heptane mixture on the oxidation of different substrates. While the use of a mixed dioxane/heptane solvent improves the oxidation of aliphatic primary and secondary alcohols it decreases the reaction rate of benzyl alcohol oxidation. Benzyl alcohol did not adsorb strongly onto the

catalyst hence decreasing the rate of reactant adsorption will not increase the reaction rate.

### 4.5 Internal Mass Transfer

For an efficient use of a catalyst particle, the reactant would diffuse throughout the particle since the fraction of active sites on the external surface is negligible (Kapteijn, Marin *et al.* 1999). In order to determine whether the reaction is limited by internal mass transfer the Wagner-Weisz-Wheeler modulus $M_W$ was calculated since it depends on experimental observables and was assumed to be first order since Weisz and Prater (1954) confirmed that deviation from first order kinetics will have negligible effects on the criterion.

$$M_W = L^2 \frac{(-r_V / C_A)_{\exp}}{D_{eff}} \quad \text{(Levenspiel 1999)} \qquad \text{Eq. 4.5.1}$$

Where $L$ is the characteristic size of a catalyst particle equal to $\frac{R}{3}$ for spheres. $r_V$ is the observed reaction rate per unit of volume of catalyst particles, $C_A$ is the initial concentration of reactants and $D_{eff}$ is the effective diffusivity defined as:

$$D_{eff} = \frac{\varepsilon_P D_{AB}}{\tau_P} \text{ where}$$

$$\frac{1}{D_{AB}} = \frac{1}{D_m} + \frac{1}{D_K}$$

and $\varepsilon_P$ is the porosity of the catalyst, $\tau_P$ is the tortuosity, $D_m$ is the molecular diffusivity and $D_K$ is the Knudsen diffusivity. The Knudsen diffusivity is only applicable to gases (Satterfield 1991) and here it assumed that the reacting oxygen is in soluble form therefore $D_{AB} = D_m$. The effective diffusivity is calculated with the average values of porosity and tortuosity of 0.4 and 4 respectively (Winterbottom and King 1999) and gave a value of $1.61\times10^{-8}$ $m^2/s$ for oxygen and $1.33\times10^{-9}$ $m^2/s$ for 2-octanol at 343K. This gives a $M_W$ value of $8.63\times10^{-3}$ and $2.77\times10^{-4}$ for oxygen and 2-octanol respectively. Both these values are much lower than 0.15 which is the Weisz-Prater (Levenspiel 1999) criterion for a diffusion free regime. Hence it can be deduced that the reaction happens throughout the catalyst particle. A sample calculation can be found in Appendix B.

### 4.6 Temperature effects and Arrhenius plot

Increasing temperature usually increases the activity of the catalyst at the expense of selectivity while carrying out the reaction at room temperature may cause catalyst poisoning by substrate adsorption (Mallat and Baiker 1994). Therefore it is not the best way to optimise conversion. In the case of oxidation of a secondary alcohol such as 2-octanol, the formation of another by-product is unlikely since further oxidation would require breaking C-C bonds. Nonetheless the investigation of the activation energy was performed over the temperature range from 323K to 353K at atmospheric pressure and

0.248M initial alcohol concentration. Initially the reaction rate proceeds according to a pseudo-first order which allows the determination of the activation energy through the Arrhenius plot.

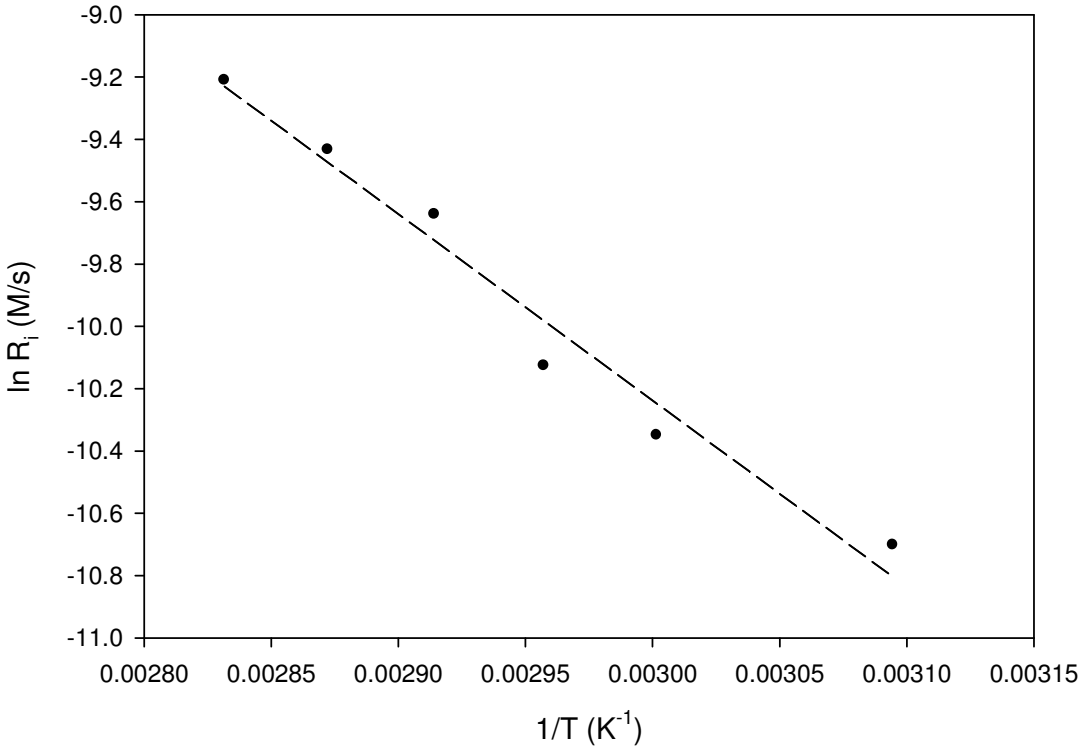


**Figure 4.8)** Arrhenius Plot for the determination of the activation energy. *Reaction conditions:* $P_{Air}$ *=1 Bar;* $C_i$ *=0.248M; rps=22.5* $s^{-1}$ *; 3g cat*

The apparent activation energy is deduced from the slope of Figure 4.8) where the best fit straight line represents $\frac{-E_a}{R}$. Hence the activation energy $E_a$ is equal to -49.8 $kJ.mol^{-1}$. Since in the previous section the internal mass transfer was calculated to be negligible then the observed activation energy is the true activation energy (Fogler 2001; Nijhuis, Dautzenberg *et al.* 2003). A low activation energy value means the

system is under mass transfer limitation and a high one means the reaction is performed in the kinetic regime and is very sensitive to the temperature.

### 4.7 Effect of pressure

The effects of oxygen pressure on the catalyst deactivation and the reaction have been extensively studied in the literature (Mallat and Baiker 1994; Kluytmans, Markusse *et al.* 2000; Keresszegi, Bürgi *et al.* 2002; Gangwal, Schaaf *et al.* 2004). Chemisorbed oxygen can further react on the surface of the catalyst to form an oxide that corrodes the metal and hence deactivates it. The alcohol, being a weak reducing agent, cannot remove the oxide from the metal which decreases the activity of the catalyst. The efficiency of the catalyst can be regained with a stream of hydrogen for example. Since in this work the deactivation of the catalyst is being investigated due to product adsorption, the experiments were completed at low oxygen pressure to eliminate any over-oxidation possibility that would mask the product adsorption effects.

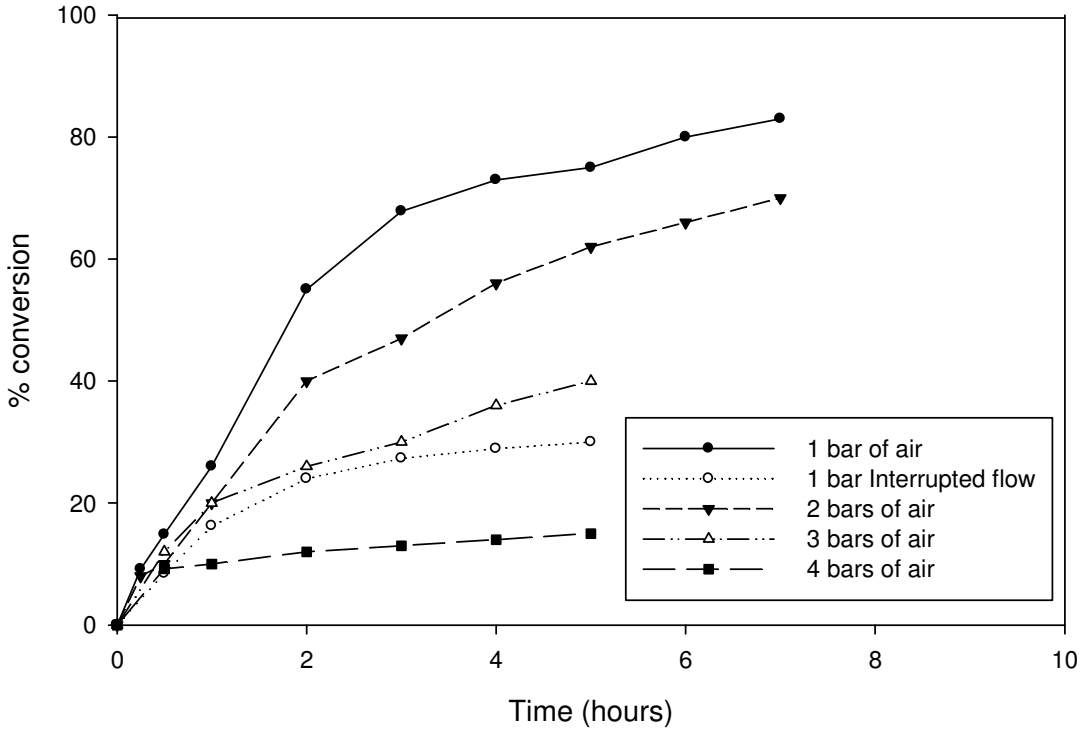


**Figure 4.9)** Pressure Effect. *Reaction mixture conditions: T=343.15 K; $C_i$=0.248M; rps=22.5 $s^{-1}$; 3g cat*

From Figure 4.9) it is apparent that an increase in air pressure reduces the conversion from the maximum value obtained at atmospheric pressure. These observations have been witnessed by many researchers including Gallezot (1997) and Gangwa *et al.* (2004). At higher oxygen pressure the catalyst tends to become over-oxidised meaning that the oxygen occupies active sites preventing the adsorption of liquid reactant. The rate of oxygen coverage of the metal surface will be faster than the rate of oxygen consumption. One way to demonstrate the over-oxidation effect is to plot the conversion with the amount of product adsorbed on the catalyst.

Figure 4.10) shows the production of ketone under 4 bar of air pressure, where the final concentration of ketone after 5 hours is 0.035M. Comparing with Figure 4.5b),

under the same conditions except 1 bar of air pressure, after 5 hours the ketone concentration is 0.085M. Clearly increasing the pressure leads to a decrease of conversion of ketone.

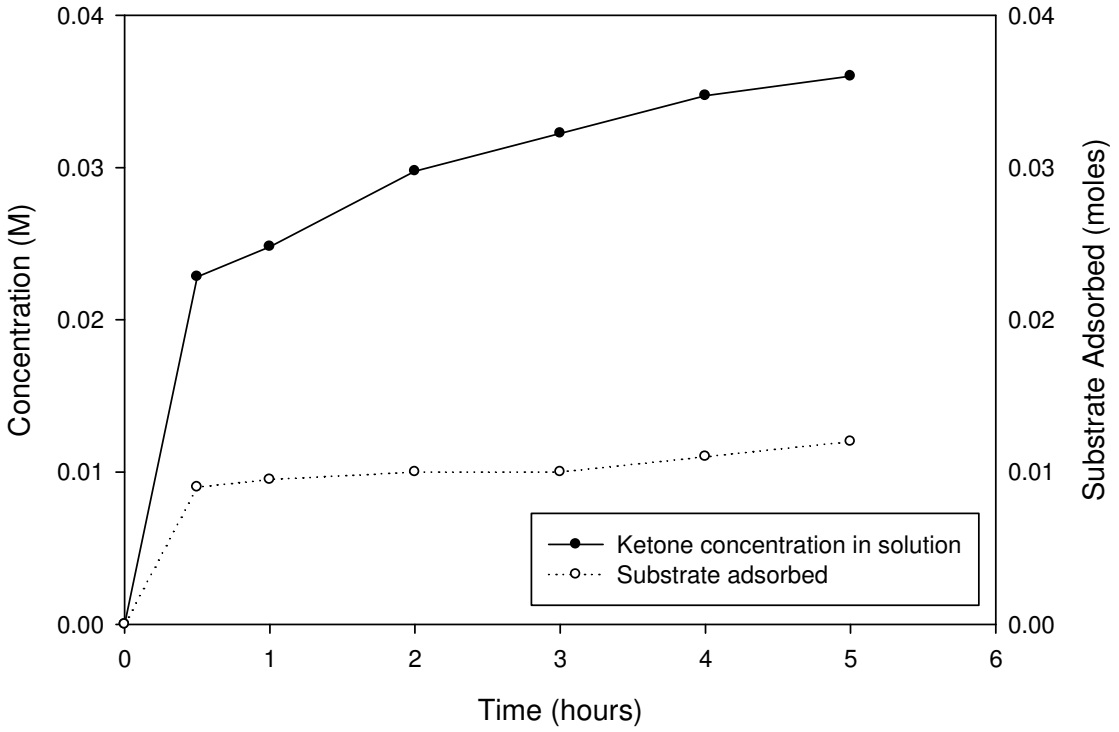


**Figure 4.10)** Conversion at 4 bars air pressure. *Reaction mixture conditions: T=343.15 K;* $P_{Air}$ *=4 Bar;* $C_i$ *=0.248M; rps=22.5* $s^{-1}$ *; 3g cat.*

A possible explanation is that the increase in oxygen pressure may have increased the oxygen concentration in the solution, therefore blocking active sites which explains the low concentration of adsorbed ketone. On the other hand when the air flow is interrupted the conversion also decreases given that not enough oxygen is present on the catalyst surface to oxidise the reactant as was observed also by Gallezot (1997). These results

suggest that there is an optimum range of oxygen concentration at which to carry out the reaction, ensuring sufficient oxygen needed by the reaction whilst preventing over-oxidation from occurring. All further experiments were carried out at atmospheric conditions as this gave the best conversion.

### 4.8 Measurement of Mass Transfer Coefficients

Because two reactants, oxygen and 2-octanol, are involved in the production of 2-octanone, either of these reagents could limit the rate of diffusion to the active sites. While the concentration of alcohol is much higher than oxygen, it is still essential to calculate the solid-liquid mass transfer coefficient $k_{SL}$ for both reactants to determine which resistance is limiting the reaction. The measurements of the different resistances $r_r, r_c$ and $r_b$ which correspond to the internal reaction, solid-liquid and gas-liquid respectively can be determined experimentally by plotting the inverse of the reaction rate versus the inverse of the catalyst loading.

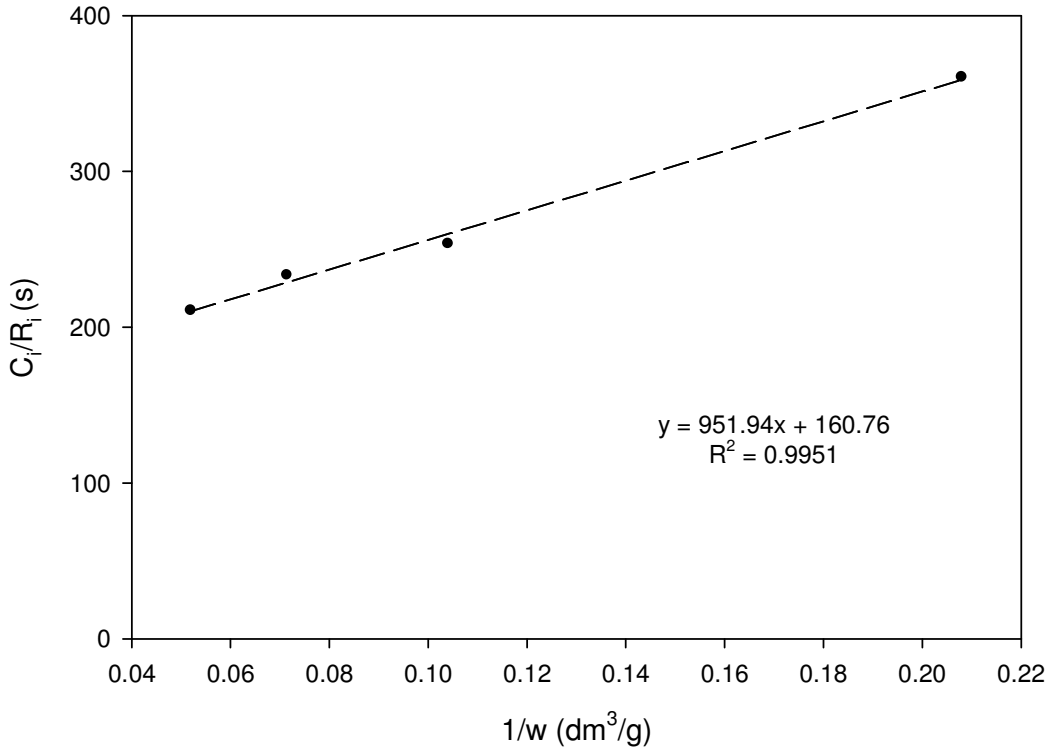


**Figure 4.11)** Solid-Liquid and Gas-Liquid mass transfer resistances for Oxygen. *Reaction mixture conditions: T=343.15 K;* $P_{Air}$ *=1 Bar; rps=22.5* $s^{-1}$

Based on the theory presented in section 2.6) the following resistances were deduced from the intercept and slope of Figure 4.11):

$$Intercept = r_b = \frac{1}{k_{GL}a_b} = 160.76\,\mathrm{s}$$

$$Slope = r_c + r_r = \frac{1}{k_{SL}a_P} + \frac{1}{\eta k} = 951.86\ gs/dm^3$$

It can be seen from Figure 4.11) that the intercept has a relatively large value, which indicates significant gas-liquid mass transfer limitation.

4.8.1) Solid-Liquid Mass Transfer

The solid-liquid mass transfer coefficient $k_{SL}$ for dissolved oxygen and 2-octanol was calculated using the following correlations in Table 4.3):

| Correlation | Author | $k_{SL}$ for dissolved $O_2$ (m/s) |
|---|---|---|
| $Sh = 2 + 0.60\,\mathrm{Re}^{0.5}\,Sc^{1/3}$ | (Fogler 2001) | $1.65\times10^{-3}$ |
| $Sh = 2 + 0.52\,\mathrm{Re}^{0.52}\,Sc^{1/3}$ | (Armenante and Kirwan 1989) | $1.56\times10^{-3}$ |
| $Sh = 2 + 0.4\,\mathrm{Re}^{1/4}\,Sc^{1/3}$ | (Kluytmans, Markusse *et al.* 2000) | $1.57\times10^{-3}$ |
| $k_{SL} = 1.19\times10^{-3}\left(\frac{N}{N_{sg}}\right)^{1.15}(Sc)^{-0.47}$ | (Kushalkar and Pangarkar 1994) | $7.22\times10^{-4}$ |

**Table 4.3)** Estimated liquid solid mass transfer coefficients over the Pt-Bi catalyst at 343K using different correlations.

The semi-empirical equation proposed by Kushalkar and Pangarkar (1994) was used in the rest of the chapter since it takes into effect the presence of gas bubbling and therefore, offers a more realistic value to the experimental setup used in this work. Consequently $r_r$ can be determined as well from the slope of Figure 4.10) and the limiting resistance for the oxidation reaction can be established. A sample calculation can be found in Appendix A.

| $k_{SL}$ for dissolved $O_2$ (m/s) | $k_{SL}$ for 2-octanol (m/s) | $a_P$ $(m^2/kg)$ | $r_c = \frac{1}{k_{SL}a_P}$ dissolved $O_2$ $(kgcat.s/m^3)$ | $r_r = \frac{1}{\eta k}$ dissolved $O_2$ $(kgcat.s/m^3)$ | $r_b = \frac{1}{k_{GL}a_b}$ (s) |
|---|---|---|---|---|---|
| $7.22\times10^{-4}$ | $1.35\times10^{-4}$ | 98.28 | 18.26 | 937.86 | 160.76 |

**Table 4.4)** Estimated mass transfer resistances over the Pt-Bi catalyst at 343K and atmospheric pressure from Figure 4.10) and Table 4.3).

From Table 4.4) it is observed that oxygen and octanol have similar values for the solid-liquid transport coefficient. However the bulk concentration of those two components in the solution is very different. While the initial concentration of alcohol is 0.248M the calculated oxygen concentration is much less as calculated below.

4.8.2) Determination of Mass Transfer Coefficients

It is very difficult to estimate the oxygen solubility in a mixed organic solvent. Even commercial oxygen probes are usually only suitable for water at low temperature. Consequently the maximum oxygen solubility was determined by assuming that the two solvents do not affect each other. Therefore based on the mole fraction of each solvent an average oxygen concentration equal to $2.8\times10^{-3}$ M was be calculated using the correlations by Battino *et al.* (1983) for each solvent. Thus it can be understood that the transport of oxygen limits the reaction rate since its concentration is much lower than the concentration of alcohol.

Oxygen has to diffuse through the gas film and into the bulk liquid where it has to be transported to the catalyst walls and then diffuse internally and react on the catalyst. These steps are described in Fogler (2001) in 5 points:

I. Oxygen dissolves from the gas phase into the liquid phase.

II. Transport from the gas-liquid surface into the bulk of solution.

III. Diffusion from the liquid bulk towards the catalyst surface.

IV. Diffusion internally in the pores of the catalyst.

V. Reaction on the catalyst.

From Figure 4.11) it is observed that the resistance from gas to liquid is considerable and is decreasing the oxygen concentration in the liquid bulk. $k_{GL}a_b$ has a value of $6.22\times10^{-3}\,s^{-1}$ determined experimentally from the intercept of Figure 4.10). However Kawase *et al.* (1997) developed a semi-empirical correlation to evaluate $k_{GL}a_b$ in three phase stirred tanks taking into effect the presence of solid particles.

$$k_{GL}a_b = C'\sqrt{D_{AB}}\,\frac{\overline{\rho}_l^{3/5}\,\varepsilon^{(9+4n)/10(1+n)}}{\left(\overline{K}/\overline{\rho}_l\right)^{1/2(1+n)}\sigma^{3/5}}\left(\frac{U_g}{U_t}\right)^{1/2}\left(\frac{\overline{\mu}_a}{\overline{\mu}_w}\right)^{-0.25} \qquad \text{Eq. 4.8.1}$$

Using this correlation the resistance to gas absorption was found to be $8.13\times10^{-3}\,s^{-1}$ which is of similar order of magnitude to the experimentally derived value.

The difference between the experimental value and the semi-empirical calculation may be due to the approximate estimations used in the calculation of bubble size $a_b$, bubble free rise velocity $U_t$ and the dissipation energy $\varepsilon$.

The gas absorbance can be increased by increasing the stirring rate or by installing a gas sparger that would decrease the bubble size and hence increase the bubble surface area. On the other hand in order to eliminate the possibilities of having over-oxidation that would mask the solvent effects, the system was kept under gas-liquid mass transfer limited regime. Hardacre *et al.* (2005) also worked in the mass transfer limited regimes in order to improve the selectivity by preventing the cinnamyl alcohol from being re-oxidised again. Therefore, reaching a kinetic regime in a reaction is not always an advantage. For that reason, assuming that the gas-liquid interface at the bubble surface is saturated with oxygen ($C_i$), the concentration in the liquid phase ($C_B$) following the mass transfer limitation would be equal to:

$$C_B = C_i - \frac{R_A}{k_B a_B}$$

$R_A$ being the initial reaction rate of an experiment. Assuming that the equilibrium oxygen concentration $C_i$ is $2.8\times10^{-3}$ M for a reaction at 343K and 0.248M of alcohol the oxygen concentration in the liquid bulk $C_B$ will be $1.03\times10^{-3}$ M, which is considerably lower than the concentration at the gas-liquid interface.

In steps II) and III) the transport from the exterior bubble surface to the catalyst surface $k_{SL}a_P$ depends on the concentration of the reactant, the particle surface area and

the stirring rate. In order to determine whether the liquid-solid mass transfer is limiting the reaction the concentration of oxygen on the catalyst surface has to be compared to the one in the bulk solution.

$$C_S = C_B - \frac{R_A}{k_{SL} a_P m}$$

Assuming the oxygen concentration in the liquid bulk $C_B$ at 343K and 0.248M alcohol concentration is $1.03\times10^{-3}$ M the calculated concentration on the catalyst surface $C_S$ is $1.00\times10^{-3}$ M. This means that the liquid-solid mass transfer is negligible and that the concentration of oxygen on the catalyst surface is almost equal to the value in the bulk solution.

Referring to steps IV) and V), the internal diffusion has already been determined to be negligible from the Weisz-Prater criterion. Therefore the reaction happens throughout the catalyst particle. Although from Table 4.3) it seems that $r_r$ is very large hence, step V) which is the resistance to reaction is a limiting step and it can be overcome by increasing the temperature (as can be seen from Figure 4.8), the amount of catalyst (as can be seen from Figure 4.11) and reactant concentration (as can be seen from Figure 4.12).

In conclusion, it appears that gas-liquid resistance is significant; however, a further increase in oxygen concentration decreases the reaction rate since oxygen binds strongly to the metal occupying active sites as is shown in Figure 4.9). It is therefore advantageous to work in such a regime as proposed also by Keresszegi *et al.* (2004b).

## 4.9 Langmuir-Hinshelwood Kinetic Model

The Langmuir-Hinshelwood (L-H) mechanism is one of the most commonly used models to describe heterogeneous catalysis since it takes into accounts the phenomenon of substrate/product adsorption and desorption. This is strongly exhibited in this study by witnessing how the ketone adsorption limits the reaction and how by decreasing the adsorption coefficient of ketone over the catalyst the reaction rate increases. Hence the L-H approach is followed here in order to model the reaction.

For the oxidation of alcohol over noble metals the details of the mechanism are still debated (Mallat and Baiker 1994; Gallezot 1997) but a general agreement exists on the following oxidative dehydrogenation mechanism assuming the oxygen dissociates on the metal (Schuurman, Kuster *et al.* 1992; Keresszegi, Ferri *et al.* 2005):

I) $A + * \xleftrightarrow{K_1} A*$

II) $O_2 + 2* \xleftrightarrow{K_2} 2O*$

III) $O* + A* \xrightarrow{k_3} P* + * + H_2O$

IV) $P* \xleftrightarrow{1/K_4} P + *$

Where A is the alcohol substrate, P is the ketone product and * denotes an active site on the catalyst. $K_1 = k_1 / k_{-1}$, $K_2 = k_2 / k_{-2}$, $K_4 = k_4 / k_{-4}$, are the equilibrium constants for the forward and reverse reactions of step I), II) and IV) respectively. Step III) is irreversible with $k_3$ as the rate constant.

While it was calculated that there was a significant transport limitation of oxygen to the catalyst, the reaction rate can be increased by changing the initial concentration of 2-octanol. Shuurman (1992) found that for the oxidation of glucoside on Pt/C, the reaction rate increases with an increase of glucoside concentration until a certain saturation value where the rate is not affected by further alcohol addition. By increasing the concentration of the alcohol reactant the active sites will be replenished more readily with this reactant hence a faster reaction rate. This allows the dependence of the reaction rate on the initial alcohol concentration to be determined.

Six likely mechanisms were considered and studied in Table 4.5). Models A) and B) are based on the model proposed by Shuurman (1992) and assume that the reaction is surface controlled and the oxygen dissociates on the metal surface, although in A) ketone is still assumed to adsorb noticeably on the metal while in B) there is no significant ketone adsorption. Models C) and D) presume that it is respectively the alcohol and the oxygen adsorption that controls the reaction while the surface reaction is fast. While model E) supposes that the reaction is surface controlled but that the oxygen adsorbs as a diatom on a single site without dissociation. Model F) considers that ketone desorption limits the reaction rate since this is what happens when the solvent is heptane. Finally model G) is based on Van den Tillaart *et al.* (1994), where they assume that the alcohol adsorbs dissociatively and oxygen chemisorbs irreversibly.

In order to determine which of the plausible Langmuir-Hinshelwood mechanisms describes best the catalysis, the "solver" function in Excel was used to estimate the kinetic parameters such as $K_1$, $K_2$ and $k_3$. After introducing the different model equations

found in Table 4.5), alcohol concentrations ranging from 0.078M to 0.276M and initial reaction rates where mass transfer limitations can be neglected, the "solver" function determines the best fit kinetic parameters. Then the Matlab software was used to incorporate the calculated mass transfer effects on the oxygen concentration and to plot different mechanistic models versus the experimental values as can be seen in Figure 4.12). The detailed Matlab script which takes the mass transfer coefficients in consideration can be found in Appendix C.

| Model<br>L-H Equation | $K_1$ | $K_2$ | $k_3$ | $K_4^*$<br>$(M)$ | Assumptions |
|---|---|---|---|---|---|
| A) $R=\frac{k_3K_1[A](K_2[O_2])^{0.5}}{(1+K_1[A]+(K_2[O_2])^{0.5}+\frac{[P]}{K_4})^2}$ | 0.005<br>$(M^{-1})$ | 42.26<br>$(M^{-1})$ | 0.1<br>$(M.g^{-1}.s^{-1})$ | 0.36 | ▪ Surface Reaction controls<br>▪ Product adsorbs<br>▪ Atomic oxygen adsorption |
| B) $R=\frac{k_3K_1[A](K_2[O_2])^{0.5}}{(1+K_1[A]+(K_2[O_2])^{0.5})^2}$ | 0.005<br>$(M^{-1})$ | 42.26<br>$(M^{-1})$ | 0.1<br>$(M.g^{-1}.s^{-1})$ | — | ▪ Surface Reaction controls<br>▪ No product adsorption<br>▪ Atomic oxygen adsorption |
| C) $R=\frac{k_1[A]}{1+\frac{[P]}{K_4}+(K_2[O_2])^{0.5}}$ | 0.000473<br>$(g^{-1}.s^{-1})$ | 42.26<br>$(M^{-1})$ | — | 0.36 | ▪ Alcohol adsorption controls<br>▪ Very fast reaction<br>▪ Atomic oxygen adsorption |
| D) $R=\frac{(k_2[O_2])^{0.5}}{1+\frac{[P]}{K_4}+K_1[A]}$ | 2.09724<br>$(M^{-1})$ | -0.3<br>$(g^{-1}.s^{-1})$ | — | 0.36 | ▪ Oxygen adsorption controls<br>▪ Very fast reaction<br>▪ Atomic oxygen adsorption |
| E) $R=\frac{k_3(K_1[A])^2K_2[O_2]}{2(1+K_1[A]+K_2[O_2]+\frac{[P]}{K_4})^3}$ | 1.825039<br>$(M^{-1})$ | 42.26<br>$(M^{-1})$ | 0.09<br>$(M.g^{-1}.s^{-1})$ | 0.36 | ▪ Surface Reaction controls<br>▪ Product adsorbs<br>▪ Diatomic oxygen adsorption |
| F) $R=\frac{k_3K_4K_1[A](K_2[O_2])^{0.5}}{(1+K_1[A]+(K_2[O_2])^{0.5}+\frac{[P]}{K_4})^2}$ | 0.005<br>$(M^{-1})$ | 42.26<br>$(M^{-1})$ | 0.1<br>$(g^{-1}.s^{-1})$ | 0.36 | ▪ Product desorption controls<br>▪ Fast reaction<br>▪ Atomic oxygen adsorption |
| G) $R=\frac{2k_2[O_2]}{(1+\frac{2k_2[O_2]}{k_3\sqrt{K_1[A]}}+2\sqrt{K_1[A]})^2}$ | 0.092<br>$(M^{-1})$ | 42.26<br>$(g^{-1}.s^{-1})$ | 0.09 | — | ▪ Alcohol adsorbs dissociatively<br>▪ Oxygen adsorbs irreversibly<br>▪ Surface reaction controls |

**Table 4.5)** Proposed models with estimated kinetic parameters and assumptions. * Determined experimentally. *Reaction mixture conditions: T=343.15 K; $P_{Air}$=1 Bar; rps=22.5 $s^{-1}$*

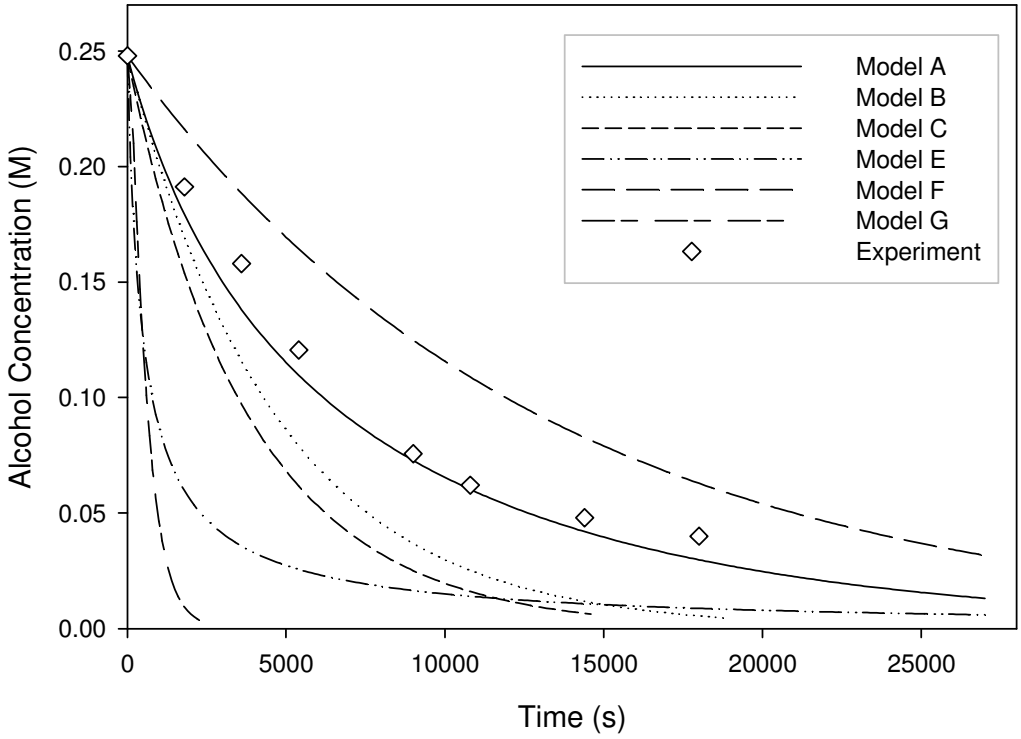


**Figure 4.12)** Models versus experimental data. *Reaction mixture conditions: T=343.15 K;* $P_{Air}$ *=1 Bar;* $C_i$ *=0.248M; rps=22.5* $s^{-1}$ *; 3g cat*

Considering Model E), oxygen adsorbs diatomically occupying only one catalyst site per molecule which generates more available free sites for alcohol adsorption. Hence, the reaction rate becomes much faster as can be seen in Figure 4.12). Since the experimental reaction rate is much slower, model E can be discarded. This has also been suggested by Lewis and Gomer (1968) who proposed that oxygen occupies two active sites when chemisorbed on platinum.

Model D) gives a negative $K_2$ which is mathematically incorrect and this disqualifies the model. From the experimental point of view, an increase in oxygen

pressure does not increase the reaction rate as can be seen from Figure 4.8) where it actually decreases with a pressure increase. Therefore, oxygen adsorption is not the rate limiting step in this case.

An attempt was made to experimentally measure the adsorption coefficient of 2-octanol on the catalyst but it was unsuccessful. There was always some conversion to ketone that has a different adsorption coefficient compared with alcohol. This effect therefore masks the true value of $K_1$, given that ketone will be adsorbed as well on the catalyst. The same problem occurs even after reducing the catalyst to eliminate any adsorbed oxygen on it and after running the experiment under a nitrogen atmosphere. Keresszegi *et al.* (2002) found that cinnamyl alcohol will still be oxidized even under argon atmosphere with a palladium catalyst. However if the reaction was controlled by the alcohol adsorption than an increase in temperature should decrease the reaction rate by preventing even more the alcohol from adsorbing on the surface (Atkins 2002). Yet with an increase in temperature the reaction rate is clearly increasing as can be seen on Figure 4.7). From the modelling point of view, model C) does not fit the experimental data as well. Hence the reaction is not controlled by alcohol adsorption and this model can be discarded.

Model F) assumes that the reaction is controlled by the ketone desorption. Thus when the ketone is produced it has to desorb from the surface to generate free sites. As can be seen from Figure 4.3) when an initial amount of ketone is added to the catalyst with only heptane as solvent before an experiment, the reaction rate becomes constant

and equal to the ketone desorption rate since the surface reaction is very fast compared to it. The reaction rate is then controlled by the rate of ketone desorption. However with the solvent mixture of dioxane-heptane an initial addition of ketone on the catalyst does not render the reaction rate constant as can be seen on Figure 4.13) although the conversion is definitely lower than without the initial presence of ketone. So if it was the ketone desorption that controls the reaction then the reaction rate should be a straight line like in Figure 4.3) when ketone is added. Moreover, model F) gives a much slower conversion compared to the experimental values which further devalues it.

Model G) proposed by Van den *et al.* (1994), considers that the alcohol adsorbs by forming an alkoxide and hydrogen on the catalyst surface using two similar active sites. However, the model shows a very fast reaction rate since oxygen is adsorbed irreversibly, contrary to the experimental data, hence disproving it.

Model A) assumes that the reaction is surface controlled and that the ketone still adsorbs on the catalyst while Model B) assumes that the reaction is surface controlled without any ketone adsorption on active sites. It can be established that model A) is more likely since the addition of ketone initially does decrease the reaction rate as can be seen from Figure 4.13). The F-value and T-value statistical parameters for Model A are less than the critical values in Table 4.6) which give a 95% confidence in the data presented.

| $K_1$ $(M^{-1})$ | $K_2$ $(M^{-1})$ | $k_3$ $(M.g^{-1}.s^{-1})$ | $K_4^*$ $(M)$ | F critical (2,21) | F calculated | T critical (0.05,8) | T calculated |
|---|---|---|---|---|---|---|---|
| 0.005 | 42.26 | 0.1 | 0.36 | 3.467 | 0.0067 | 2.36 | 2.31 |

**Table 4.6)** Estimated kinetic and statistical parameters for model A. **Determined experimentally from an adsorption equilibrium experiment. Reaction mixture conditions: T=343.15 K; $P_{Air}$ =1 Bar; stirring speed =22.5 $s^{-1}$*

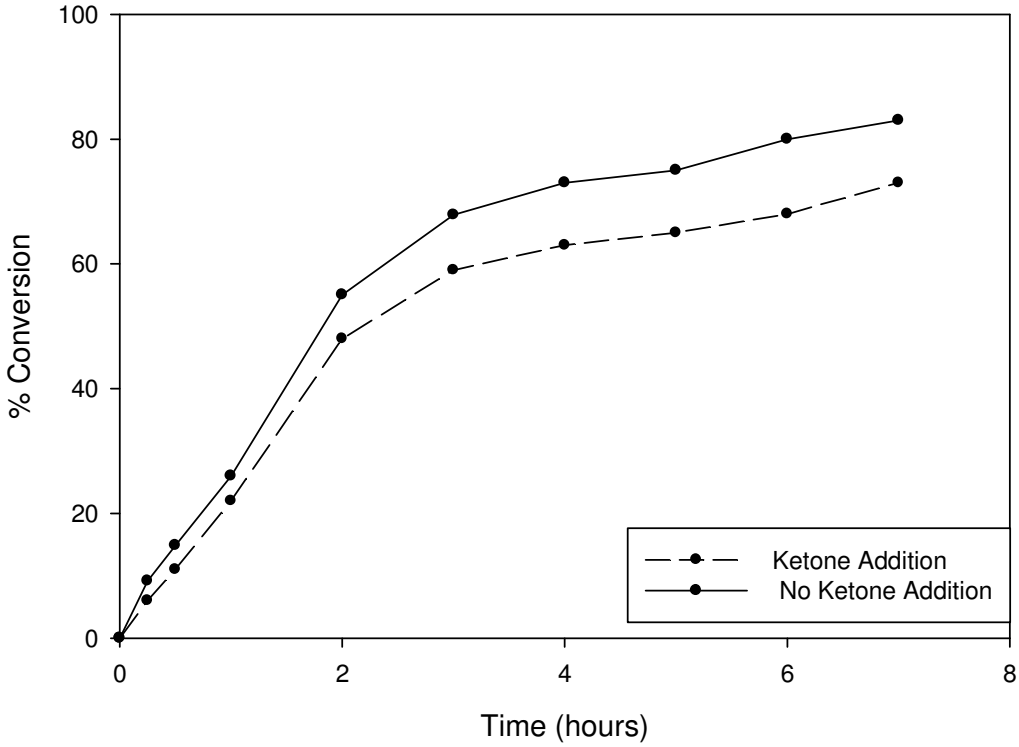


**Figure 4.13)** Initial ketone addition effects on the solvent mixture. *Reaction mixture conditions: T=343.15 K; $P_{Air}$ =1 Bar; $C_i$ =0.248M; rps=22.5 $s^{-1}$; 10 ml added ketone.*

The solvent mixture decreases the strong adsorption of ketone without eliminating it. This is understandable, otherwise even the similar alcohol reactant molecule will not adsorb on the catalyst as was witnessed with the ineffective DMSO solvent. Model A) has been described as well by Shuurman (1992) but without the effects of product adsorption since the substrate is glucoside which is readily soluble in the water solvent

used. Figure 4.14) compares the experimental data with Model A) for a different initial alcohol concentration which further validates Model A).

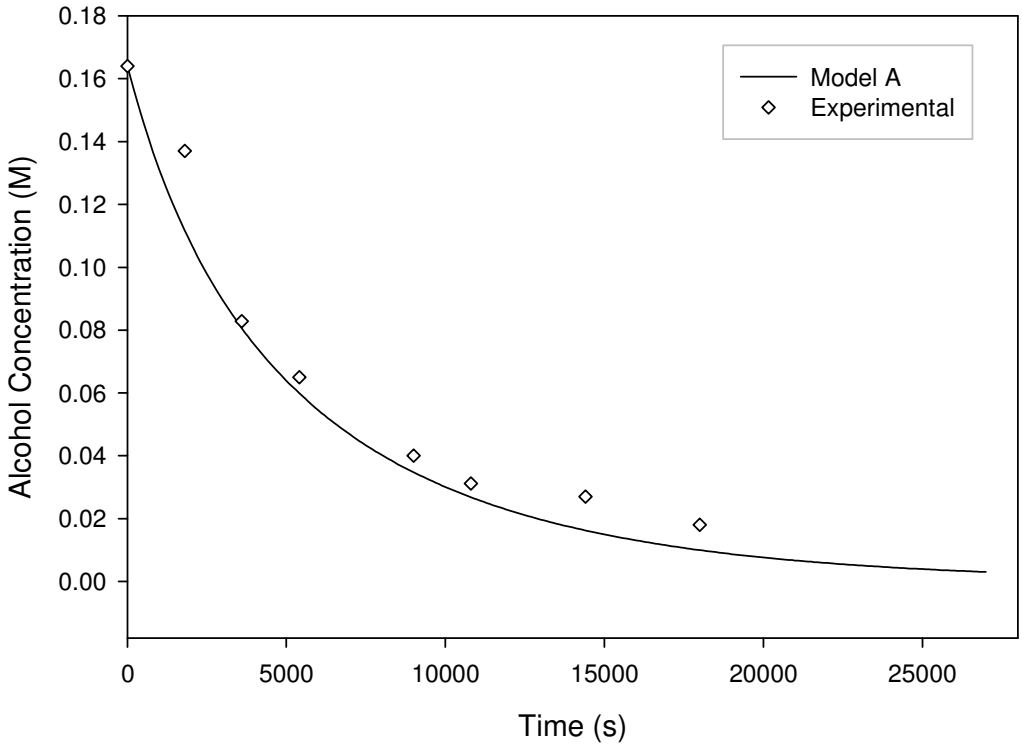


**Figure 4.14)** Model A at a different concentration. *Reaction mixture conditions: T=343.15 K;* $P_{Air}$ *=1 Bar;* $C_i$ *=0.164M; rps=22.5* $s^{-1}$

## 4.10 Catalyst pre-treatment and recycling.

A desired characteristic in any commercial catalyst is the ability to re-use it without any activity loss. When the catalyst was washed with acetone and water after a reaction and then dried at 333 K overnight it showed a lower activity then the fresh

catalyst. Besson and Gallezot (2003) suggested cleaning the catalyst in basic medium to remove adsorbed by-products, while Gangwal *et al.* (2002) suggested that strongly chemisorbed oxygen can be removed by introducing a strong reducing agent to the catalyst medium. This might be explained by the fact that acetone/water is able to remove only some of the adsorbed organic products but is not able to eliminate strongly chemisorbed oxygen and organic by-products which occupy active sites from the metal surface. In the first procedure, in order to remove any remaining adsorbed organics the catalyst was immersed in a 2M NaOH heated aqueous solution and was stirred for 2 hours.

The best way to eliminate the oxygen is to reduce the catalyst. On the other hand extra care should be given for the reduction of this catalyst since it has a carbon support that can be flammable in the presence of hydrogen and even explosive if it is immersed in an organic solvent. Therefore the used catalyst was reduced in water after the initial washing at 333 K for 2 hours at 3 bar of hydrogen since the latter has a low solubility in water. The subsequent procedure restored the initial activity of the catalyst. Furthermore the pre-treatment of the catalyst before a reaction was investigated as well. Two cases were studied: inert treatment (used as received) and reduced catalyst before reaction. For this catalyst, an initial reduction step before reaction did not change the conversion outcome which means that the catalyst was not in an oxidised form and that the catalyst batch was a fresh one as can be seen in Table 4.6).

| Initial Reaction Rate | 1st Cleaning step (Acetone/water wash and drying) | 2nd Cleaning step (Alkali solution wash and reduction by hydrogen) |
|---|---|---|
| First Run | 0.23M/hr | 0.23M/hr |
| 2nd Run | 0.085M/hr | 0.22M/hr |
| 3rd run | _ | 0.23M/hr |

**Table 4.7)** Initial reaction rates after cleaning the catalyst. *Reaction conditions: T=343.15 K;* $P_{Air}$ *=1 Bar;* $C_i$ *=0.248M; 3g cat; rps=22.5* $s^{-1}$ *Flow=0.680L/min.*

### 4.11 Catalyst characterisation using CO Pulse Chemisorption

5%Pt-1%Bi/Carbon can be characterised using CO chemisorption which consists of introducing a pattern of known amount of carbon monoxide onto the catalyst after purging it with argon or helium to remove any adsorbed species. The CO will strongly adsorb on the platinum surface occupying a single active site per molecule. The remaining CO amount can be quantified with a TCD detector after passing through the catalyst bed. Usually the first pulse will be completely adsorbed by the catalyst depending on the metal loading and the TCD will detect the second CO pulse pattern. When CO is no longer adsorbed by the catalyst (saturation level) the chemisorption stops and the adsorbed amount can be quantified to give the metal surface area, metal dispersion and the active particle diameter. The relatively small dispersion of platinum

shown in Table 4.8) means that a small portion of the metal was available as an active oxidation surface. However, small dispersion limits the over-oxidation of products and hence maintains the selectivity.

| Metal Dispersion: | Metallic Surface Area | Active Particle Diameter |
|---|---|---|
| 6.0% | 0.75 m²/g | 18nm |

**Table 4.8)** Catalyst characterisation using CO chemisorption

*Summary*

The oxidation of 2-octanol has been reported to be difficult to oxidise by the literature (Anderson, Griffin *et al.* 2003; Keresszegi, Grunwaldt *et al.* 2004). Here it has been shown that the activity can be enhanced by decreasing the adsorption coefficient of the product on the catalyst using a 16-18% v/v dioxane in heptane mixture. This novel way of tackling chemical poisoning will maintain the desired reaction rate while in common solvents such as heptane, the product will adsorb strongly on the catalyst preventing the regeneration of active sites. In order to prevent over-oxidation consequences the catalysis was performed at low pressure and under some gas-liquid mass transfer effects. Mass transfer coefficients have been determined experimentally and empirically using the appropriate correlations for the system used. A Langmuir-Hinshelwood mechanism based on Schuurman *et al.* (1992) describes adequately the reaction profile.

# V) SELECTIVE OXIDATION OF BENZYL ALCOHOL ON 2.5%Au-2.5%Pd/TITANIA

While gold and palladium catalysts have been extensively studied for the oxidation of alcohols (Schwank 1985; Tsujino, Ohigashi *et al.* 1992; Kimura, Kimura *et al.* 1993; Bronnimann, Bodnar *et al.* 1994; Bamwenda, Tsubota *et al.* 1997; Bond 2000; Hongli, Qinghong *et al.* 2005; Hughes, Xu *et al.* 2005; Abad, Corma *et al.* 2008), the use of bimetallic gold-palladium is a relatively recent approach towards selective heterogeneous oxidation (Hutchings and Haruta 2005). It is crucial to investigate the mechanism and optimise the reaction conditions to maximise production of benzaldehyde. This would be necessary in order to commercialise this novel catalyst. Benzyl alcohol (BnOH) is a very reactive alcohol and has many reaction pathways which make it ideal for the selectivity study with the Au-Pd/titania catalyst (Enache, Edwards *et al.* 2006). Whilst the oxidation of BnOH with this bimetallic catalyst has been reported in the literature, the need to further explore the selectivity and optimal conditions has

been raised to better understand the chemical and physical properties of the Au-Pd/titania catalyst (Enache, Edwards *et al.* 2006; Enache, Barker *et al.* 2007).

Initially, preliminary experiments were conducted with a fresh batch of catalyst for the BnOH oxidation as reference reactions. Then the selectivity and mechanism were studied by changing engineering parameters such as the reactor design, impeller stirring speed, system pressure and the catalyst pre-treatment. The activation energy and mass transfer coefficients are then evaluated before attempting to model simplistically the kinetics of the reaction. Finally, the catalyst is characterised using SEM-EDX and XRD.

## 5.1) Initial oxidation of BnOH with Au-Pd/Titania

The Au-Pd/Titania catalyst was first tested "as received" to evaluate its activity and selectivity in the BnOH oxidation and the results are shown in Figure 5.1).

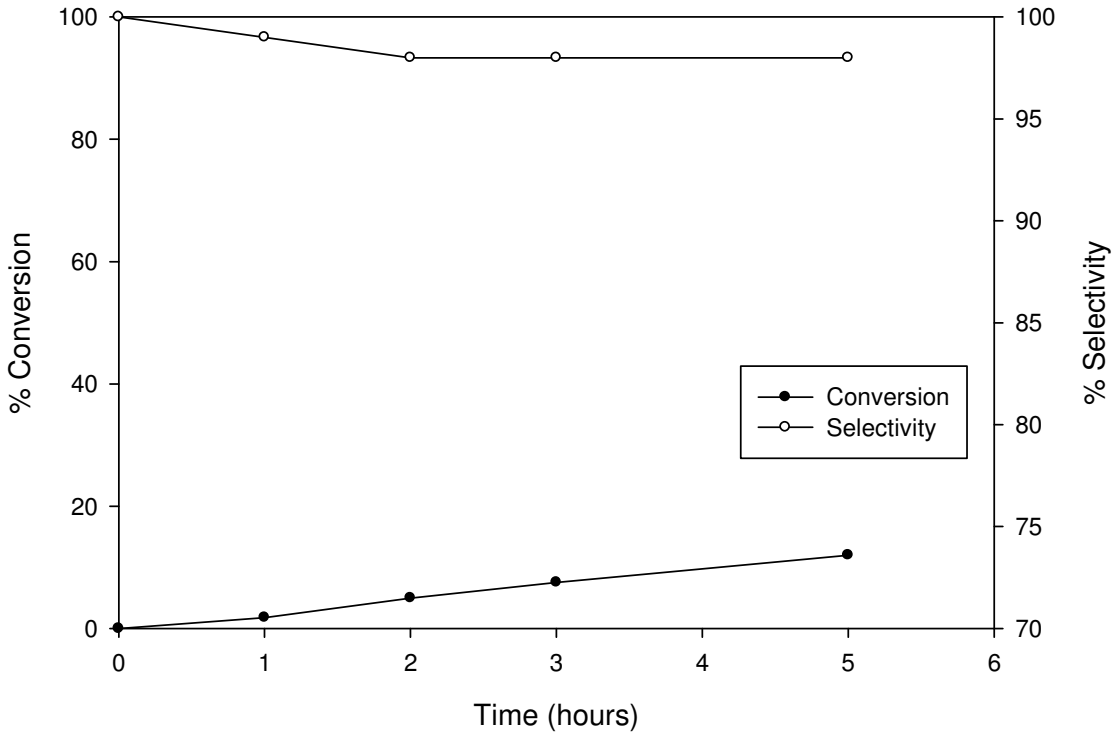


**Figure 5.1)** BnOH oxidation with untreated catalyst. *Reaction conditions: T=363.15 K; Flow= 550ml/min;* $P_{Air}$ *=6 Bar; 300ml BnOH solvent-free; rps=15.0* $s^{-1}$

It can be seen from Figure 5.1) that using fresh catalyst gives a low benzaldehyde production. The only other by-product that reduced the selectivity was toluene where the possible reaction mechanisms are discussed in section 2.2.1.1). This result might suggest that the catalyst was in an oxidised state or that it was covered with impurities such as water or oxides, hence some of the active sites were unavailable for the adsorption of BnOH. In order to validate this supposition, a Temperature Programmed Reduction (TPR) was performed on the fresh catalyst.

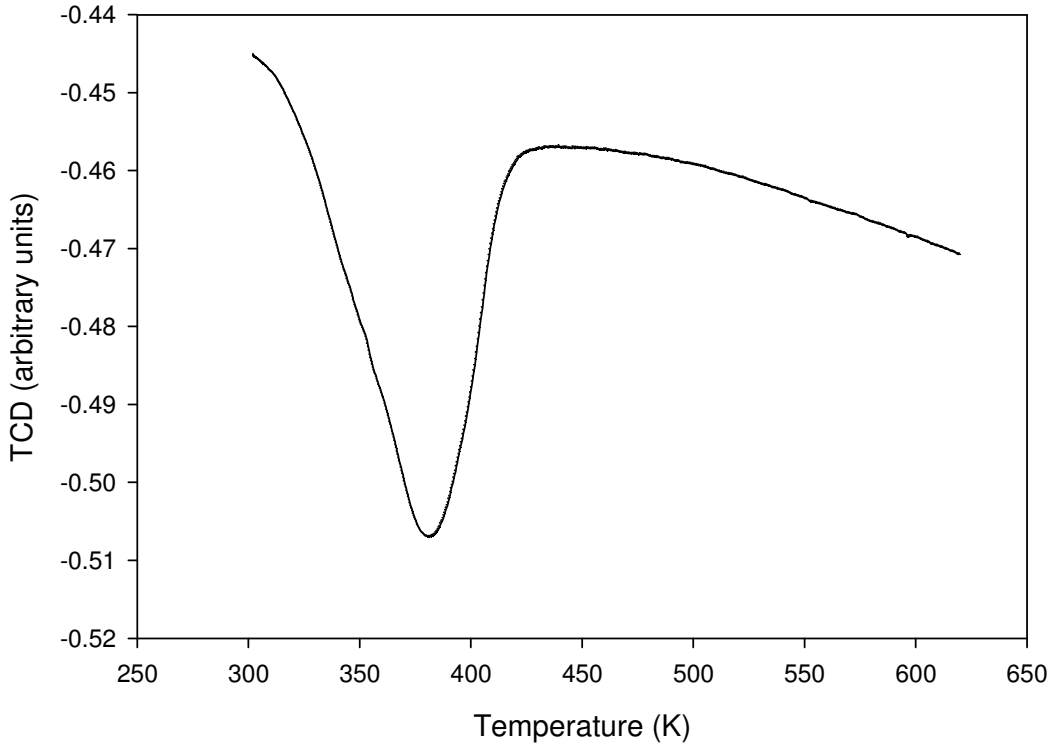


**Figure 5.2**) TPR of Au-Pd/Titania catalyst. *10%$H_2$/Argon flow=50ml/min; 5K/min up to 620K.*

Figure 5.2) shows a strong desorption peak at 380K which demonstrates the reduction of the catalyst. The catalyst also changed colour from dark red to grey which further suggests that the catalyst was in an oxidised state prior to carrying out the experiment.

### 5.2) Selectivity and Mechanism Investigation

In order to avoid the problem of using an oxidised catalyst, a fresh batch was reduced in the stirred tank using isopropanol as solvent under 2 bar of hydrogen at room

temperature while stirring at $20.0s^{-1}$. The catalyst was then dried and tested for the BnOH oxidation. Figure 5.3) shows the conversion of BnOH and product selectivity with reduced catalyst.

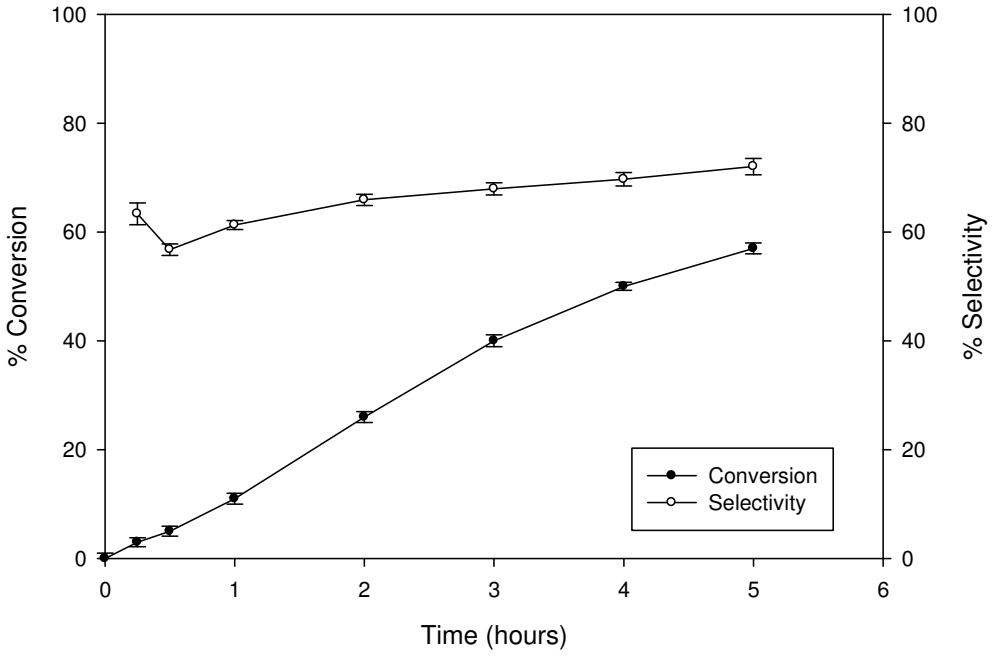


**Figure 5.3)** BnOH oxidation with reduced catalyst. *Reproduced 3 times. Reaction conditions: T=363.15 K; Flow= 550ml/min;* $P_{Air}$ *=4 Bar; 300ml BnOH solvent-free; rps=15.0* $s^{-1}$

Comparing Figure 5.3) with Figure 5.1), it can be seen that reducing the catalyst considerably increases the conversion and therefore the production of benzaldehyde (BnO) and toluene. An initial reduction step has been reported to remove sub-surface oxygen from the catalyst surface freeing the active sites especially when catalysts have been stored for a long period prior to use (Gangwal, van der Schaaf *et al.* 2005). However, while the reaction rate increases considerably compared to the use of the

catalyst with inert treatment, the selectivity towards BnO decreased to 70% with the reduced catalyst. Enache *et al.* (2006) reported that a higher oxygen pressure increases the selectivity towards BnO. However, their work was done in 40ml of solution without gas sparging, where the inlet of the oxygen stream was open but not the outlet retaining the total pressure constant. Therefore, in order to further understand the effects of scale up with this catalyst for commercial purposes, a series of engineering factors were investigated. Parameters such as air pressure, stirring speed, and reactor design were studied to try to improve and investigate the mass transfer of oxygen to the catalyst surface.

### 5.2.1) Pressure Effects

The effect of pressure on selectivity has been studied in the range of 1-6 bar of air.

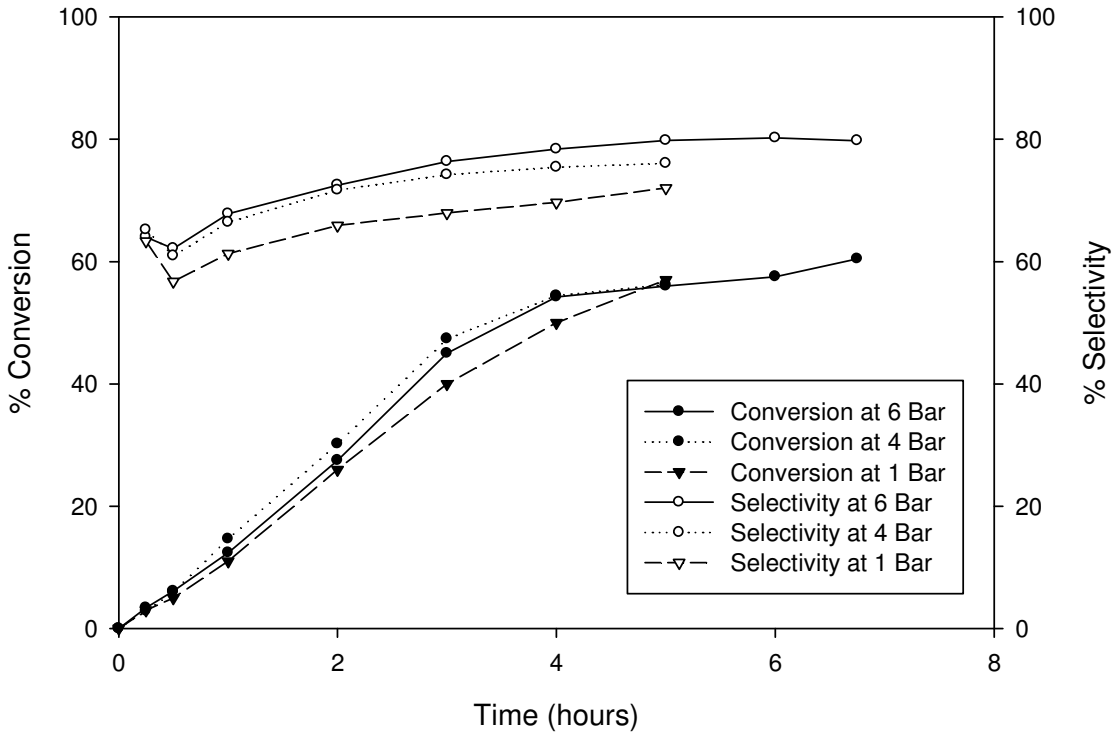


**Figure 5.4)** BnOH oxidation with reduced catalyst at different air pressures. *Reaction conditions: T=363.15 K; Flow= 550ml/min;* $P_{Air}$ *=1-6 Bar; 300ml BnOH solvent-free; rps=15.0* $s^{-1}$.

As can be seen from Figure 5.4), conversion is virtually unaffected by changes in air pressure, while the selectivity increases until a certain level. The conversion is similar at 1 and 6 bar of air. This result suggests that the reaction is zero order in oxygen but the reaction path, or selectivity, is affected by the oxygen concentration. These results support theories from the literature, where Enache *et al.* (2006) and Prati *et al.* (2007b) suggested that the selectivity is dependant on the oxygen concentration but not the reaction rate. However, Enache *et al.* (2006) used pure oxygen and the pressure was varied from 1 to 10 bar while in the current work, air (five times less oxygen) was used

from 1 to 6 bar. This might explain why they witnessed different by-products, such as esters and carboxylic acids, since their production requires another stochiometric mole of oxygen (Figure 2.2). Figure 5.4) also demonstrates that the selectivity reaches a maximum of 78% at 6 bar of air after 4 hours of reaction. This might imply that the mass transfer from gas to liquid might be inefficient, preventing a fast transfer of oxygen to the catalyst which enhances the production of BnO. One way of enhancing the oxygen transport is to increase the stirring speed of the impeller which should increase the gas bubbles surface area (Nienow 1998; Kresta, Edward PL *et al.* 2004).

### 5.2.2) Stirring Effects

The stirring speed effect on the selectivity was investigated by increasing it from 9 to 20 rps with the PBT-U.

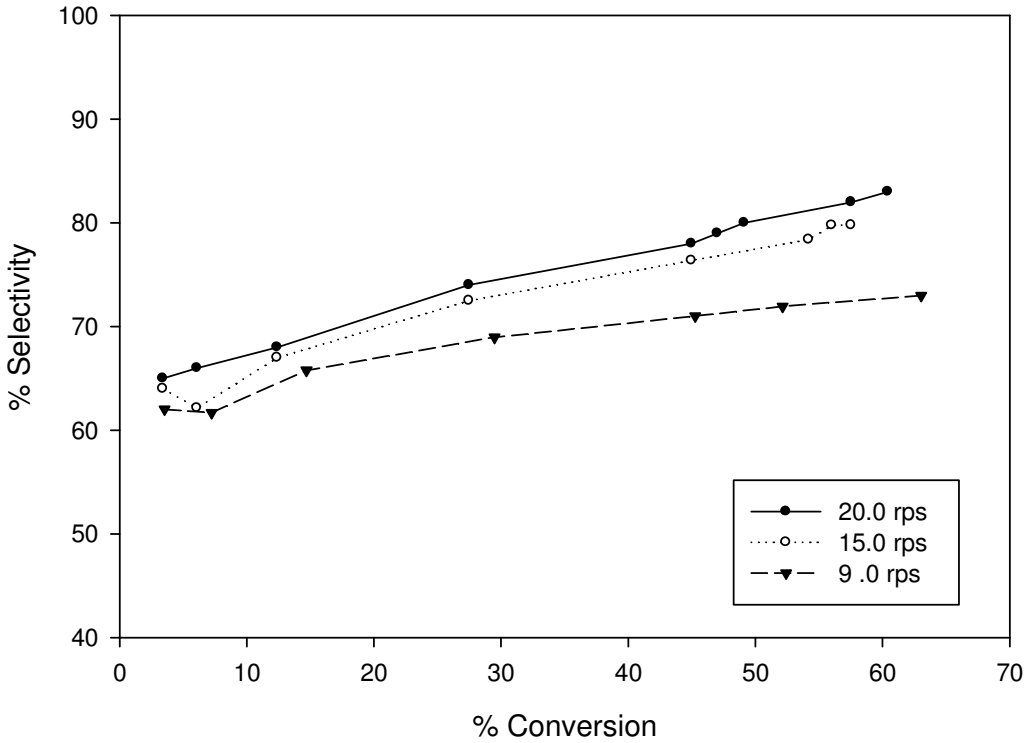


**Figure 5.5)** BnOH oxidation with reduced catalyst at different stirring speeds. *Reaction conditions: T=363.15 K; Flow= 550ml/min;* $P_{Air}$ *=6 bar air; 300ml BnOH solvent-free*

Figure 5.5) is a plot of the selectivity versus the conversion. This plot illustrates how the product distribution evolves with the course of the reaction, noting that in this case conversion is not significantly influenced by the stirring speed. Selectivity clearly increases with stirring speed, up to a maximum of 83%, since a higher impeller rotation increases the number of bubbles and the bubble surface area, $a_b$ (Kresta, Edward PL *et al.* 2004). Given that the yield of BnO is dependant on the transport of oxygen to the catalyst, the reactor configuration had to be optimised to improve the mass transfer coefficients.

5.2.3) Reactor Optimisation

All previous experiments were performed with a PBT-U having the gas sparged underneath the impeller with a single orifice pipe. One way to increase the gas/liquid interface is to place a disc shower sparger which produces smaller bubbles at the same gas flow. Since the gas-liquid mass transfer coefficient is proportional to the energy dissipated into the vessel (Kawase, K; *et al.* 1997), a Rushton turbine which has a higher power number should be used (Zhou and Kresta 1996). The energy dissipated can be calculated *via* Eq. 2.5.1.2.3. using the same impeller dimensions and stirring speed, the energy dissipated with the PBT-U is $3.47 m^2/s^3$ while the energy dissipated from the Rushton turbine is $12.02 m^2/s^3$. The disc sparger diameter designed to improve gas bubbles dispersion was selected to be 0.8 times the impeller diameter, having a sparger diameter of 3.2 cm in this work with 21 holes equally spaced as can be seen in Figure 3.2). Figure 5.6) shows the differences between the previous reactor and the optimised reactor.

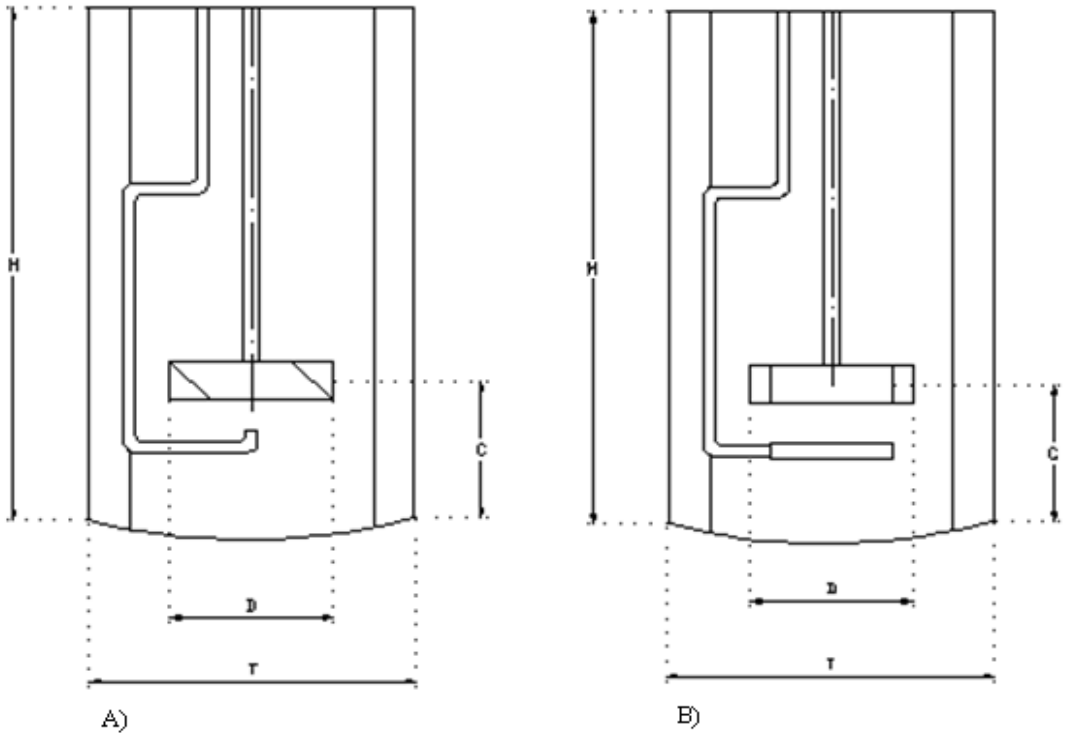


**Figure 5.6)** A) Before optimisation. B) After optimisation. *Tank diameter T=8cm; Impeller Diameter D=4cm; Baffle width =1cm; Clearage C=3cm; Height H=13cm.*

Using configuration B) from Figure 5.6), the oxidation of BnOH was carried out and the results are shown in Figure 5.7).

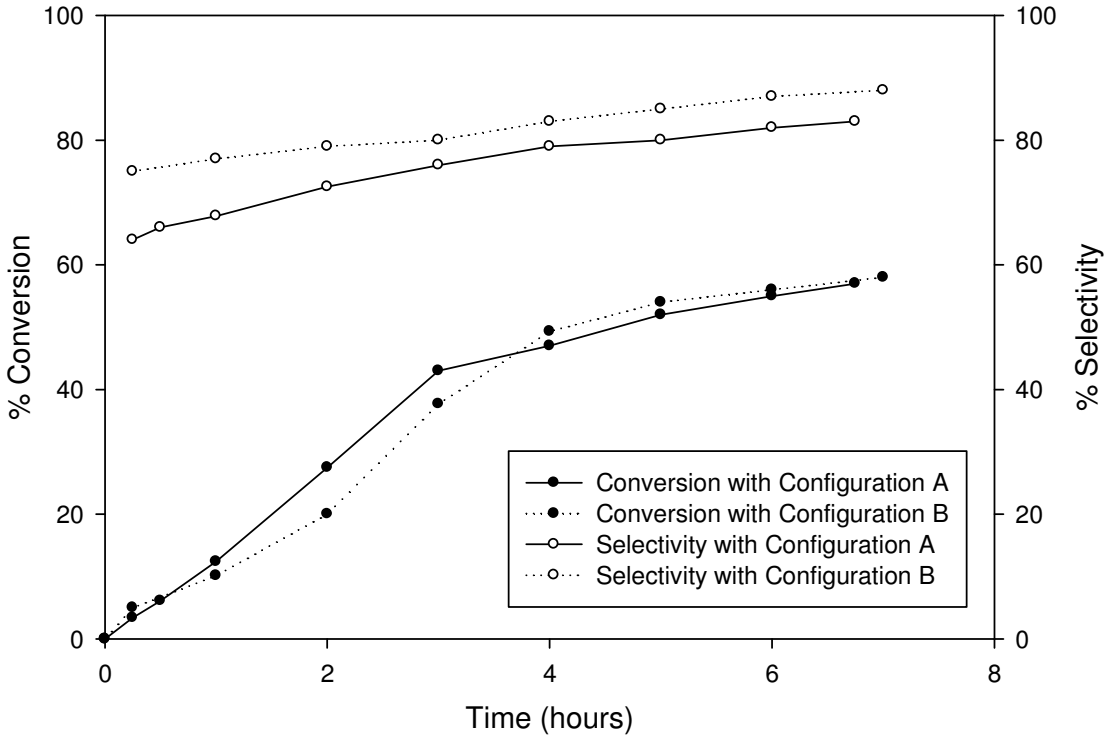


**Figure 5.7)** Oxidation with the different reactor configuration *Reaction conditions: T=363.15 K; Flow= 550ml/min;* $P_{Air}$ *=6 bar air; 300ml BnOH solvent-free; rps=20.0* $s^{-1}$.

From Figure 5.7), it can be deduced that while the conversion is unaffected, the selectivity increases by ~5% up to 88%. Although this increment is relatively low, the means of obtaining it are straightforward and on a high scale production could make a significant economical difference.

5.2.4) Mechanism Investigation

Investigation of the reaction mechanism of BnOH oxidation to gain an understanding of how the products and by-products are formed may allow for

optimisation of reaction conditions to further increase selectivity. Keresszegi *et al.* (2005), Enache *et al.* (2006) and Enache *et al.* (2007) have suggested that toluene might be produced during the BnOH oxidation with Au-Pd/titania due to either a hydrogenation from adsorbed hydrogen or an oxygen loss process from the reactant as can be seen in Figure 2.2). In order to determine the precise mechanism a series of experiments was carried out. The hydrogenation of BnOH with the Au-Pd/titania catalyst was carried out to investigate the origins of toluene production. Indeed, the hydrogenation of BnOH to toluene showed that the reaction rate is significant as can be seen from Figure 5.8)

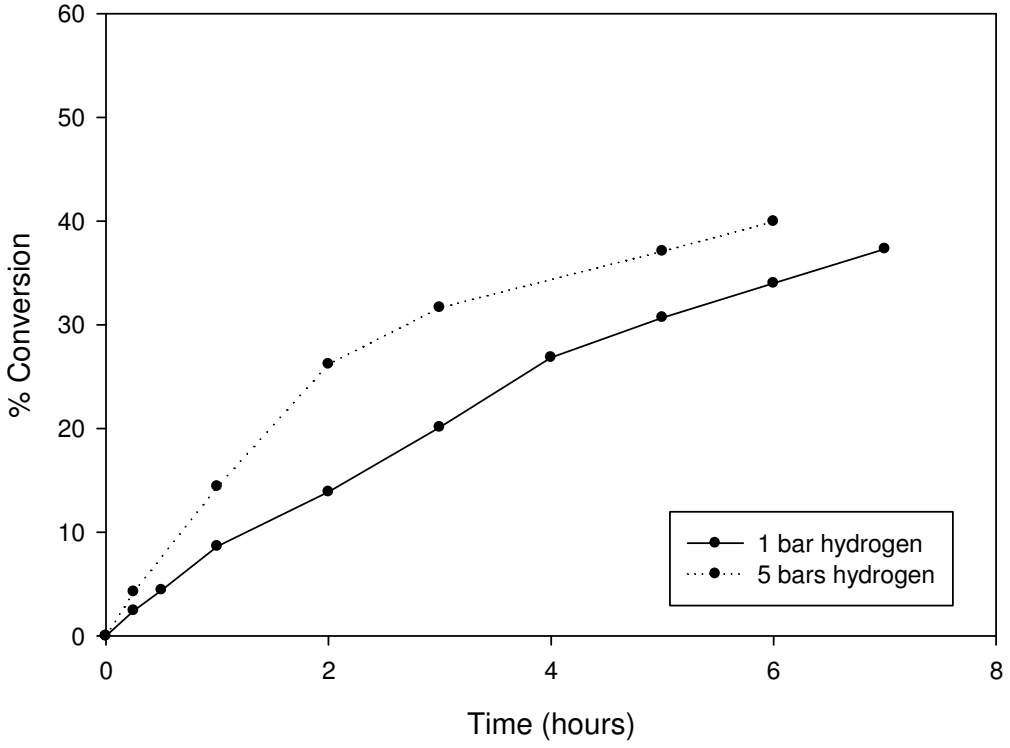


**Figure 5.8)** Hydrogenation of BnOH. *Reaction conditions: T=363.15 K; Flow= 550ml/min; 300ml BnOH solvent-free; rps=20.0* $s^{-1}$.

Figure 5.8) shows that toluene can be formed by hydrogenation of BnOH using the Au-Pd/titania catalyst. Therefore, if hydrogen is causing the formation of toluene then it must come from the dehydrogenation of BnOH. In order to verify this proposition, BnOH was oxidised anaerobically in the presence of Au-Pd/titania. Pure nitrogen was bubbled into the benzyl alcohol prior to using it as a reactant in order to remove any dissolved oxygen before it was added to the reactor, along with the catalyst, under a nitrogen atmosphere.

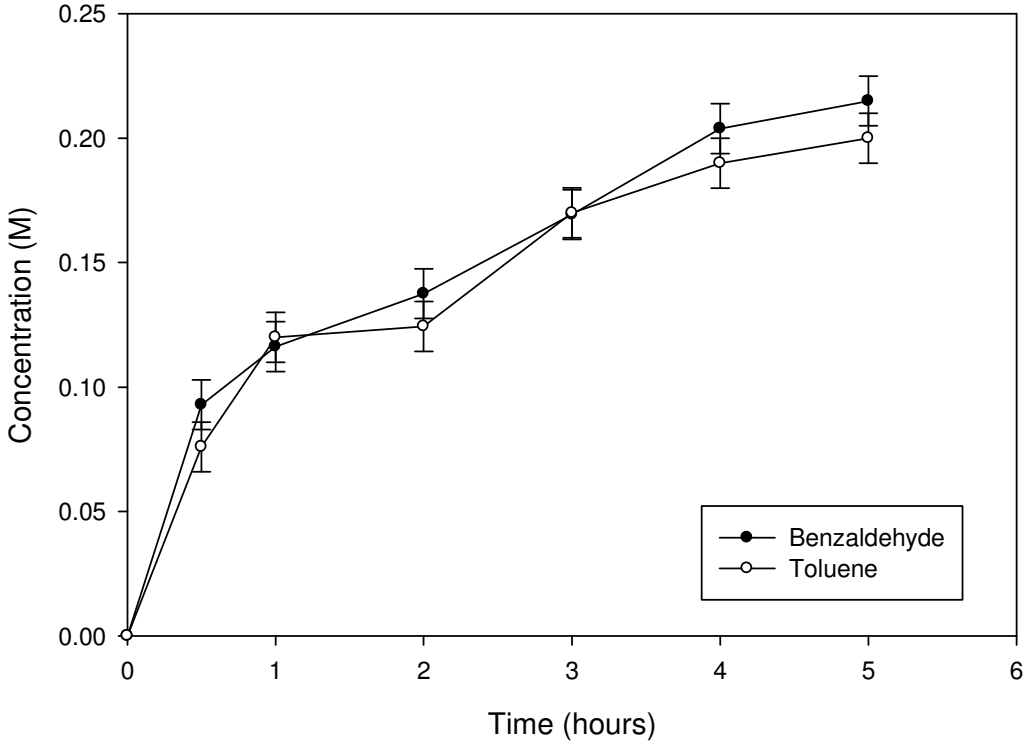


**Figure 5.9)** Anaerobic oxidation of BnOH. *Reaction conditions: T=363.15 K; 300ml BnOH solvent-free; rps=20.0* $s^{-1}$ *; 1 bar* $N_2$.

Figure 5.9) clearly demonstrates that under an inert atmosphere, benzaldehyde and toluene are produced in equal amounts. It can be deduced from Figures 5.8) and 5.9) that the oxidation of BnOH may occur *via* the formation of two metal hydrides M-H which can either be oxidised by supplied oxygen or used to hydrogenate a BnOH molecule, producing toluene and water. Since the anaerobic reaction is very slow, the adsorbed hydrogen is readily removed by oxygen to form water, rather than undergoing a hydrogenation reaction with BnOH in aerobic conditions. These results explain why the selectivity is sensitive to oxygen concentration and mass transfer coefficients, as was previously established. Moreover, the hydrogenation of BnO was carried out to investigate if the reaction is reversible.

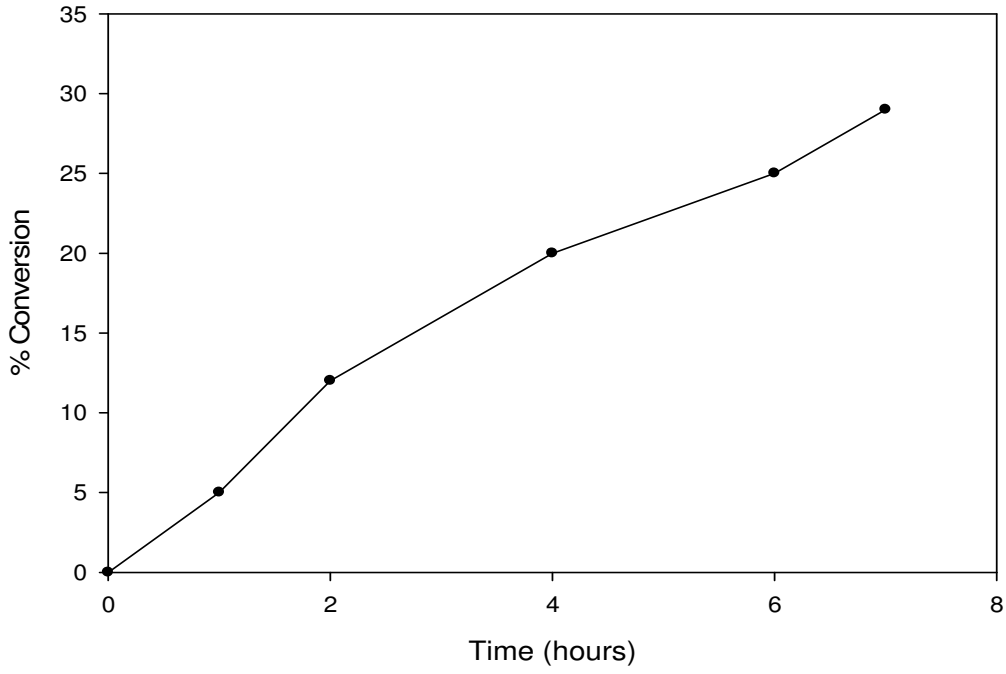


**Figure 5.10)** BnO hydrogenation. *Reaction conditions: T=363.15 K; Flow= 550ml/min; 300ml BnOH;* $P_{H_2} = 1\,bar$*; rps=20.0*

Figure 5.10) shows the hydrogenation of BnO under 1 bar of hydrogen. It can be noted that the reaction is slower than the hydrogenation of BnOH under similar conditions. Therefore the oxidation of BnOH is reversible using the bimetallic catalyst. From the previous data and conclusions the following mechanism can be established:

$$I) \qquad \varphi - CH_2OH + * \xleftrightarrow{K_1} \varphi - CH_2OH *$$

$$II) \qquad O_2 + 2* \xleftrightarrow{K_2} 2O*$$

$$III) \qquad \varphi - CH_2OH * + 2* \underset{k_3'}{\overset{k_3}{\rightleftarrows}} \varphi - CHO + 2H* + *$$

$$IV) \qquad O* + 2H* \xrightarrow{k_4} H_2O + 3*$$

$$V) \qquad \varphi - CH_2OH * + 2H* \xrightarrow{k_5} \varphi - CH_3 + H_2O + 3*$$

The presence of water in the solution has no effects since an initial addition of 15ml of water to the reaction does not affect the reaction rate or the selectivity. The observation that the BnOH conversion rate is independent of the oxygen concentration yet the reaction can yield toluene or BnO means that both their production rates must be similar. The need to reduce the catalyst before its use seems contradictory to obtaining a high selectivity since palladium can adsorb a large amount of hydrogen which can react with the BnOH to form toluene at the very start of the reaction. Therefore, a pre-treatment step may be needed to remove as much hydrogen as possible from the catalyst surface before using it, without oxidising the noble metals. Heating the catalyst to remove hydrogen requires high temperatures which may not be suitable since sintering of the metal particles occurs.

5.2.5) Catalyst pre-treatment

An efficient way to remove adsorbed hydrogen without oxidising the catalysts consists of carrying out a hydrogenation reaction. Therefore, 1-pentyne was chosen as a hydrogen acceptor since it is easily hydrogenated (Jackson, Hamilton *et al.* 2001; Hamilton, Jackson *et al.* 2002; Teschner, Vass *et al.* 2006; Jackson and Monaghan 2007). The pre-treatment step consists of a reaction between the reduced catalyst with a concentrated solution of pentyne anaerobically. Subsequently, reduced catalyst batches of 10g were immersed in a 3M solution of 1-pentyne in heptane at room temperature and a stirring speed of 16 $s^{-1}$ for 6 hours under a nitrogen atmosphere. Regrettably, the amount of hydrogen adsorbed on the catalyst could not be determined since the catalyst has only 5% metal loading and it is mostly the palladium that absorbs hydrogen. Therefore, the amount of pentene and pentane formed could not be analysed quantitatively using GC since the amount of hydrogen adsorbed per gram of catalyst is very low. The catalyst is then washed with acetone and dried overnight at 313K.

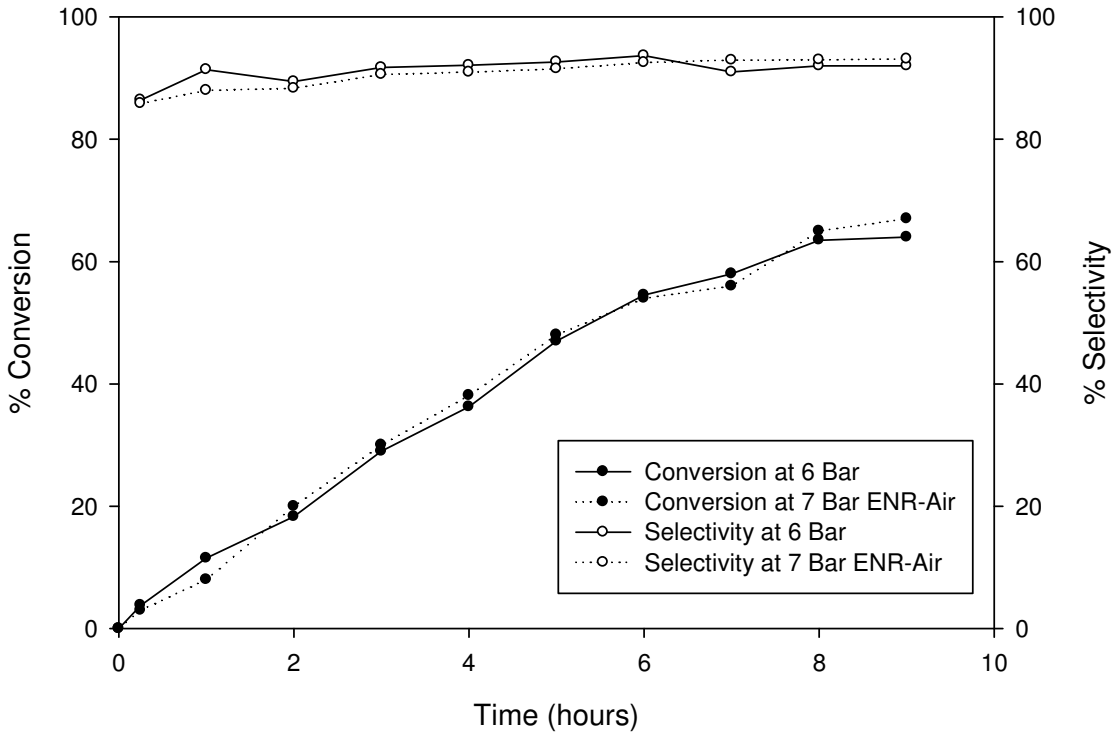


**Figure 5.11)** BnOH oxidation with treated catalyst. *Reaction conditions: T=363.15 K; Flow= 550ml/min; ENR-Air=40% $O_2$ Enriched Air; 300ml BnOH solvent-free; rps=20.0 $s^{-1}$.*

Figure 5.11) shows the oxidation of BnOH with catalyst pre-used for the hydrogenation of pentyne. The selectivity increases considerably, from 84% to 93% compared to Figure 5.7), without a change in the conversion after 7 hours of reaction. Enache *et al.* (2007) obtained a similar selectivity, however their system required the use of 2 bar of pure oxygen. When using a similar oxygen partial pressure as used in this work, 1.2 bar, their selectivity was around 80%. This aspect is especially important in industry for safety purposes and to avoid any hazard associated with the use of pure oxygen. Therefore, by treating the catalyst to a pentyne hydrogenation, it becomes

possible to attain the same selectivity without the use of a high oxygen partial pressure. A likely explanation for the increase in selectivity is the deposition of carbon from the pentyne onto the catalyst as can be seen in Figure 5.17) which reduced the amounts of active sites responsible for the toluene production and hence increased considerably the selectivity.

An additional increase in oxygen pressure, by using enriched air for instance, did not further increase the selectivity. It can be deduced that with this reactor configuration and at 6 bar of air, the selectivity becomes independent of the oxygen concentration. Therefore, the initial production of toluene seems to be an inevitable primary by-product as suggested by Enache *et al.* (2007). Since the oxidation is being carried in solvent free conditions where the catalyst is immersed in the BnOH reactant, the hydrogenation of the latter seems unavoidable by the stripped hydrogen from BnOH oxidation. Moreover, the initial pentyne hydrogenation to strip as much hydrogen from the reduced catalyst as possible does not necessarily remove all of the adsorbed hydrogen from the catalyst surface. However, the production of toluene is negligible and suggestions on ways to further eliminate it are presented in the Future Recommendation section in Chapter 8. Hence, by applying an optimum reactor configuration and by pre-treating the catalyst it becomes possible to considerably increase the selectivity and activity of the Au-Pd/titania catalyst for the oxidation of alcohols.

### 5.3) Temperature effects

It was demonstrated previously that the selectivity of the BnOH reaction is dependant on the oxygen concentration. Therefore, an increase in temperature should

decrease the oxygen solubility and, hence, the selectivity as well. Also, the rate constant $k_5$ in step V) from Section 5.2.4) of the mechanism will increase with temperature, significantly increasing the formation of side products.

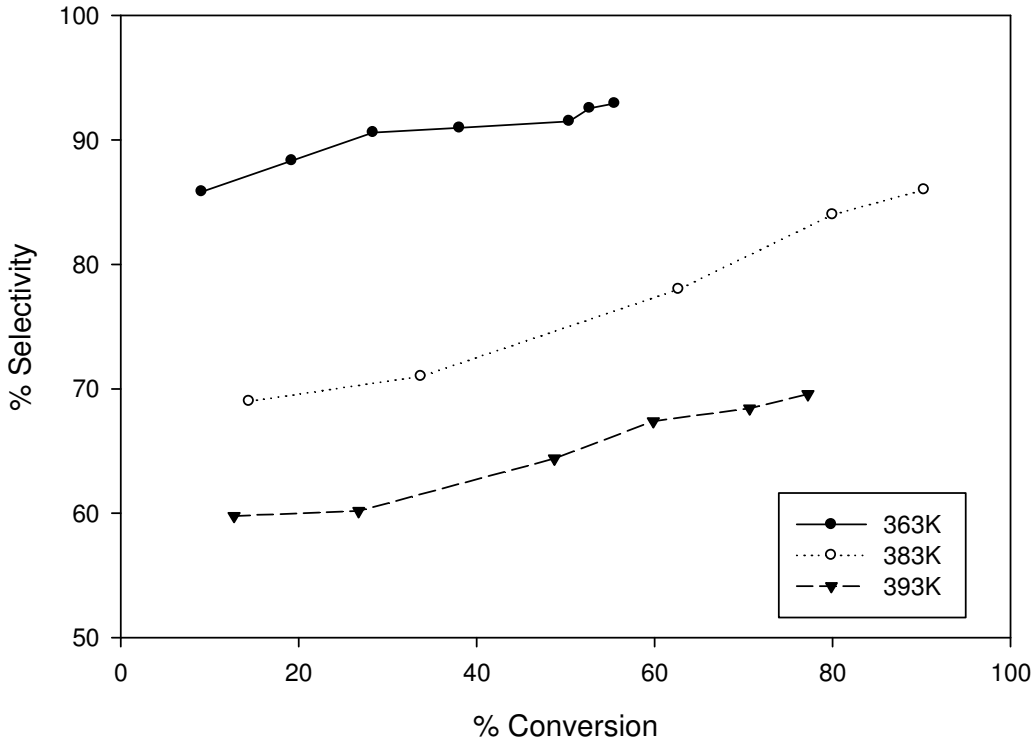


**Figure 5.12)** Selectivity towards BnO versus conversion at different temperatures. *Reaction conditions: Flow= 550ml/min;* $P_{Air}$ *=6 Bar; 300ml BnOH solvent-free; rps=20.0* $s^{-1}$.

Figure 5.12) shows how the selectivity decreases with temperature, but increases with conversion at constant conversion. Even though the conversion is faster at higher temperatures, the toluene production also increases at higher temperatures. Therefore, the optimum temperature for a high selectivity and conversion seems to be 363K. The

investigation of the activation energy was performed over the temperature range from 343K to 393K at 6 bar pressure. Initially, the reaction rate proceeds linearly which allows the determination of the activation energy through an Arrhenius plot.

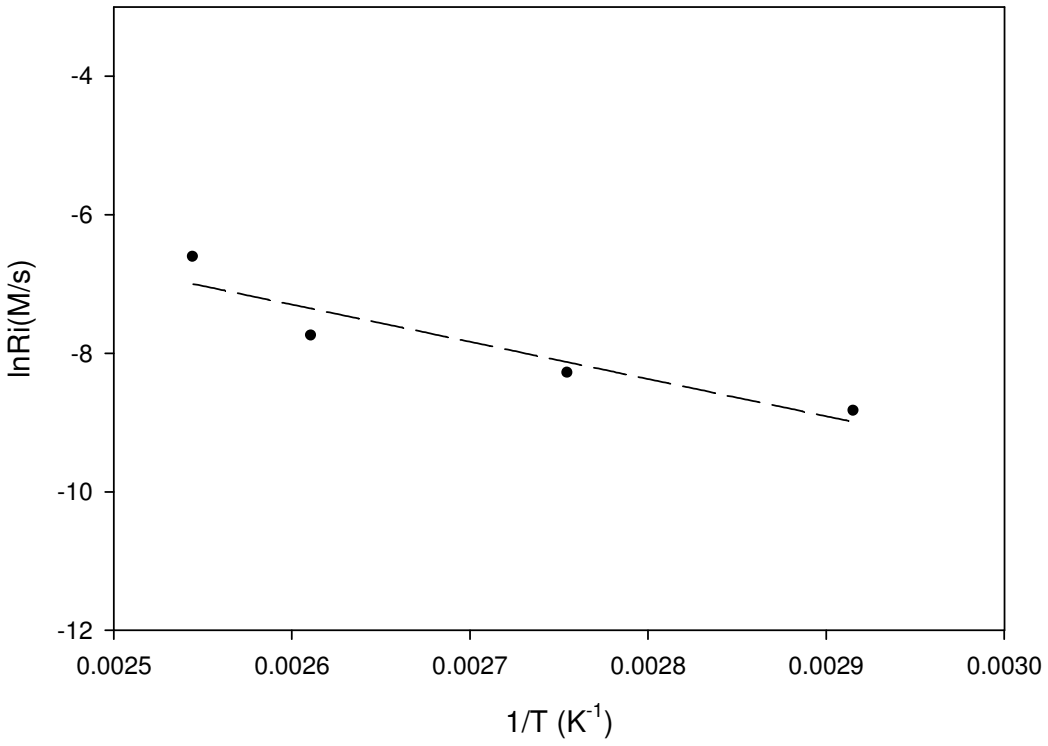


**Figure 5.13)** Arrhenius Plot for the determination of the activation energy. *Reaction conditions:* $P_{Air}$ *=6 Bar; rps=20.0* $s^{-1}$.

The apparent activation energy is deduced from the slope of Figure 5.13) where the line of best fit represents $\frac{-E_a}{R}$. The activation energy $E_a$ is equal to -44.6 $kJ.mol^{-1}$. This experimental value seems very similar to the reported activation energy by Enache *et al.* (2006) of 45.8 $kJ.mol^{-1}$.

**5.4) Measurement of Mass Transfer Coefficients**

The mass transfer coefficients can be determined by plotting $\frac{C_i}{R_i} vs. \frac{1}{w}$ in a similar way to Figure 2.10) using a calculated saturation oxygen concentration at the gas-liquid film of $7.10\times10^{-3}$ M (Golovanov and Zhenodarova 2005).

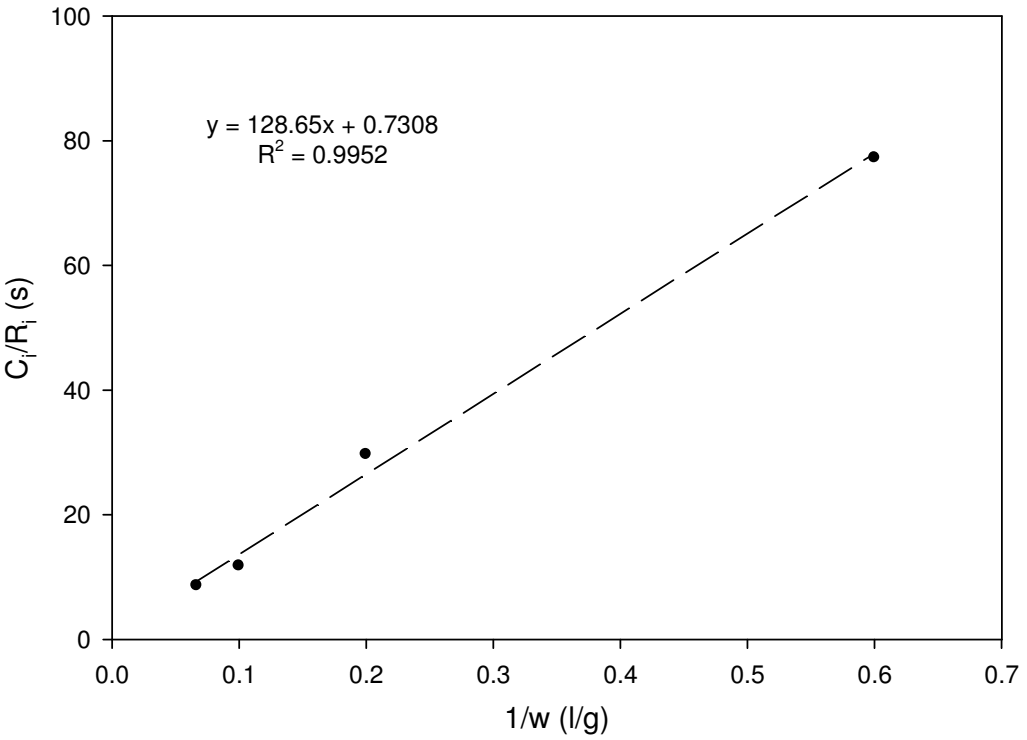


**Figure 5.14)** Solid-Liquid and Gas Liquid mass transfer resistances for Oxygen.
*Reaction mixture conditions: T=363.15 K; $P_{Air}$ =6 Bar; rps=20.0 $s^{-1}$*

From Figure 5.14) the gas-liquid and liquid-solid mass transfer internal resistances can be determined by the following equations:

$Intercept = r_b = \frac{1}{k_{GL} a_b} = 0.7308$ s: Resistance to gas absorption

$Slope = r_c + r_r = \frac{1}{k_{SL} a_P} + \frac{1}{\eta k} = 128.65\ gs/dm^3$: Resistance to liquid-solid mass transfer and internal diffusion with surface reaction respectively.

It seems from Figure 5.14) that the resistance to gas absorption is negligible. This is further validated when the pressure is varied without any effect on the reaction rate as Figure 5.5) shows. Enache *et al.* (2006) and Prati *et al.* (2007a) also suggested that the pressure of oxygen does not influence the reaction rate. Therefore, it can be deduced that the rate of oxygen transport, both external and internal, does not limit the reaction rate. Moreover, the catalyst is immersed in the solvent-free BnOH reactant and hence the reaction cannot be limited by the transport of BnOH. The reaction is occurring in the kinetic regime and is not limited by mass transfer. Hence, the resistance represented by the slope only represents the surface reaction;

$Slope = \frac{1}{k_{SL} a_P} + \frac{1}{\eta k} = \frac{1}{k} = 128.65\ gcat.s/dm^3$. Hence the value of $k$ is $7.7 \times 10^{-3}\ dm^3.s^{-1}.gcat^{-1}$

## 5.5) Kinetic Evaluation

The air pressure variation and the optimisation of gas-liquid mass transfer affected the selectivity but not the reaction rate, which means that the oxidation of BnOH is zero order in oxygen, as was previously demonstrated. Also from Figure 5.11), it is apparent that the reaction rate starts to decrease after 50% conversion. This might be due to either the reversible reaction of the BnOH oxidation or the decreasing alcohol concentration. From Figure 5.8) and 5.10), under the same conditions, it appears that the BnOH hydrogenation is more thermodynamically favourable than the BnO hydrogenation. Therefore, it can be assumed from Figure 5.15) that the reverse reaction or BnO hydrogenation will produce less BnOH than the amount of toluene produced during the oxidation of BnOH.

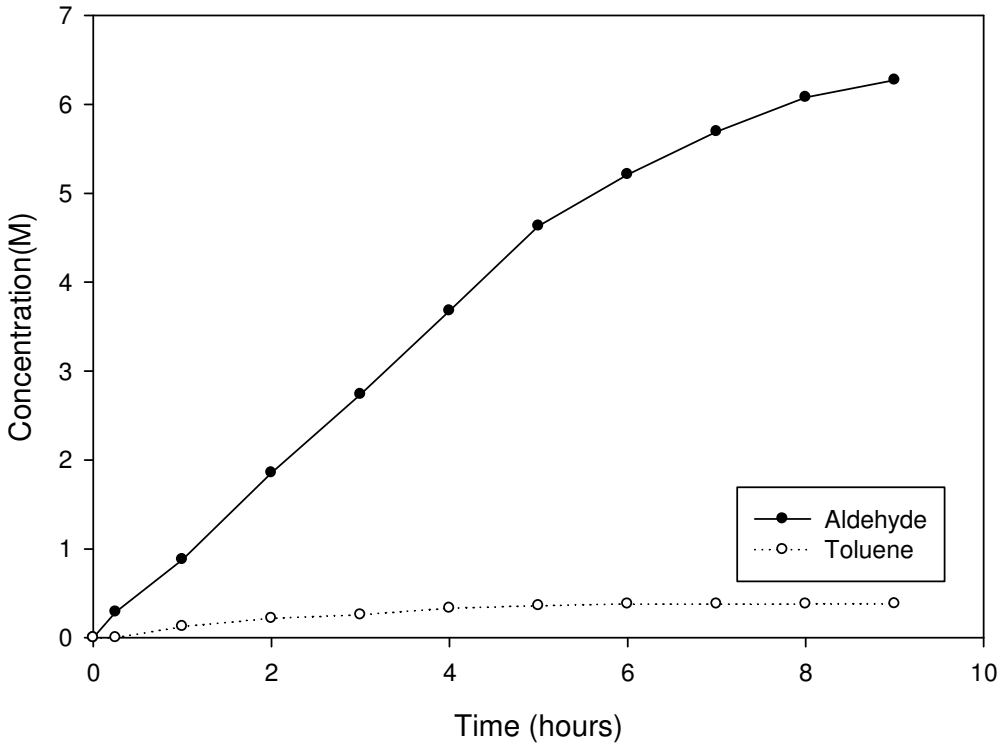


**Figure 5.15**) BnOH oxidation with treated catalyst. *Reaction conditions: T=363.15 K; Flow= 550ml/min;* $P_{Air}$ *=6 Bar; 300ml BnOH solvent-free; rps=20.0* $s^{-1}$.

Hence, the reverse of step III) can be neglected in the modelling of the BnOH oxidation kinetics. The remaining explanation for the decrease in activity after ~50% conversion might be a change in the reaction order. The reaction starts in zero order oxygen and BnOH since in solvent-free conditions the active sites are saturated with reactants, but after the conversion and dilution of the alcohol the reaction rate becomes dependant on the concentration of the latter. One way to determine the kinetic dependency on the BnOH concentration is to plot the initial reaction rate with different starting concentrations of alcohol, as shown in Figure 5.16).

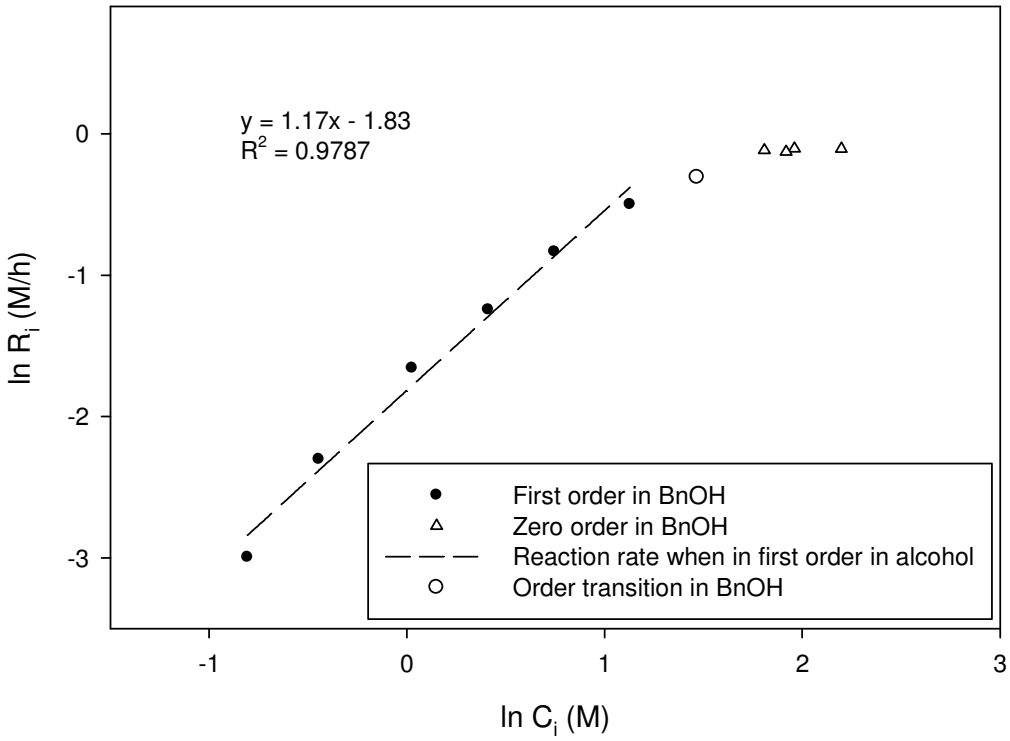


**Figure 5.16)** Initial reaction rate at different BnOH starting concentrations. *Reaction conditions: T=363.15 K; Flow= 550ml/min; 1.5gcat;* $P_{Air}$ *=6 Bar.*

Figure 5.16) shows that the oxidation of BnOH is first order with respect to alcohol when its concentration is below ~32% of the solution. At concentrations higher than ~63% the reaction is zero order in BnOH and oxygen. A zero reaction order at high concentration has also been reported by Schuurman *et al.* (1992) for the oxidation of glucoside. Between 30% and 60%, the reaction order in BnOH seems to be decreasing as the reaction rate becomes increasingly independent of the alcohol concentration. Opre *et al.* (2005) reported as well a first order in BnOH at low concentration and zero order at higher concentrations for the reaction rate with a ruthenium based catalyst. Also, from

Figures 5.16), $k_3 = 0.16h^{-1}$ and at high concentrations when the reaction is zero order, the reaction rate is $K_3 = 1.22M.h^{-1}$ ,

$R = k_3 C_{BnOH}$ ; $0 < X_{BnOH} <\sim 0.3$
$R = K_3$ ; $\sim 0.6 < X_{BnOH}$

Finally, the catalyst was characterized after being reduced and deprived of hydrogen by a pentyne hydrogenation.

**5.6) Catalyst Characterisation**

The catalyst was analysed using SEM-EDX to visualise the particles and determine the composition as shown in Figure 5.17). The bright spots represent the presence of noble metals on the Titania.

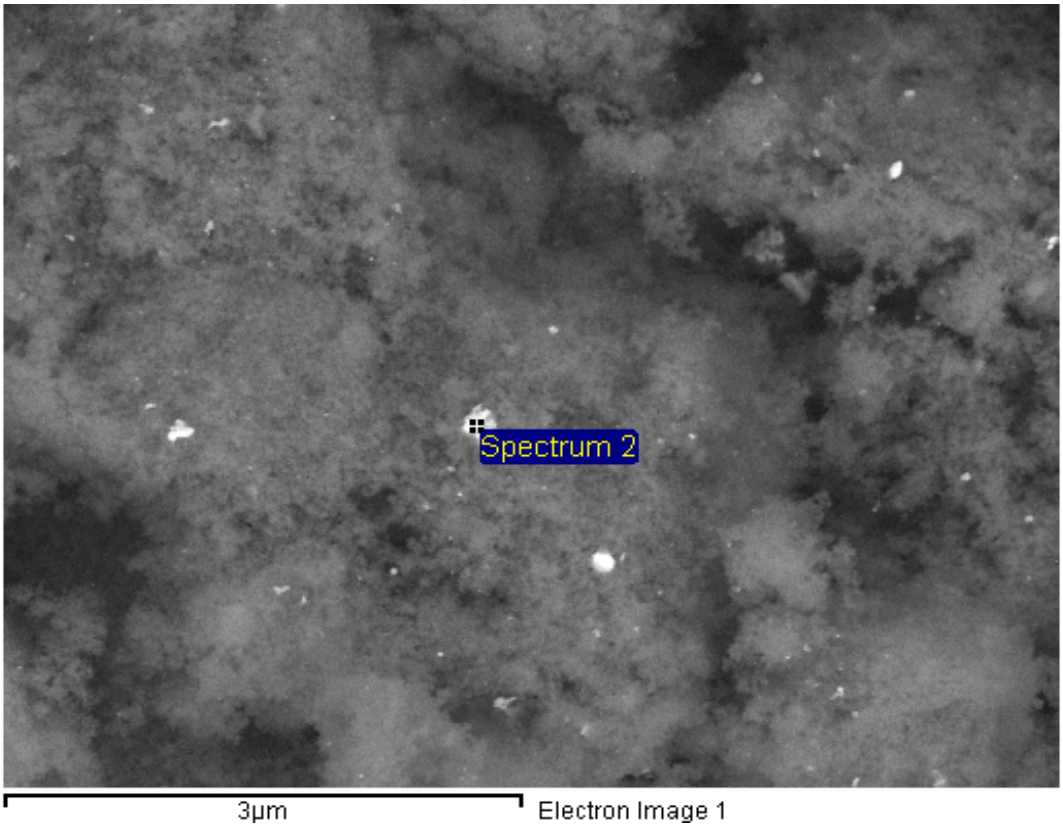


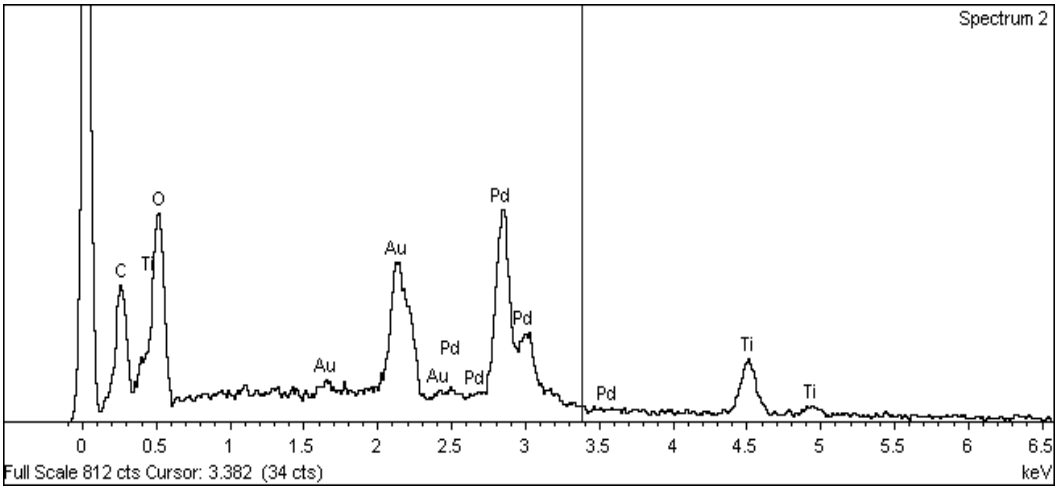


**Figure 5.17)** SEM-EDX of the Au-Pt/Titania catalyst.

The results from SEM-EDX and XRD do confirm the presence of gold and palladium. However, palladium is much more strongly exhibited than gold in agreement with the proposed gold core palladium shell structure. The presence of carbon may be due to some impurities left from the initial hydrogenation of pentyne. The metal particle is estimated to be around 17nm and the titania is in the anatase phase from the XRD.

*Summary*

The oxidation of benzyl alcohol with this novel Au-Pd/titania was studied over a range of conditions in order to optimise the selectivity and rate and to further understand the mechanism of the reaction. While the reaction was performed in the kinetic regime the reactor design, engineering parameters and the pre-treatment of the catalyst significantly improved the benzaldehyde selectivity up to 93% without the use of high oxygen pressure, which causes a hazard in industrial applications.

# VI) SELECTIVE OXIDATION OF ALCOHOLS ON METAL OXIDES

The investigation of heterogeneous catalysts consisting of transition metals other than the noble metals is well documented in the literature since they provide a much cheaper alternative than expensive platinum group metals (PGM). Therefore, the purpose of this chapter is to investigate different metal oxides for the liquid phase oxidation of different alcohol categories such as primary octanol, secondary 2-pentanol and aromatic benzyl alcohol. The mechanism of metal oxide catalysis is explained before discussing the investigation of a variety of catalysts. The catalysts contained 5% active metal loading and were provided by Johnson Matthey. The trial catalysts included $AgO/SiO_2$, $Fe_2O_3/SiO_2$, $CuO/SiO_2$, $CuO/Al_2O_3$ and were tested in this work at different pressures and temperatures. The catalysts have also been characterised with TPR and XRD.

## 6.1) Introduction and Mechanism

The hydrocarbon oxidation with metal oxides (MO) catalysts proceeds by a different mechanism than for PGM catalysts. Usually, the noble metals oxidise the alcohol by a Langmuir-Hinshelwood type mechanism. First the hydrogen of the hydroxyl function chemisorbs onto the metal surface where the substrate will detach to yield a ketone. The supplied oxygen is activated by the noble metal to react with the adsorbed hydrogen to yield water and thus cleans the active surface (Gallezot 1997).

In the 1950's, the SOHIO company (now BP) found that a lattice oxygen in MO is more selective to oxidize hydrocarbons than gaseous oxygen but preferred not to publish information about this new mechanism for commercial purposes. However in 1954, Mars and van Krevelen (1954) were able to oxidise benzene and naphthalene with a vanadia based oxide catalyst without the knowledge of the SOHIO work (Grasselli 2001). Hence, the reaction path elucidated was called the Mars and van Krevelen (MK) mechanism. This oxidation process can be summarized by the following 7 steps as described by Grasselli (2002):

1. The lattice oxygen of the metal oxide reacts with two chemisorbed hydrogen atoms coming from the substrate to yield water and hence oxidises the alcohol.
2. The metal-oxygen bond must be of intermediate strength. A strong bond will render the catalyst inert. A weak bond will result in total oxidation of the substrate or loss of oxygen in the solution.

3. The host structure of the metal oxide should withstand the formation of anion vacancies without collapsing and allow the migration of lattice $O^{2-}$ and electron transfer rapidly through it.
4. The catalyst should be able to perform redox cycles to oxidise the substrate and to replenish its anion vacancies by supplied oxygen.
5. The sites must be multifunctional in order to carry out hydrogen chemisorption, oxygen inclusion and substrate desorption.
6. The neighbouring lattice oxygen should be spaced enough in order not to over-oxidise the same substrate.
7. Different phases in the solid structure of the catalyst can co-operate (one does the catalysis while the other replenishes the anion vacancies created).

The following scheme summarises the different steps undertaken in a MK mechanism.

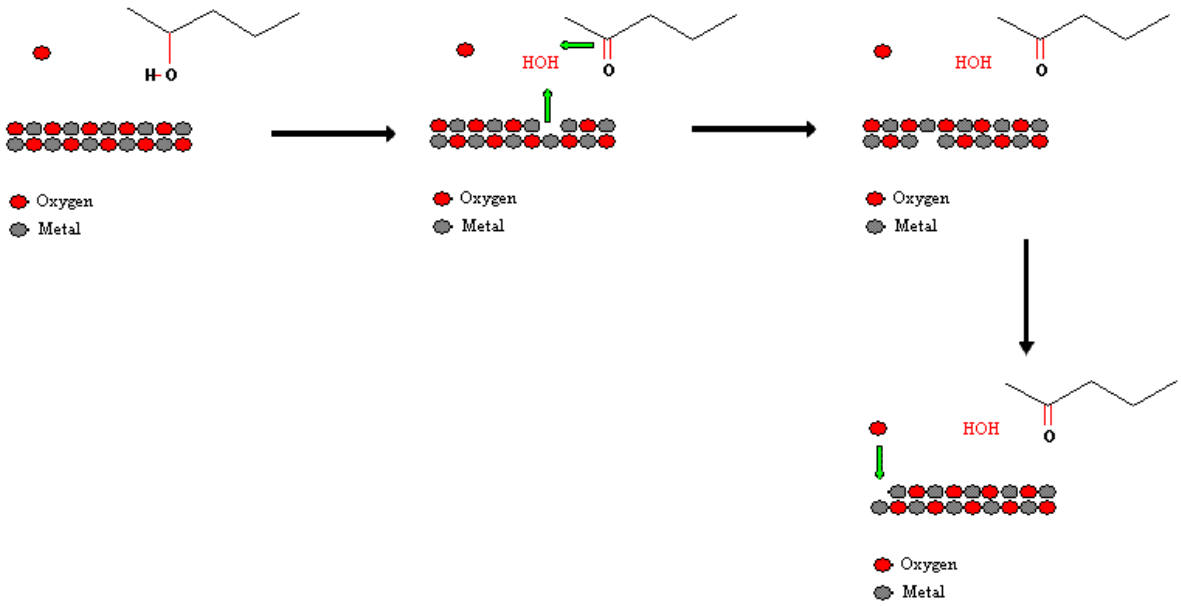


**Figure 6.1)** Mars and van Krevelen oxidation mechanism illustration.

In order to establish if the MK mechanism is occurring during an oxidation, the use of oxygen isotopes can prove the reaction pathway (Weng and Delmon 1992). By providing an $O^{18}$ atmosphere during the reaction, the initial product and water created can be analysed to determine which oxygen isotope they include. If they contain $O^{16}$ only, then the oxygen from the lattice metal was used. If they do incorporate $O^{18}$, then the oxygen was inserted from the atmosphere through a Langmuir-Hinshelwood mechanism (Grootendorst, Verbeek *et al.* 1995).

Some researchers have used hydrogenation of carboxylic acids with MO catalysts to yield carbonyl compounds through the MK mechanism. For example, the hydrogenation of benzoic acid with ZnO produced benzaldehyde at temperature above 575K (de Lange, van Ommen *et al.* 2001). The supplied hydrogen reduces the MO and produces water. Consequently, the vacancy created is replenished by absorbing oxygen from the carboxylic group of the substrate. Therefore, the carboxylic acid is transformed into a carbonyl compound and the MO is regenerated before it undergoes another redox cycle (Grootendorst, Verbeek *et al.* 1995; Sakata, van Tol-Koutstaal *et al.* 1997).

MO catalysts have been successfully used for gas phase oxidation reactions at high temperatures (Doornkamp, Clement *et al.* 1999; Doornkamp and Ponec 2000; Grasselli 2002). However, the literature on liquid phase oxidation of hydrocarbons with MO undergoing a MK mechanism is very scarce (Chuang, Cheng *et al.* 1992). Actually, Makwana *et al.* (2002) reported only a few existing works involving a MK mechanism with transition metal oxide for the liquid phase reaction. Some are based on a homogeneous reaction of various hydrocarbons such as anthracene to anthraquinone and

diphenylmethane to benzophenone with 99% selectivity with a phosphovanadomolybdate catalyst (Khenkin and Neumann 2000). However, a noble metal oxide such as Ru–Co-hydroxyapatite, has been reported to undergo a MK mechanism for the oxidation of benzyl alcohol at 333K (Opre, Grunwaldt *et al.* 2005). Some have reported a radical mechanism with MO, however such a reaction path usually involves unselective oxidation or even total oxidation of the reactant to carbon dioxide and water (Pintar and Levec 1992; Pintar and Levec 1992). The major reason for the use of MO in the gas phase reaction is the temperature dependency of the M-O bond (Doornkamp, Clement *et al.* 1999). The energy of the bond has to be appropriately balanced to allow the MO to be reduced by the substrate and oxidised by supplied oxygen. Evidently, M-O bonds become flexible at high temperature which is unsuitable for general liquid phase oxidation. Conversely, manganese oxide on an octahedral molecular sieve was able to efficiently oxidise benzyl alcohol at 383K up to 90% and 100% selectivity (Makwana, Son *et al.* 2002) which demonstrate the potential of MO catalysts in liquid phase oxidation.

## 6.2) Alcohol Oxidation and TPR Characterisation

Before starting the alcohol oxidation, the catalysts were characterised by XRD to classify their nature. The XRD was performed at the School of Chemistry, University of Birmingham and the identification of the different catalysts is in Table 6.1).

| $AgO / SiO_2$ | $Fe_2O_3 / SiO_2$ | $CuO / Al_2O_3$ | $CuO / SiO_2$ (uncalcined) | $CuO / SiO_2$ (Calcined) |
|---|---|---|---|---|
| Undefined | Hematite | Undefined | Undefined | Tenorite |

**Table 6.1)** XRD identification of various catalysts

*Experimental Setup*

The 500ml Baskerville reactor was used for the testing of the different metal oxide catalysts. The PBT-U was in place with the single orifice sparging pipe set under the impeller. Pictures of the different catalysts and XRD data can be found in Appendix E.

6.2.1) $AgO / SiO_2$

The literature on silver oxide oxidation of alcohols in the liquid phase is very scarce. Initially silver oxide on silica has a mild yellow colour at room temperature. However, it was observed that the catalyst changed colour to dark brown immediately upon submersion into a hot solution at 373K. This observation suggested a change of catalyst oxidation state. The most likely cause is loss of oxygen from silver. In order to verify the cause of irreversible colour change, a TPR was performed on the catalyst.

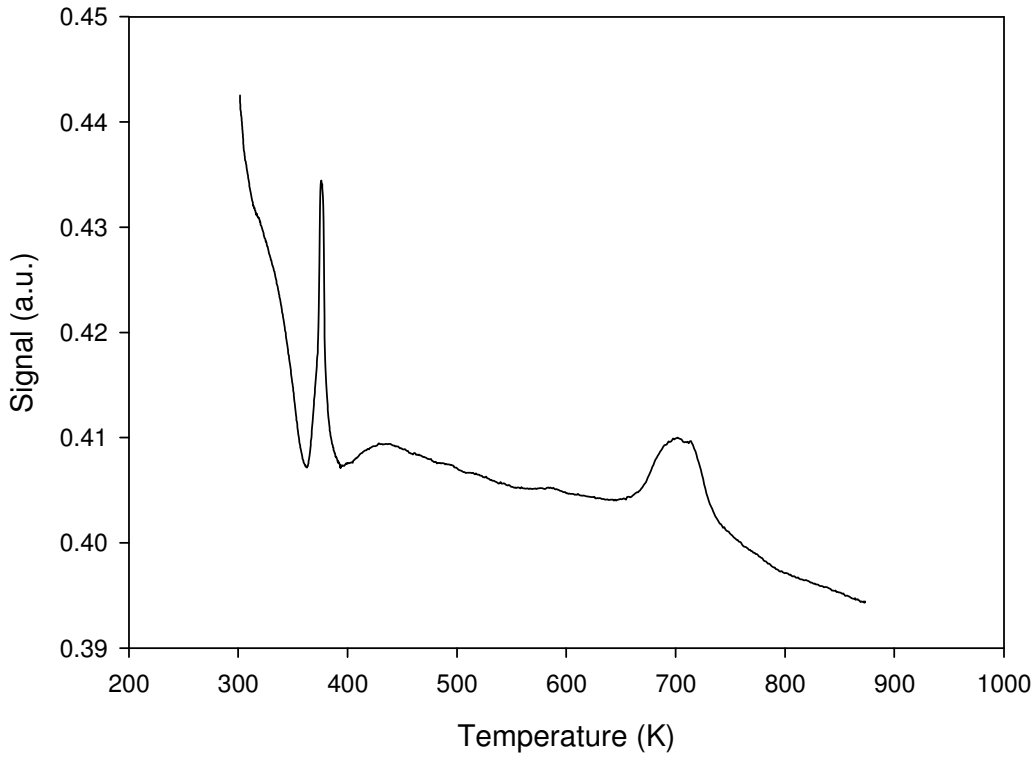


**Figure 6.2)** TPR of silver oxide. *10%$H_2$/Argon flow=50ml/min; 5K/min up to 890K.*

Figure 6.2) shows the TPR of fresh silver oxide catalyst. There seems to be a considerable desorption at temperatures below 370K. This is possibly due to the loss of impurities from the surface as the catalyst is subjected to heat and a reductive gas flow. However, a sharp peak is localised at 380K which exhibits the reduction of the catalyst phase. Another peak occurs at 670K. The phase transformation from AgO to $Ag_2O$ or $Ag_2O_3$ happens just above 373K while the phase transformation from $Ag_2O$ to Ag and O occurs at 673K (Waterhouse, Bowmaker *et al.* 2001). Hence, comparing the experimental observation of the catalyst colour change upon submersion into a solution at 373K with the literature, it seems that the catalyst abruptly lost oxygen upon immersion

into a hot solution since the temperature corresponded to 370K causing a phase change. The lattice oxygen did not oxidise the substrate due to the swift release of oxygen. The catalyst could not be re-oxidised through the bubbling of air since the oxygen partial pressure was too low and the temperature too high. In order to prevent the abrupt oxygen loss from the catalyst, the reaction was carried out at various temperatures and 6 bar of air pressure.

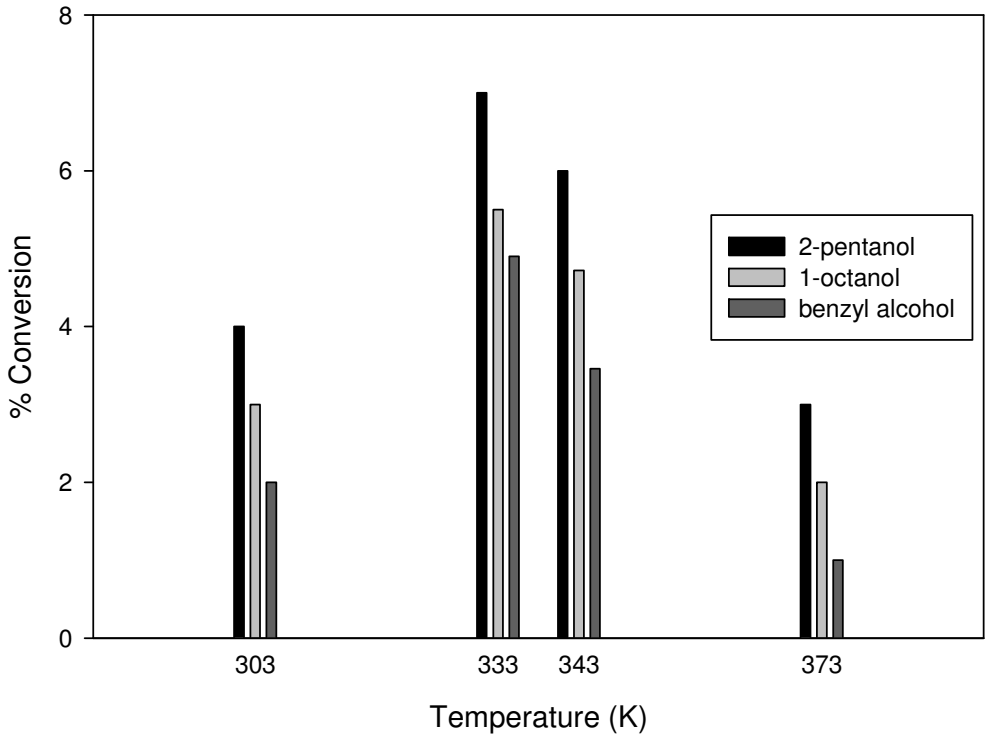


**Figure 6.3)** Various alcohol oxidations at different temperatures with silver oxide. *Reaction conditions: Flow= 550ml/min;* $P_{Air}$ *=6 Bars; C=0.248M in 300ml Heptane; rps=22.5* $s^{-1}$ *; 6g cat.*

Figure 6.3) shows the oxidation of different alcohols at various temperatures after 6 hours of reaction. While the production of 2-pentanone, 1-octanone and benzaldehyde is negligible, it can be seen that the conversion passes through a maximum with an initial temperature increase before it starts to decrease after 340K. Indeed, it was previously shown with the help of the TPR that AgO loses oxygen swiftly when the temperature is raised beyond 370K. Therefore, the catalyst was releasing oxygen even faster as the temperature was increased after 340K. Since it is the lattice oxygen that reacts with the alcohol, the fast oxygen loss from the catalyst would eventually decrease the reaction rate. At temperature lower than 340K, the lattice oxygen would react with the alcohol to produce the carbonyl compounds. A temperature increase would enhance the reaction rate as long as it does not go beyond ~360K which then starts causing the abrupt oxygen release into the solution.

Upon collection of the used catalyst, its colour was dark brown confirming that it did lose oxygen to become $Ag_2O$ and was not re-oxidised to AgO. The silver-oxygen bond of 213kJ/mole is weak and it can be easily broken but cannot be regenerated under the liquid phase reaction conditions (Dean 1999). Hence, this catalyst is ineffective for mild liquid phase oxidation. This can be further established when the concentration is studied with time.

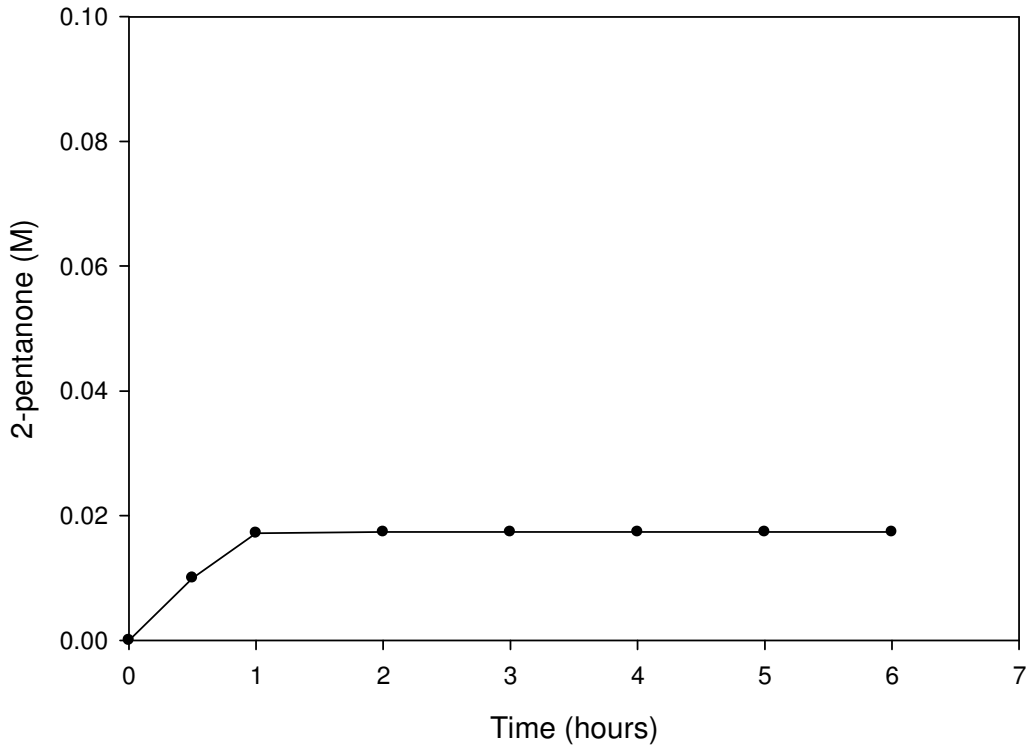


**Figure 6.4)** 2-pentanol oxidation with silver oxide. *Reaction conditions: Flow= 550ml/min;* $P_{Air}$ *=6 Bars; Ci=0.248M in 300ml Heptane; rps=22.5* $s^{-1}$ *; T=333K; 6g cat.*

Figure 6.4) shows that the reaction stops after one hour since the AgO has irreversibly become $Ag_2O$ which is inert. High pressures, beyond the capacity of the experimental setup, might allow the re-oxidation of the catalyst and this possibility is worth being investigated in future works.

*6.2.2)* $Fe_2O_3 / SiO_2$

In order to determine the optimum temperature where iron oxide will be able to exchange lattice oxygen, a TPR was performed on fresh catalyst and the results are shown in Figure 6.5).

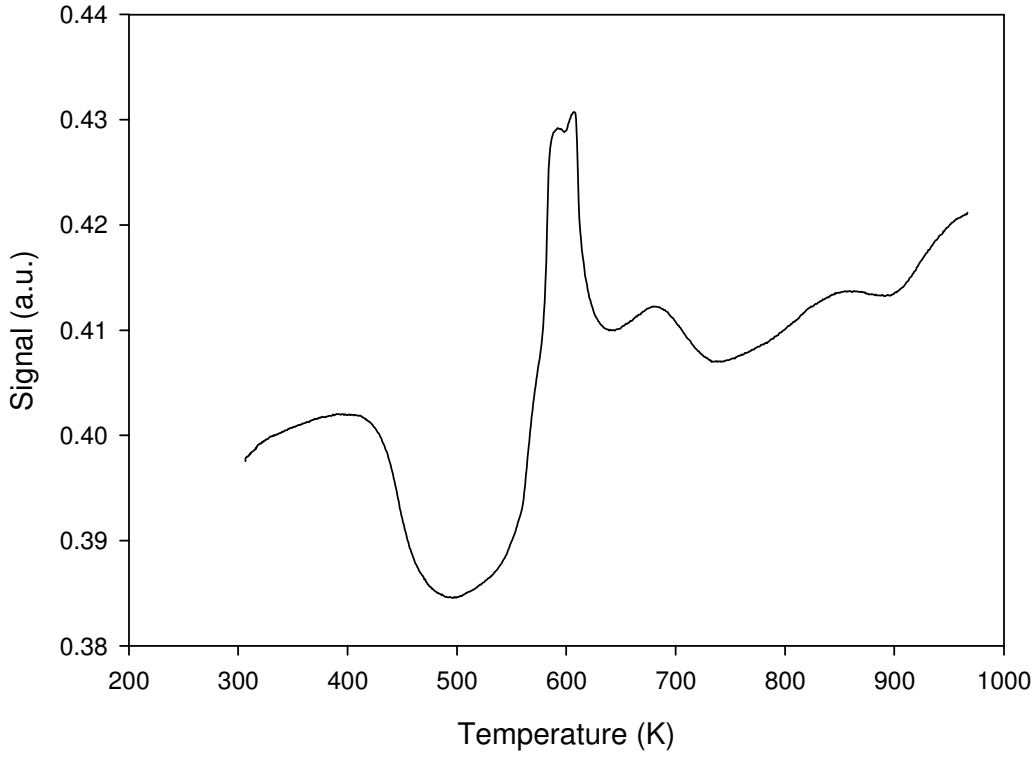


**Figure 6.5)** TPR of iron oxide. *10%$H_2$/Argon flow=50ml/min; 5K/min up to 980K*.

From Figure 6.5) iron oxide reduces at 590K with a broad peak at 400K. The latter peak may be caused due to water desorption since iron oxide is hydrophilic (Zeng, Quaye *et al.* 2004). Hematite is the form of iron oxide that reduces at 590K (Iwamoto, Yoda *et al.* 1978; Lemaitre, Delannay *et al.* 1982). These results clearly confirm the XRD results in

Table 6.1) that the catalyst is hematite. The catalyst is therefore very stable and the Fe-O bond has an energy value of 409kJ/mole (Dean 1999). Hence, it might be expected to require a very high temperature for the alcohol oxidation to allow the lattice oxygen to be flexible within the catalyst. Figure 6.6) shows the attempted oxidation of different alcohols at various temperatures.

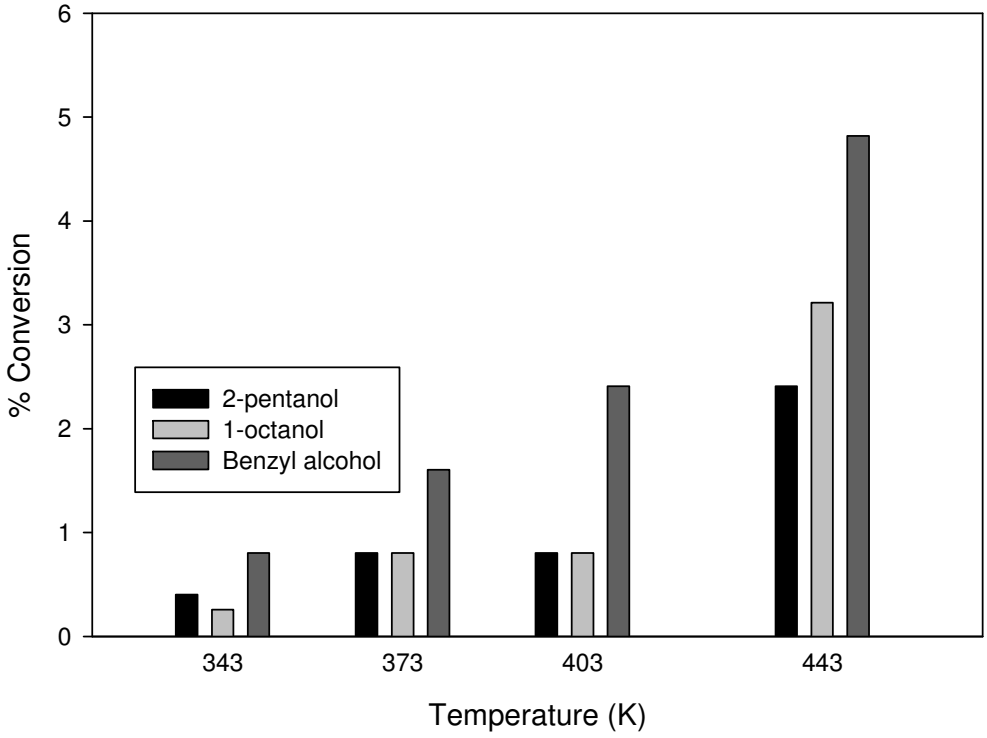


**Figure 6.6)** Various alcohol oxidations at different temperatures with iron oxide. *Reaction conditions: Flow= 550ml/min;* $P_{Air}$ *=5 Bars; C=0.248M in 300ml Decane; rps=22.5* $s^{-1}$*; 6g cat.*

As predicted, the reaction rate for all the alcohols increased due to an enhanced flexibility of the Fe-O bond as the temperature was increased. In all the experiments with the iron

oxide catalyst the original red colour remained unaltered at the end of the experiment, suggesting that the catalyst did not change phase after 8 hours of reaction. It can be concluded that this catalyst is unsuitable for liquid phase oxidations, however it might be active for gas phase oxidations at high temperatures (Weng and Delmon 1992).

### *6.2.3) $CuO/SiO_2$ and $CuO/Al_2O_3$*

Different copper samples were tried for the alcohol oxidation evaluation. The $CuO/Al_2O_3$ was supplied uncalcined and two samples of, one calcined and one uncalcined on silica. An initial TPR was performed on the copper on alumina sample.

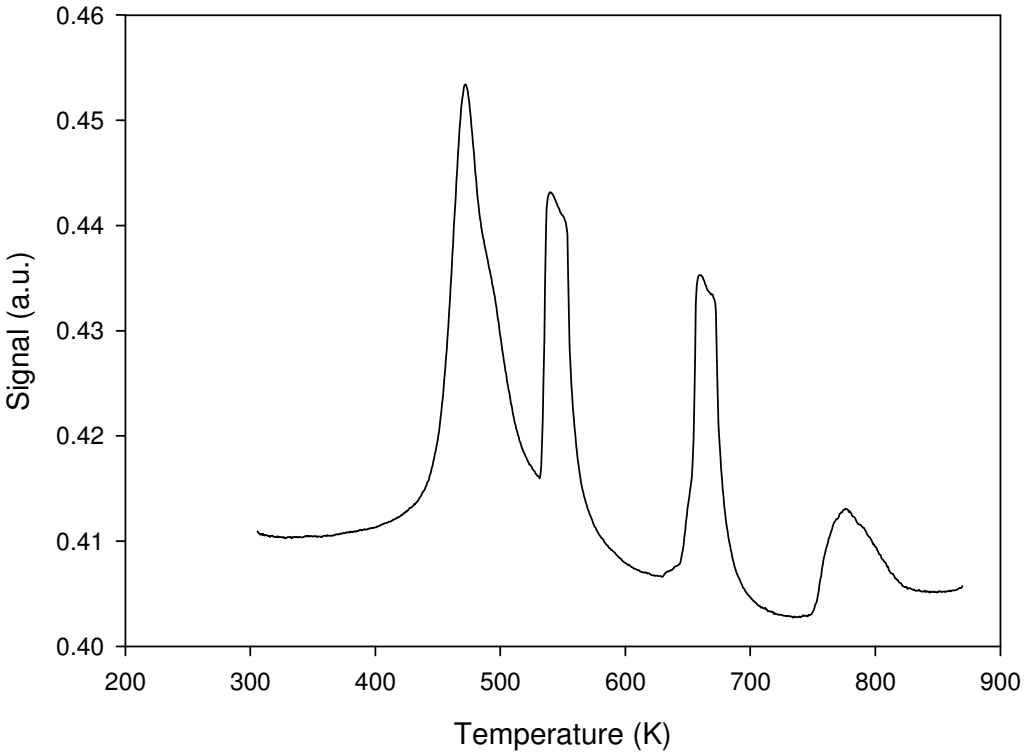


**Figure 6.7)** TPR of copper oxide on alumina. *10%$H_2$/Argon flow=50ml/min; 5K/min up to 880K.*

Figure 6.7) shows the different peaks exhibited during the Temperature Programmed Reduction of $CuO/Al_2O_3$. It is obvious that the structure of this uncalcined sample contained different oxide phases which reduce at different temperatures. The seventh principle as explained by Grasselli (2002) clarifies that different structural phases may perform different roles in a reaction scheme. Unfortunately, the catalyst showed no activity at all, even after trying the following matrix of experiments with addition of hydrogen peroxide (Miyahara, Kanzaki *et al.* 2001) in Table 6.2).

| Pressure (Bars) | Temperature (K) | 50% w/w $H_2O_2$ | Solvent | Alcohol |
|---|---|---|---|---|
| 1, 4, 8 | 303, 373, 430 | 0 or 15ml | Octane & Decane | benzyl alcohol |
| 1, 4, 8 | 303, 373 | 0 or 15ml | Heptane & Octane | 2-pentanol |
| 1, 4, 8 | 303, 373, 430 | 0 or 15ml | Octane & Decane | 1-octanol |

**Table 6.2)** Different reaction conditions for copper oxide on alumina

Consequently, both uncalcined and calcined silica supported catalysts were then tried. The TPR of both copper on silica catalysts is shown in Figure 6.8).

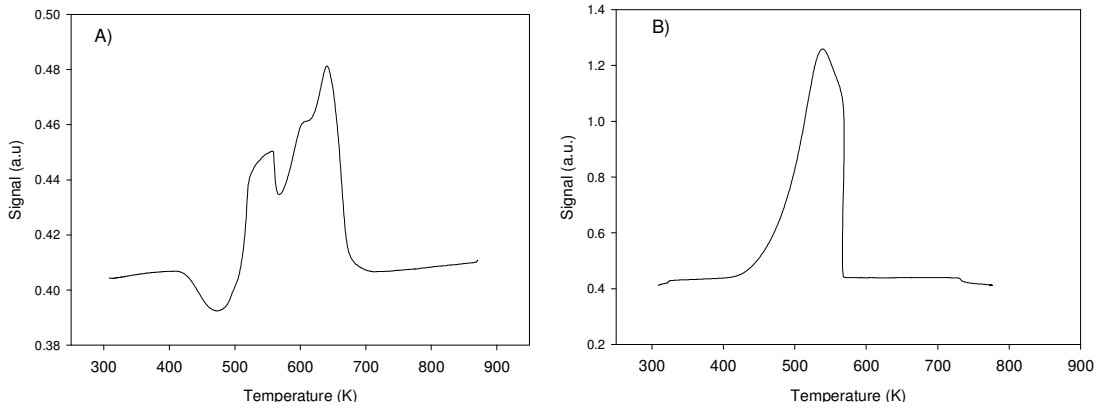


**Figure 6.8)** TPR of copper oxide on silica. *10%$H_2$/Argon flow=50ml/min; 5K/min up to 800K. A) Uncalcined and B) Calcined*

The figures above show clearly that the calcined catalyst has one distinctive oxide phase while the uncalcined sample has different oxide phases whose reduction temperatures

overlap. Nonetheless, the activity of both samples was tested in the oxidation of the three alcohols and the results are shown in Figure 6.9).

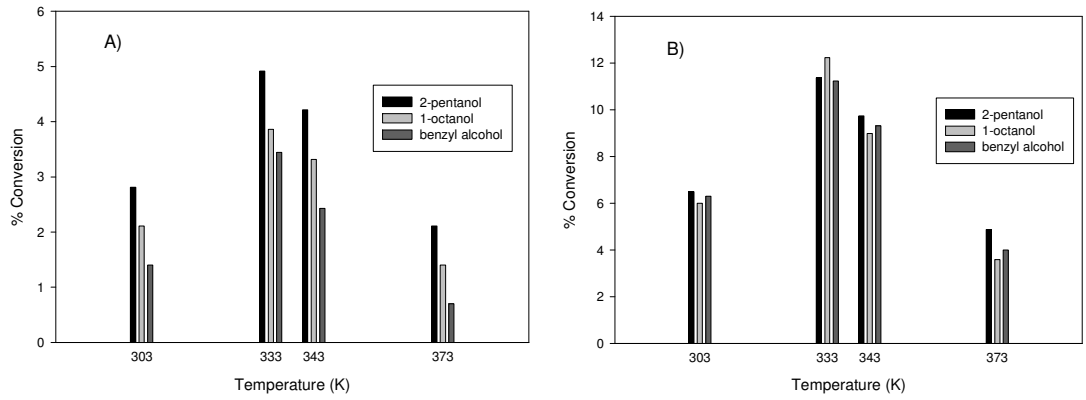


**Figure 6.9)** Various alcohol oxidations at different pressures with copper oxide. *Reaction conditions: Flow= 550ml/min; $P_{Air}$=5 Bars; C=0.248M in 300ml Decane; time=7 hours; rps=20.0 $s^{-1}$ ; 6g cat. A) Uncalcined and B) Calcined.*

Figure 6.9) shows the superior activity of the calcined sample over the uncalcined catalyst. It is interesting to note that of all the metal oxide catalysts tested, the calcined $CuO/SiO_2$ showed the most promising results in terms of conversion at 333K. Although the reduction temperature from Figure 6.8) is 530K, the catalyst starts to lose activity as the oxidation reaction temperature increases. This highlights the possibility that it is becoming increasingly more difficult to re-oxidise both catalysts when the temperature is augmented. Therefore, the air pressure effect was studied on the reaction at 333K in order to determine whether higher pressure could more effectively regenerate the catalyst surface.

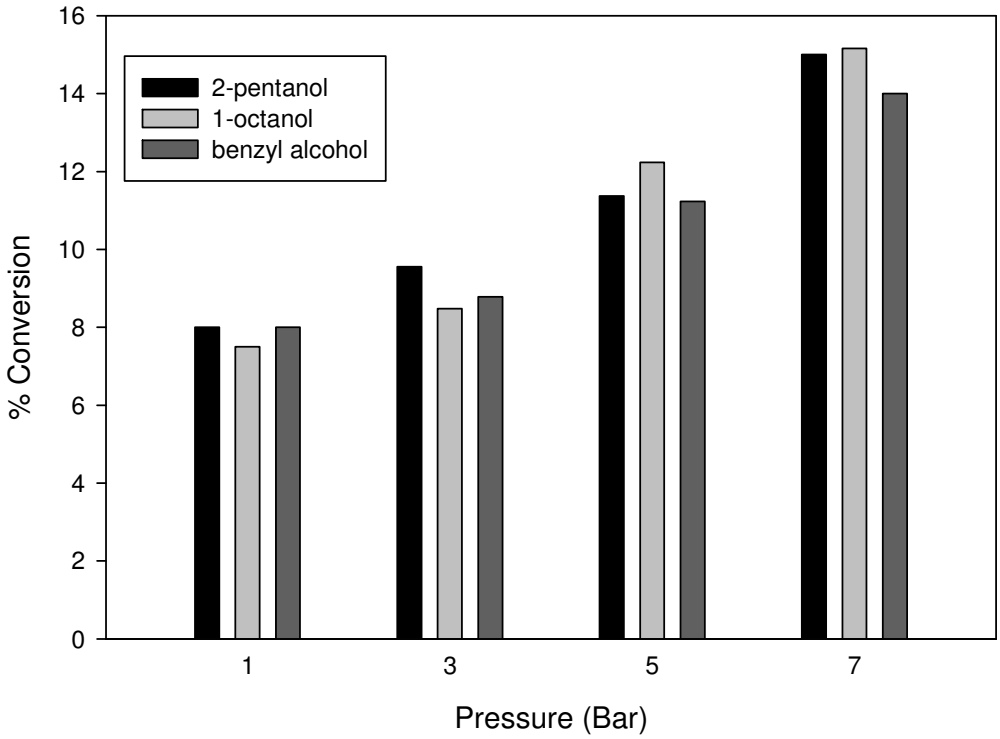


**Figure 6.10)** Various alcohol oxidations at different temperatures with calcined copper oxide. *Reaction conditions: Flow= 550ml/min; T=333K; C=0.248M in 300ml Heptane; rps=20.0* $s^{-1}$***;*** *time=7 hours****;*** *6g cat.*

Figure 6.10) shows a constant increase in reaction rate for all three alcohols as the pressure increases. The Cu-O bond energy is 343kJ/mole which seems to be the appropriate intermediate metal-oxygen bond strength. Although the conversion increases slightly, the pressure effect underlines and confirms the importance of the catalyst re-oxidation. The addition of 50%w/w $H_2O_2$ did not improve the oxidation, since it was followed by oxygen evolution from the solution. This observation was explained in the literature as well (Miyahara, Kanzaki *et al.* 2001). Unfortunately, the equipment does not allow any further increase in air pressure to push the conversion any higher. Although

the conversion was low, it is interesting to note that the reaction rate was constant at 0.005M/hr, contrary to silver oxide which lost its activity after one hour since it changed into $Ag_2O$. Figure 11) shows that the calcined $CuO/SiO_2$ catalyst is the most promising Metal Oxide based catalyst since its activity is continuous.

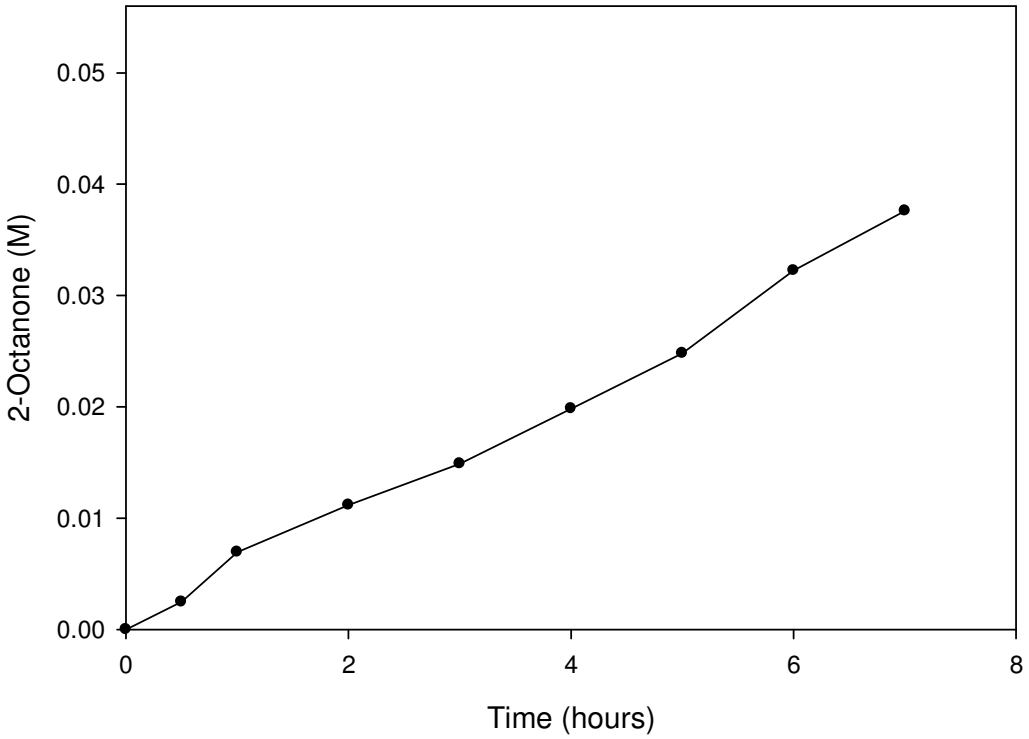


**Figure 6.11)** 2-octanol with calcined copper oxide on silica. *Reaction conditions: Flow= 550ml/min; T=333K; C=0.248M in 300ml octane; rps=20.0* $s^{-1}$ ***;*** *time=7 hours; P=7Bar**;*** *6g cat.*

Summarising the results from the copper oxide catalyst, it seems that calcination or having a single oxide phase considerably increases the activity of the catalyst. The alumina supported catalyst had various oxide phases, which made the catalyst ineffective

in the oxidation of alcohols. The uncalcined silica supported catalyst showed only low activity since it also had different oxide phases. However, the calcined silica supported copper catalyst showed promising results and an appropriate metal-oxygen bond energy. It seems however, that the oxygen partial pressure limits the activity of the catalyst.

*Summary*

In this chapter, the testing of tested three different metal oxide catalysts for the oxidation of primary, secondary and aromatic alcohols is reported. The silica supported silver oxide had a very weak Ag-O bond and it easily lost oxygen without being able to re-oxidise. Iron oxide had the opposite problem of silver oxide: the Fe-O bond is too strong. This catalyst was not active because under these reaction conditions and temperature, the metal oxide bond is not flexible enough. Uncalcined copper oxide on alumina with different oxide phases was inert, probably due to an incompatible bulk structure of the catalyst (Grasselli 2002). The calcined copper oxide catalyst on silica showed the most potential since the strength of the Cu-O bond seemed to have an appropriate intermediate energy. Increasing the oxygen partial pressure increases the conversion since it speeds up the re-oxidation of the copper catalyst.

# VII) CONCLUSIONS AND RECOMMENDATIONS

## 7.1) Conclusions

### 7.1.1) 2-Octanol Oxidation with 5%Pt-1%Bi/carbon

The oxidation of 2-octanol was investigated with 5%wtPt-1%wtBi/carbon to understand the reasons of the low activity reported in literature and to establish a solution. The sudden loss of the high reaction rate after 15 minutes during the oxidation of 2-octanol with 5%Pt-1%Bi/carbon in heptane was investigated. There were three likely causes including overoxidation, leaching and poisoning. It was found that the latter cause was occurring due to the strong adsorption of 2-octanone on the catalyst surface. The amount of adsorbed ketone was found to be 0.006moles/gram of catalyst. Therefore, the solvent choice was investigated to try to remove the adsorbed ketone from the active surface. P-xylene and dioxane each proved to be inadequate to dissolve the adsorbed ketone from the catalyst and DMSO bound even more strongly than 2-octanone

on the active surface. Finally, a mixture of 16-18% v/v dioxane in heptane was able to effectively regenerate active sites and allow a constant reaction rate of 0.07M/hr.

The Arrhenius plot was studied with temperatures ranging from 323K to 353K and the activation energy was calculated to be -49.8 kJ/mol from a straight line fitted to the data. The 30 microns diameter particulate powder catalyst did not show any internal mass transfer limitations but considerable external mass transfer limitations were found. The gas-liquid mass transfer $k_{GL}a_b$ was found to be $6.22\times10^{-3}$ $s^{-1}$ experimentally and $8.13\times10^{-3}$ $s^{-1}$ semi-empirically using Kawase *et al.* (1997) formula. The liquid-solid mass transfer coefficient $k_{SL}$ was found to be $7.22\times10^{-4}$ m $s^{-1}$ using the semi-empirical formula developed by Kushalkar and Pangarkar (1994) and the experimental data. However, since the objective of this work was to study the catalyst deactivation due to chemical poisoning, the system was kept under oxygen mass transfer limitations to avoid the creation of overoxidation which would mask the poisoning effect. This was evidenced by increasing the pressure of the reactor where a decrease in reaction rate was manifested.

Different rate laws representing six likely mechanisms were investigated as well to be able to model the conversion with time. The model based on Shuurman (1992) with an additional effect of strong product adsorption described effectively the experimental data and had the following expression:

$$R = \frac{k_3 K_1 [A](K_2[O_2])^{0.5}}{(1 + K_1[A] + (K_2[O_2])^{0.5} + \frac{[P]}{K_4})^2}$$

Finally, the catalyst was characterised with CO chemisorption and was determined to have a 6% metal dispersion, 0.75 m²/g metallic surface area and 18 nm active particle diameter.

7.1.2) Benzyl Alcohol Oxidation with 2.5%Au-2.5%Pd

The recently developed 2.5wt %Au-2.5wt %Pd Johnson Matthey catalyst was investigated for the oxidation of benzyl alcohol. Studies of this novel catalyst have been recently reported in the literature, where the need to further understand the reaction mechanism and engineering parameters have been raised. The catalyst showed a negligible conversion when used as received which prompted the investigation into a reduction step with hydrogen. Indeed, this reductive pre-treatment dramatically improved the conversion at the expense of the selectivity for the oxidation of benzyl alcohol. The reduction might have cleaned the catalyst surface from impurities such as water and oxides, clearing the active sites. The conversion increased by ~50% after the reduction but the selectivity decreased by ~25% to 70%.

The oxygen effects on the reaction rate and selectivity were then investigated by increasing the pressure and stirring speed to enhance gas-liquid mass transfer. While the reaction rate was zero order in oxygen, the selectivity increased to 83% when the pressure was 6 bar and the stirring speed 20.0 $s^{-1}$. Those findings suggest that the selectivity is enhanced with an increase in oxygen concentration. Therefore, the reactor configuration was redesigned to improve gas-liquid mass transfer. The PBT-U was replaced with a Rushton Turbine to increase the power input. The energy dissipated with the PBT-U was 3.47 $m^2/s^3$ while the energy dissipated from the Rushton turbine was

12.02 $m^2/s^3$. The single orifice sparger was replaced with a disc shower head with 21 holes to maximise the number of bubbles. As a consequence, the selectivity was increased by ~5% up to 88%.

Moreover, the mechanism of the reaction was investigated to determine the origins of the toluene production. Toluene and benzaldehyde were produced in equal amounts in anaerobic conditions and benzyl alcohol is easily hydrogenated to toluene. Hence, it was deduced that toluene is produced by hydrogenation of benzyl alcohol originating from the dehydrogenation of the latter. This explained why the selectivity was sensitive to the oxygen concentration since the gaseous reactant removes effectively surface hydrogen before it reacts with benzyl alcohol to produce toluene. Since the catalyst was being reduced before use to free active sites, it would then be covered in hydrogen. Therefore, the catalyst was used in an anaerobic hydrogenation reaction of pentyne to remove any remaining traces of hydrogen on the catalyst. This second treatment step of the catalyst boosted the selectivity to 93%. The EDX showed carbon deposition on the catalyst after the pentyne hydrogenation which suggests that some active sites were blocked during the alcohol oxidation. This is a likely explanation for the selectivity increase since the reaction rate of the toluene production decreased.

Since the reaction was performed in solvent free conditions to minimise chemical wastes and was zero order in oxygen, no mass transfer of reactant affected the reaction rate. The Arrhenius plot was studied for temperatures between 343K and 393K, where the activation energy was determined to be -44.6 $kJ.mol^{-1}$. Therefore, the reaction could be easily and simplistically described with a power law model with the following equations:

$R = k_3 C_{BnOH}$; $0 < X_{BnOH} <\sim 0.3$
$R = K_3$; $\sim 0.6 < X_{BnOH}$

At 363K, it was found that $k_3 = 0.16\,\text{h}^{-1}$ at low concentrations. At high concentrations, the reaction is zero order and the reaction rate is $K_3 = 1.22\,\text{M.h}^{-1}$. Between 30% and 60%, the reaction order in BnOH decreases as the reaction rate becomes increasingly independent of the alcohol concentration.

Finally, the catalyst was characterised with EDX and XRD to verify the presence of gold and palladium where a stronger presence of palladium was exhibited in agreement with the proposed gold core palladium shell structure. The metal particle is estimated to be around 17nm and the Titania is in the anatase phase as deduced from the XRD.

7.1.4) Alcohol Oxidation with Transition Metal Oxides

The $AgO/SiO_2$, $Fe_2O_3/SiO_2$, $CuO/SiO_2$ and $CuO/Al_2O_3$ Transition Metal Oxides were studied as an alternative to the more expensive and rare PGM based catalysts. While the catalysts studied did not show good potential as an effective heterogeneous oxidation catalyst, the following conclusions were deduced:

1. Ag-O bond is too weak with a bond energy of 213kJ/mole as deduced from the XRD characterisation. Therefore it easily lost oxygen without being able to be re-oxidised.

2. The hematite form of iron oxide has a strong iron-oxygen bond equivalent to 409kJ/mole, rendering the catalyst inert since the lattice oxygen is inflexible.

3. Uncalcined CuO catalyst containing different structural phases was not active. However, the calcined sample showed an increasing conversion with a pressure increase up to 15% for the 1-octanol oxidation at 7 bar.

## 7.2) Recommendations for Future Works

The following are suggestions which would further extend the work presented in this thesis.

- *Structured Catalyst*

The work done in this thesis was performed in the Stirred Tank Reactor. Other efficient reactors such as the trickle bed, coated capillary and bubble column could affect mass transfer coefficients. Indeed, the selectivity studied with the 2.5%Au-2.5%Pd was shown to be dependent on the oxygen transport. Also, a coated capillary column would help study the effects of hydrodynamics on the reaction rate and selectivity.

- *Metal Oxides*

While the metal oxide catalysts studied in this chapter gave a negligible conversion, they might show a more promising activity under the right conditions. As proposed by Grasselli (2002), only some structural phases for the same catalyst composition may be active. Hence, the almost inert hematite iron oxide may be more active under a different phase such as maghemite for example. Moreover, the calcined CuO catalyst gave an

increasing conversion with oxygen partial pressure. Working in a coated CuO capillary as suggested above, may improve the re-oxidation of the copper catalyst which would enhance the reaction rate.

- *Catalyst Characterisation*

While TPR, Chemisorption and XRD were used to describe the catalysts phase and structure, other methods would complete the characterisation. Techniques such as EXAFS (Extended X-Ray Absorption Fine Structure) and Cyclic Voltammetery would help understand the bonding between the gold and palladium in the 2.5%Au-2.5%Pd catalyst. Indeed, the core/shell structure synergy between Au and Pd is still not entirely comprehended.

- *Oxygen probe*

The use of an oxygen probe suitable with an organic solvent would allow a qualitative and quantitative insight into the effects of pressure, mass transfer and modelling on the reaction. Common oxygen probes are usually incompatible with organic solutions and are imprecise at high temperatures. Nonetheless, sophisticated and expensive probe instrument do exist that provide specific data with conditions such as the ones used in this work.

# Appendix A:

## External Mass Transfer Sample Calculation for Chapter IV)

A1) Mass transfer coefficient for $O_2$

The solid-liquid mass transfer coefficient $k_{SL}$ can be determined experimentally by plotting the inverse of the initial reaction rate versus the inverse of the catalyst loading assuming the reaction behaves with a first order in reactants initially as was explained in section 2.6) (Fogler 2001).

Plotting $C_i / R_i$ versus $1/w$ the resulting line will have the following relationships:

$$Intercept = r_b = \frac{1}{k_{GL} a_b}$$

$$Slope = r_c + r_r = \frac{1}{k_{SL} a_P} + \frac{1}{\eta k}$$

Where $r_r, r_c$ and $r_b$ are the internal and reaction, solid-liquid and gas-liquid resistances respectively.

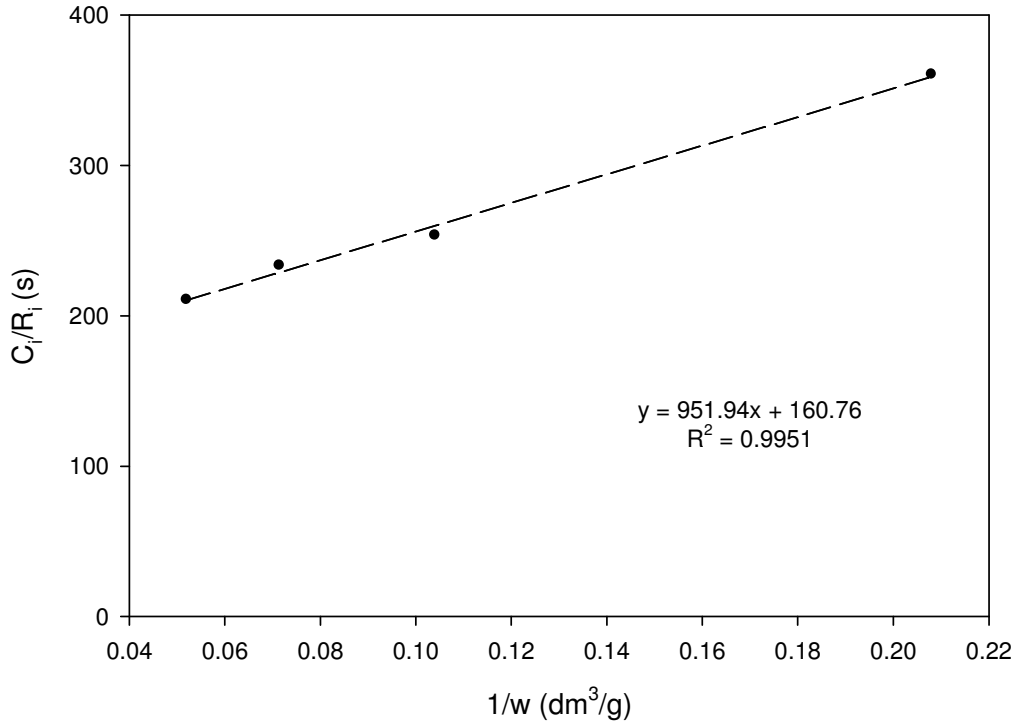


**Figure A1)** Solid-Liquid and Gas-Liquid mass transfer resistances for Oxygen. *Reaction mixture conditions: T=343.15 K;* $P_{Air}$ *=1 Bar; rps=22.5* $s^{-1}$

From Figure A1) it can be deduced that the sum of liquid-solid transport resistance and internal diffusion is equal to 951.94 $gcat.s/dm^3$. $k_{SL}$ can be calculated using the following semi-empirical equation (Kushalkar and Pangarkar 1994).

$$k_{SL} = 1.19\times10^{-3}\left(\frac{N}{N_{sg}}\right)^{1.15}(Sc)^{-0.47}$$

A2) Calculation of Nsg and Ns

Bujalski *et al.* (1998) observed that for upward pumping in three phase stirred tanks:

$$N_{sg} = N_S \left(1 + Q_{VG}\right)^{0.11}$$

Where $Q_{VG}$ is the vessel volume per minute flow and is equal to 0.73 vvm.

Zwietering (1958) found that:

$$N_S = \frac{S \upsilon^{0.1} d_p^{0.2} (g \Delta\rho / \rho_L)^{0.45} X^{0.13}}{D^{0.85}}$$

The following data was used to calculate Ns:

$$\text{S= } 2\left(\frac{T}{D}\right)^{1.33} = 2\left(\frac{8.0}{4.0}\right)^{1.33} = 5.03 \text{ Nienow, 1975}$$

$$N_S = \frac{S \upsilon^{0.1} d_p^{0.2} (g \Delta\rho / \rho_L)^{0.45} X^{0.13}}{d_i^{0.85}} = \frac{5.03 \times (4.64 \times 10^{-7})^{0.1} \times (30 \times 10^{-6})^{0.2} (9.81 \times 1.72)^{0.45} 1.289^{0.13}}{0.04^{0.85}} = 8.28 rps$$

$$N_{sg} = N_S \left(1 + Q_{VG}\right)^{0.11} = 8.28(1 + 0.73)^{0.11} = 8.79 rps$$

$$Sc = \frac{\upsilon}{D_{AB}} = \frac{4.64 \times 10^{-7}}{1.61 \times 10^{-8}} = 28.82$$

A3) Determination of the Resistances

Determination of $r_c$:

$$k_{SL} = 1.19\times10^{-3}\left(\frac{N}{N_{sg}}\right)^{1.15}(Sc)^{-0.47} = 1.19\times10^{-3}\left(\frac{22.5}{13.6}\right)^{1.15}(28.82)^{-0.47} = 7.22\times10^{-4}\,m/s$$

$$a_p = \frac{6}{d_p\rho_c} = \frac{6}{30\times10^{-6}\times2035} = 98.28 m^2/kg\ .$$

$$r_c = \frac{1}{k_{SL}a_P} = 18.26 kgcat.s/m^3$$

$$r_c = 14.08 gcat.s/dm^3$$

Determination of $r_r$:

$$Slope = \frac{1}{k_{SL}a_P} + \frac{1}{\eta k} = 951.94\ gcat.s/dm^3$$

$$Slope = \frac{1}{k_{SL}a_P} + \frac{1}{\eta k} = \frac{1}{7.22\times10^{-4}\times98.28} + \frac{1}{\eta k} = 951.94 gcat.s/dm^3$$

$$r_r = \frac{1}{\eta k} = 951.94 - \frac{1}{7.22\times10^{-4}\times98.28} = 937.86 gcat.s/dm^3$$

Determination of $r_b$:

$$Intercept = r_b = \frac{1}{k_{GL}a_b} = 160.76 s$$

Determination of $k_{GL}$:

Kawase *et al.* (1997) developed a semi-empirical correlation to evaluate $k_{GL}a_b$ in three phase stirred tanks.

$$k_{GL}a_b = C'\sqrt{D}\,\frac{\overline{\rho}_l^{3/5}\,\varepsilon^{(9+4n)/10(1+n)}}{\left(\overline{K}/\overline{\rho}_l\right)^{1/2(1+n)}\sigma^{3/5}}\left(\frac{U_g}{U_t}\right)^{1/2}\left(\frac{\overline{\mu}_a}{\overline{\mu}_w}\right)^{-0.25}$$

Calculation of the speed of free bubble rise $U_t$:

*Bubble diameter and surface area estimation*

An approximate estimation about the bubble diameter can be determined using the correlation found in Hu *et al* (2005)

$$d_b / d_i = 0.74We^{-0.58}$$

Therefore,

$$We = \rho_L N^2 d_i^3 / \sigma = 745.5 \times 22.5^2 \times 0.039^3 / 0.01686 = 1327$$

$$d_b / d_i = 0.74We^{-0.58} = 0.74 \times 1327^{-0.58} = 0.0114\,;\; d_b = 0.04 \times 0.0114 = 4.57 \times 10^{-4}\,m$$

$$a_b = 6.56 \times 10^{-7}\,m^2$$

The speed of bubble free rise is determined by:

$$U_t = d_b^2(\rho_G - \rho_L)g/18\mu$$

$$U_t = d_b^2(\rho_G - \rho_L)g/18\mu = (4.57 \times 10^{-4})^2 \times \left|(1.168 - 745.5)\right| \times 9.81/(18 \times 0.347 \times 10^{-3}) = 0.23 m/s$$

Calculation of the dissipation energy $\varepsilon$

$$\varepsilon = \frac{P_0 \times N^3 \times d_i^5}{V}$$

$$\varepsilon = \frac{1.27 \times N^3 \times d_i^5}{V} = \frac{1.27 \times 22.5^3 \times 0.039^5}{312 \times 10^{-4}} = 0.0418 W / kg$$

Therefore assuming the solution is Newtonian for simplicity and that the density of the solution is the same as the slurry since the solid concentration is negligible:

$$k_{GL}a_b = C'\sqrt{D}\,\frac{\overline{\rho}_l^{3/5}\,\varepsilon^{(9+4n)/10(1+n)}}{\left(\overline{K}/\overline{\rho}_l\right)^{1/2(1+n)}\sigma^{3/5}}\left(\frac{U_g}{U_t}\right)^{1/2}\left(\frac{\overline{\mu}_a}{\overline{\mu}_w}\right)^{-0.25}$$

$$k_{GL}a_b = 0.675\sqrt{16.1\times10^{-9}}\,\frac{745.5^{3/5}\times0.0418}{\left(0.347\times10^{-3}/745.5\right)^{1/4}(16.86\times10^{-3})^{3/5}}\left(\frac{0.002}{0.23}\right)^{1/2}\left(\frac{0.347\times10^{-3}}{4.012\times10^{-4}}\right)^{-0.25}$$

$$k_{GL}a_b = 8.56\times10^{-5}\,\frac{2.21}{2.25\times10^{-3}}\times0.09\times1.03 = 8.13\times10^{-3}\,\mathrm{s}^{-1}$$

# Appendix B:

## Internal Mass Transfer Sample Calculation for Chapter IV)

B1) Wagner-Weisz-Wheeler modulus $M_W$

In order to determine whether the reaction is limited by internal mass transfer the Wagner-Weisz-Wheeler modulus $M_W$ was calculated since it depends on experimental observables.

$$M_W = L^2 \frac{(-r_V / C_A)_{\exp}}{D_{eff}}$$ (Levenspiel 1999)

Where L is the characteristic size of a catalyst particle equal to $\frac{R}{3}$ for spheres. $r_V$ is the observed reaction rate per unit of volume of catalyst particles, $C_A$ is the initial concentration of reactants and $D_{eff}$ is the effective diffusivity defined as:

$$D_{eff} = \frac{\varepsilon_P D}{\tau_P}$$ where

$$\frac{1}{D} = \frac{1}{D_m} + \frac{1}{D_K}$$

$\varepsilon_P$ is the porosity of the catalyst, $\tau_P$ is the tortuosity, $D_m$ is the molecular diffusivity and $D_K$ is the Knudsen diffusivity. The Knudsen diffusivity is only applicable to gases (Satterfield 1991) and it is assumed that the reacting oxygen is in soluble form therefore $D = D_m$. The effective diffusivity was calculated with the average values of porosity and

tortuosity of 0.4 and 4 respectively (Winterbottom and King 1999) and gives a value of $1.61\times10^{-8}\ m^2.s^{-1}$ for oxygen and $1.33\times10^{-9}\ m^2.s^{-1}$ for 2-octanol at 343K.

The initial concentration of oxygen and 2-octanol are $6.58\times10^{-1}\ moles.m^{-3}$ and $248\ moles.m^{-3}$ respectively and $L = 5\times10^{-6}\,m$. The initial reaction rate based on the volume of catalyst in the reactor is $r_V = 3.66\ moles.m_{cat}^{-3}.s^{-1}$.

$$M_W = L^2\frac{(-r_V/C_A)_{\exp}}{D_{eff}} = (5\times10^{-6})^2\frac{(3.66/6.58\times10^{-1})}{1.61\times10^{-8}} = 8.63\times10^{-3}$$ For oxygen

$$M_W = L^2\frac{(-r_V/C_A)_{\exp}}{D_{eff}} = (5\times10^{-6})^2\frac{(3.66/248)}{1.33\times10^{-9}} = 2.77\times10^{-4}$$ For 2-octanol.

Both these values are much lower than 0.15 which is the Weisz-Prater (Levenspiel 1999) criterion for a diffusion free regime. Hence it can be deduced that the reaction happens on the outer surface of the catalyst.

# Appendix C:

## Matlab Program Sample for Chapter IV)

C1) Derivation of Model A)

Each proposed rate law in Table 4.5) was integrated into an equation in which it is a function of time. For example:

Model A: $$f(t) = \frac{-d[A]}{dt} = \frac{k_3 K_1 [A](K_2[O_2])^{0.5}}{(1 + K_1[A] + (K_2[O_2])^{0.5} + \frac{[P]}{K_4})^2}$$

For simplification, let

$$[P] = ([A_0] - [A])$$
$$a = k_3 K_1 (K_2[O_2])^{0.5}$$
$$b = 1 + (K_2[O_2])^{0.5} + \frac{[A_0]}{K_4}$$
$$c = K_1 - \frac{1}{K_4}$$

Model A can then be integrated into the following

$$\frac{-d[A]}{dt} = \frac{a[A]}{(b + c[A])^2}$$

$$\frac{-dt}{d[A]} = \frac{(b + c[A])^2}{a[A]}$$

$$-\int dt = \int_{[A_i]}^{[A]} \left[ \frac{b^2}{a[A]} + \frac{2bc}{a} + \frac{c^2[A]}{a} \right]$$

$$-t = \left[ \frac{b^2}{a} \ln[A] + \frac{2bc}{a}[A] + \frac{c^2[A]^2}{2a} \right]_{A_i}^{A}$$

$$f(t) = 0 = \frac{b^2}{a} \ln[A] + \frac{2bc}{a}[A] + \frac{c^2[A]^2}{2a} - \frac{b^2}{a} \ln[A_i] - \frac{2bc}{a}[A_i] - \frac{c^2[A_i]^2}{2a} + t$$

The final equation will hence be used in Excel to determine the kinetic parameters and in Matlab to include the mass transfer effects. Eventually, the Matlab plot should describe the experimental data.

C2) Kinetic Parameters

Initial reaction rates with different starting alcohol concentrations were performed in the Laboratory setup to exclude mass transfer limitations and to determine the effects of initial alcohol concentration on the reaction rate. The air flow and stirring were increased until any further increase does not change the rate, where it can then be assumed that there are no masking mass transfer effects and the reactions happening are in the kinetic regime. The reaction rate initially increases linearly initially since no significant amount of product is being formed to slow the catalysis. The kinetic parameters $K_1$, $K_2$ and $k_3$ were determined with the help of Excel by using the "solver"

function. The initial experimental reaction rates were plotted against different initial alcohol concentration in Figure C1). After introducing the derived equation f(t), the solver function determines statistically the kinetic parameters with minimum error.

The following graph represents the experimental data and the modelled data using the "solver" function to find and minimise the errors as much as possible in the kinetic parameters.

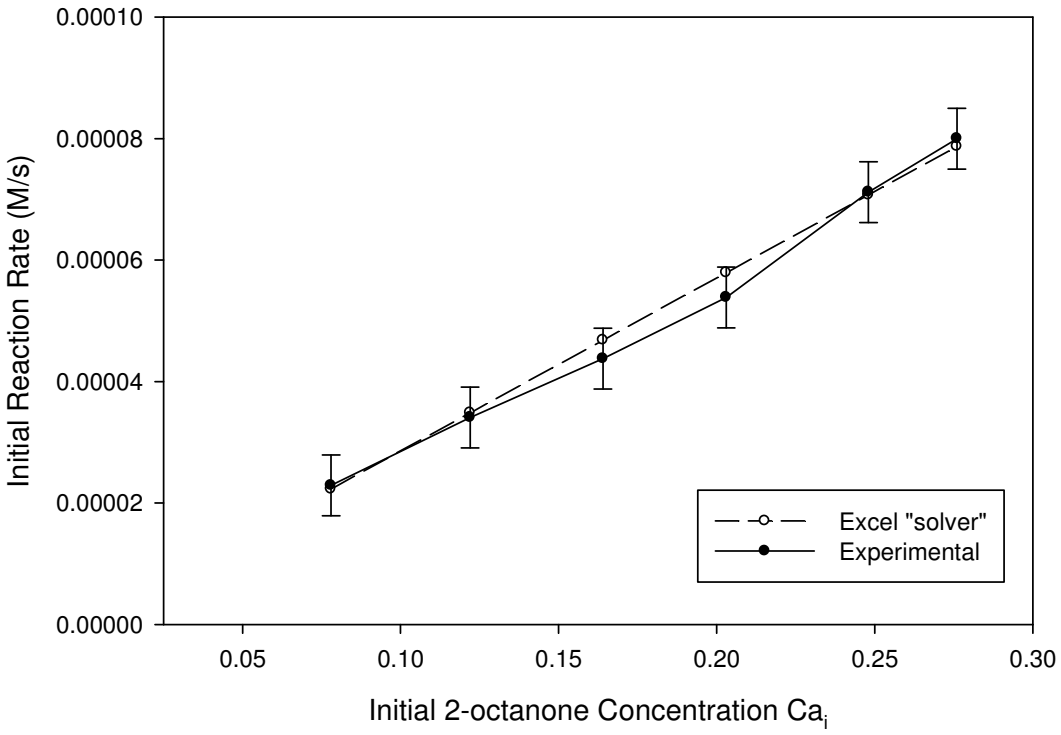


**Figure C1)** Plot of the experimental reaction rate and of the Excel rate law with calculated kinetic parameters using function f(t). *Reaction mixture conditions: T=343.15 K;* $P_{Air}$ *=1 Bar; rps=22.5* $s^{-1}$ *; 0.3g cat.*

The kinetic parameters $K_1$, $K_2$ and $k_3$ determined by Excel and used in Figure C1) are the following:

$K_1$= 0.005
$K_2$= 42.26
$k_3$= 0.3

C3) Matlab

After developing the integrated form of the rate law and determining the values of the kinetic parameters, the Matlab script could be written. The values in Table C1) were used.

| $[O_2]$ (M) | $K_1 (M^{-1})$ | $K_2 (M^{-1})$ | 3 x $k_3$ $(M.g^{-1}.s^{-1})$ | $K_4 (M)$ | CAi (M) |
|---|---|---|---|---|---|
| 0.001 | 0.005 | 42.26 | 0.3 | 0.36 | 0.248 |

**Table C1)** Parameters used in the modelling of the experimental data in Figure 4.12)

From Table C1), the oxygen concentration was calculated from section 4.8 and Appendix A. CAi is the initial concentration of 2-octanol used. $K_4$ was determined experimentally from Figure 4.6). The following Matlab script was used and Figure C2) shows the resulting plot.

1. function [CA,Time,Redexp,Texp]= Model A

2. $[O_2]$=0.001;
3. k1=0.005;
4. k2=42.26
5. k3=0.3
6. k4=0.36
7. CAi=0.248;
8. a=k3*k1*(k2*$[O_2]$)^0.5;
9. b=1+(k2*$[O_2]$)^0.5+CAi/k4;
10. c=(k1-1/k4);
11. Redexp=[0.248, 0.191231219, 0.1580577956, 0.1205995312, 0.07569495,0.06209932,0.048,0.04];
12. Texp=[0, 1800, 3600, 5400, 9000, 10800, 14400, 18000 ];
13. Time=[0:100:1.5*Texp(1,max(length(Texp)))]
14. CA=[];
15. for i=1:max(length(Time))
16. CA(i)=fsolve(@(x)((b^2/a*log((x))+2*b*c/a*x+c^2/(a*2)*x^2)-((b^2/a*log((CAi))+2*b*c/a*CAi+c^2/(a*2)*CAi^2))+Time(i)),CAi); i=i+1;
17. end
18. plot(Texp,Redexp,'o',Time,CA);

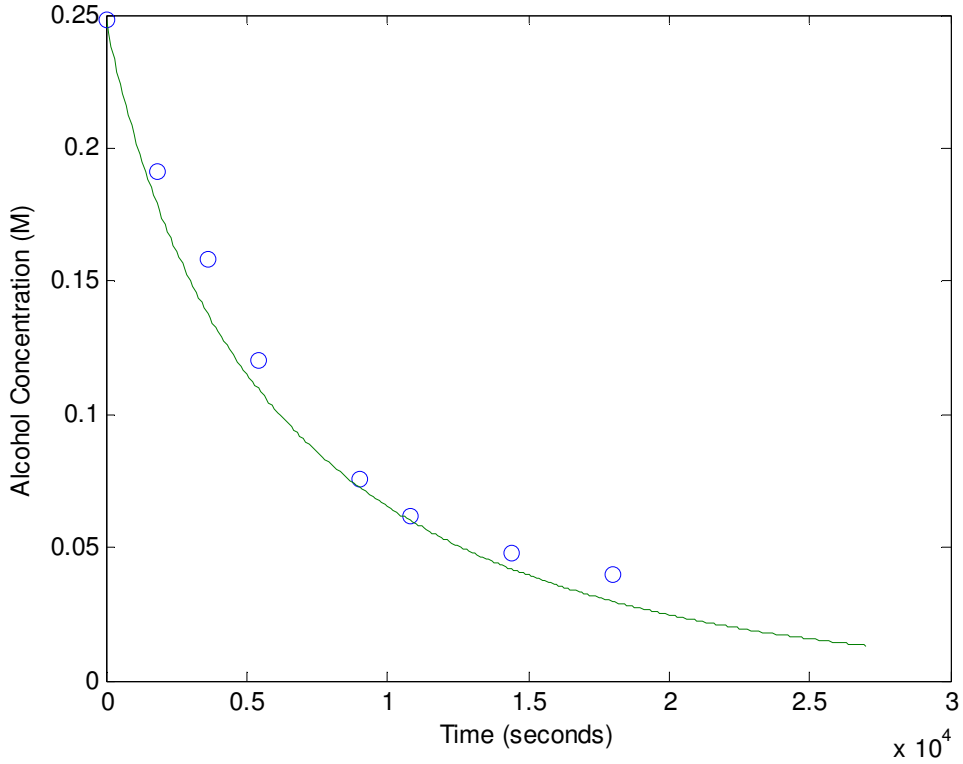


**Figure C2)** Plot of the Matlab Scrip for Model A).

# Appendix D:

## Supplementary Information used for calculations

D1) Additional Data

| Name of Reagent | Form | Purity | Molecular Weight | b.p °C | Sp. gr |
|---|---|---|---|---|---|
| Heptane | Liquid | 99 % | 100.21 g/mol | 371.6 K | 0.684 |
| DMSO | Liquid | 99 % | 78.13 g/mol | 462 K | 1.1004 |
| p-Xylene | Liquid | 99 % | 106.16 g/mol | 412 K, | 0.861 |
| 1-4, Dioxane | Liquid | 99 % | 88.11 g/mol | 374K | 1.033 |
| 2-Octanol | Liquid | 99 % | 130.23 g/mol | 451K | 0.819 |
| Benzyl Alcohol | Liquid | 99 % | 108.14 g/mol | 478K | 1.044 |
| 2-Pentanol | Liquid | 99 % | 72.15 g/mol | 391K | 0.809 |
| 1-Octanol | Liquid | 99 % | 130.23 g/mol | 468K | 0.824 |
| Water | Liquid | >99.5 % | 18 | 373K | 0.990 |
| Hydrogen | Gas | >99.99 % | 2 | - | 0.08 |
| Nitrogen | Gas | >99.99 % | 28 | - | 1 |
| Air | Gas | - | 29 | - | 1 |

**Table D1)** Physical properties of reagents, solvents and gases

| Platinum-Bismuth | |
|---|---|
| Support type | Carbon |
| Support size | ~30 microns |
| Catalyst metal loading | 5 % |
| Catalyst dispersion | 6.0% |
| Particle density | 2.35 g/cm³ |
| Active Particle Diameter | 18nm |
| Metallic Surface Area | 0.75 m²/g - |
| Water content | 55% |
| Surface Area | ~1000 m²/g |

| Gold-Palladium | |
|---|---|
| Support type | Titania |
| Support size | ~30 microns |
| Au Catalyst loading | 2.5 % |
| Pd Catalyst loading | 2.5 % |
| Particle density | 4.80 g/cm³ |
| Support phase | Anatase |
| Active Particle Diameter | 17nm |
| Water content | — |
| Surface Area | ~100 m²/g |

**Table D2)** Properties of catalysts

| Name | Equation | Relation |
|---|---|---|
| Reynolds Number | $\mathrm{Re} = \frac{\rho_L N D^2}{\mu}$ | $\frac{inertial\ \ force}{viscous\ \ force}$ |
| Sherwood number | $Sh = \frac{k_{SL} d_P}{D_m}$ | $\frac{mass\ diffusivity}{molecular\ diffusivity}$ |
| Schmidt number | $Sc = \frac{\mu}{\rho\ D_m}$ | $\frac{kinematic\ viscosity}{molecular\ diffusivity}$ |

**Table D3)** Dimensionless groups

D2) Diffusivity of Oxygen and 2-Octanol in various solvents for Chapter 4

The diffusivity of a substance in a mixed solvent is affected by the viscosity and mole fraction of the different solvent constituents.

$D_m \mu_m^{0.8} = \sum x_i D_{Ai} \mu_i^{0.8}$ (Poling, Prausnitz *et al.* 2001))

The diffusivity of a substance in a pure solvent can be estimated using the following semi-empirical equation (Chang and Wilke 1955).

$$D_{AB} = \frac{7.4\times10^{-8}(\phi M_B)^{1/2}T}{\eta_B V_A^{0.6}}$$

Where $\phi$=association factor of solvent B, dimensionless

$M_B$= Molecular weight of solvent B, g/mol

$V_A$=molar volume of solute A at its normal boiling temperature, $cm^3/mol$

$\eta_B$= viscosity of solvent B, cP

T=temperature, K

The association factors for the solvents used are equal to 1. $V_A$ is 14 and 189 $cm^3.mol^{-1}$ for oxygen and 2-octanol respectively using Schroeder's additive method properties (Poling, Prausnitz *et al.* 2001). Table C1) summarises the results calculated.

| | Diffusivity coefficient in heptane($10^{-9}m^2.s^{-1}$) | Diffusivity coefficient in dioxane($10^{-9}m^2.s^{-1}$) | Diffusivity coefficient in octanol($10^{-9}m^2.s^{-1}$) | Diffusivity coefficient in mixture($10^{-9}m^2.s^{-1}$) |
|---|---|---|---|---|
| Oxygen | 15.0 | 14.1 | 17.9 | 16.1 |
| Octanol | 4.05 | 1.74 | 0.72 | 1.33 |

**Table D4)** Diffusivity of oxygen and 2-octanol in the solvent mixture at 343K

D3) Solvent Viscosity and Density for Chapter 4

The viscosity of heptane, dioxane and 2-octanol at 343 K were calculated as following. The viscosity is a function of temperature with the general form: $\ln \mu = A + \frac{B}{T} + CT + DT^2$ where A, B, C and D are constant parameters characteristics of each substance (Yaws 2003).

| | A | B | C | D | $\mu$ (cP) |
|---|---|---|---|---|---|
| Dioxane | -7.5724 | 1.3813E3 | 0.0136 | -1.1464E-5 | 0.590 |
| Heptane | -5.7782 | 8.0587E2 | 0.0134 | -1.4794E-5 | 0.267 |
| 2-Octanol | -17.262 | 3.2080E3 | -2.258E-5 | -2.2582E-5 | 1.732 |

**Table D5)** Viscosity of solvents at 343K

But since the reaction is performed in a mixture of dioxane, heptane and 2-octanol as a reactant, the viscosity of the whole mixture must be taken into account. Liquid viscosity is very sensitive to the structure of the constituent molecules (Poling, Prausnitz *et al.* 2001). Therefore the resulting viscosity of the mixture can be determined by:

$\ln \mu_m = \sum_i x_i \ln \mu_i + \sum_{i \neq j} x_i x_j G_{ij}$ (Grunberg and Nissan 1949)

Where x is the liquid mole fraction and G is a group interaction parameter that can be found in literature (Isdale 1979).

| x(heptane) | x(dioxane) | x(octanol) | $G_{12}$ (heptane-dioxane) | $G_{13}$ (octanol-dioxane) | $G_{23}$ (heptane-octanol) |
|---|---|---|---|---|---|
| 0.722 | 0.245 | 0.032 | 0.076 | -0.343 | -0.239 |

**Table D6)** parameters for the determination of the solvent mixture viscosity

The viscosity of the mixture hence becomes 0.347 cP or $0.347 \times 10^{-3} kg.s^{-1}.m^{-1}$

The density of the mixture was determined experimentally at 343K to be $745.5 \times 10^{-3} g.cm^{-3}$.

D4) Surface Tension Determination for Chapter 4

The surface tension of pure liquids as a function of temperature can be calculated using the following equations and have a general form:

$\sigma = A(1-T/T_c)^n$ Where A and n are listed empirical values that can be found in (Yaws 2003).

| Pure Liquid at the experimental temperature | $\sigma = A(1-T/T_c)^n$ N/m |
|---|---|
| n-Heptane (343K) | 0.015 |
| 1-4 Dioxane (343K) | 0.026 |
| Benzyl Alcohol (343K) | 0.029 |

**Table D7)** Surface tension values

For a mixture of heptane and dioxane the resulting surface tension can be calculated from the following equation (Poling, Prausnitz *et al.* 2001)

$$\sigma_m^{1/4} = \frac{\rho_{Lm} \sum_{i=1}^{n} x_i \sigma_i^{1/4}}{\rho_{Li}}$$

Where $\sigma_m$ is the surface tension of the mixture, $\rho_{Li}$ and $\rho_{Lm}$ are the molar density of the pure liquid and mixture respectively, and $x_i$ is the mole fraction.

| | $x_i$ | $\rho_{Li}$ (mol/L) | $\sigma_i$ (N/m) |
|---|---|---|---|
| Heptane | 0.745 | 6.82 | 0.015 |
| Dioxane | 0.255 | 11.7 | 0.026 |

**Table D8)** Parameters used to evaluate the surface tension of the mixture

At 343K, $\rho_{Lm}$ is 7.67 mol/l. Therefore,

$$\sigma_m^{1/4} = \frac{\rho_{Lm} \sum_{i=1}^{n} x_i \sigma_i^{1/4}}{\rho_{Li}} = 2.026 \text{ mN/m}$$

As a result $\sigma_m$=16.86 mN/m

# Appendix E:

## Transition Metal Oxide

E1) XRD data of the Metal Oxides

The following data was provided by the University of Birmingham, School of Chemistry upon the XRD analysis of the Transition Metal Oxide which allowed the identification of the catalyst phases.

| Catalyst | 1) d-Spacing ( $\mathring{A}$ ) /Relative intensity | 2) d-Spacing ( $\mathring{A}$ ) /Relative intensity | 3) d-Spacing ( $\mathring{A}$ ) /Relative intensity | Phase |
|---|---|---|---|---|
| $AgO / SiO_2$ | 2.08/100% | 8.53/94% | 2.37/82.5% | Undefined |
| $Fe_2O_3 / SiO_2$ | 2.7/80% | 1.69/43% | 2.52/50% | Hematite |
| $CuO / SiO_2$ calcined | 2.53/100% | 2.99/97.3% | — | Tenorite |
| $CuO / Al_2O_3$ | 1.39/100% | 1.99/65% | 2.53/58% | Undefined |

**Table E1)** XRD data provided for the identification of the different phases

E2) Metal Oxides Pictures

A)

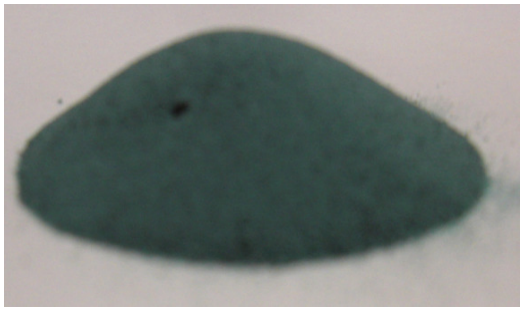

B)

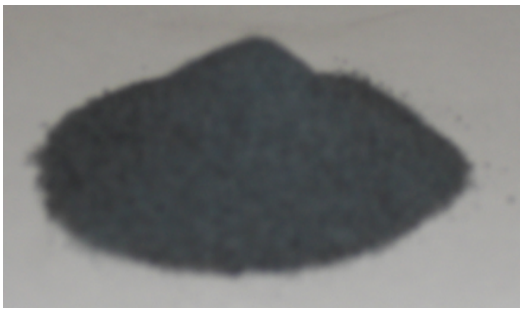

C)

D)

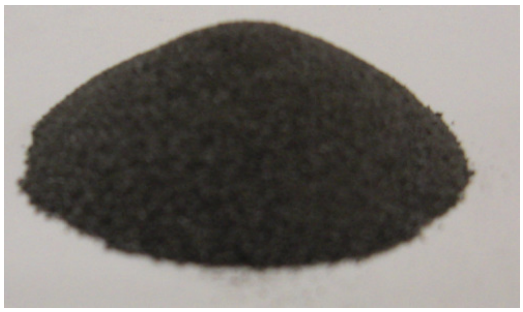

E)

**Figure E1)** TMO catalyst Pictures. *A) Iron oxide on Silica; B) Copper oxide on Alumina; C) Calcined Copper Oxide on Silica; D) Silver oxide on Silica; E) Used Silver Oxide on Silica*

Abad, Corma, et al. (2008). "Catalyst Parameters Determining Activity and Selectivity of Supported Gold Nanoparticles for the Aerobic Oxidation of Alcohols: The Molecular Reaction Mechanism." Chemistry - A European Journal **14**(1): 212-222.

Abad, A., P. Concepción;, et al. (2005). "A Collaborative Effect between Gold and a Support Induces the Selective Oxidation of Alcohols13." Angewandte Chemie International Edition **44**(26): 4066-4069.

Alvarez, A. and J. Ancheyta (2008). "Modeling residue hydroprocessing in a multi-fixed-bed reactor system." Applied Catalysis A: General **351**(2): 148-158.

Anderson, R., K. Griffin, et al. (2003). "Selective Oxidation of Alcohols to Carbonyl Compounds and Carboxylic Acids with Platinum Group Metal Catalysts." Advanced Synthesis & Catalysis **345**(4): 517-523.

Armenante, P. M. and D. J. Kirwan (1989). "Mass transfer to microparticles in agitated systems." Chemical Engineering Science **44**(12): 2781-2796.

Atkins, P. (2002). Physical Chemistry, Oxford University Press.

Aubin, J., N. Le Sauze, et al. (2004). "PIV measurements of flow in an aerated tank stirred by a down- and an up-pumping axial flow impeller." Experimental Thermal and Fluid Science
5th international conference on Gas-Liquid and Gas-Liquid-Solid Reactor Engineering **28**(5): 447-456.

Auer, E., A. Freund, et al. (1998). "Carbons as supports for industrial precious metal catalysts." Applied Catalysis A: General **173**(2): 259-271.

Bae, I. T., X. Xing, et al. (1990). "In situ Fourier transform infrared reflection absorption spectroscopic studies of glucose oxidation on platinum in acid." Journal of Electroanalytical Chemistry **284**(2): 335-349.

Bamwenda, G. R., S. Tsubota, et al. (1997). "The influence of the preparation methods on the catalytic activity of platinum and gold supported on TiO2 for CO oxidation." Catalysis Letters **44**(1): 83-87.

Battino, R., T. Rettich, et al. (1983). "The solubility of oxygen and ozone in liquids." Journal of Physical Chemistry Reference Data **12**(2): 163.

Besson, M. and P. Gallezot (2003). "Deactivation of metal catalysts in liquid phase organic reactions." Catalysis Today
Catalyst Lifecycle Meeting **81**(4): 547-559.

Blaser, H.-U., A. Indolese, et al. (2001). "Supported palladium catalysts for fine chemicals synthesis." Journal of Molecular Catalysis A: Chemical **173**(1-2): 3-18.

Bond, G. C. (1962). An Introduction to Catalysis by Metals.

Bond, G. C. (2000). "Diagnostic use of compensation phenomena in heterogeneous catalysis-: Reactions of alkanes on platinum and palladium catalysts." Applied Catalysis A: General **191**(1-2): 23-34.

Bond, G. C. and D. T. Thompson (1999). "Catalysis by gold." Catalysis Reviews-Science and Engineering **41**(3-4): 319-388.

Boudart, M. (1972). "Two-step catalytic reactions." AIChE Journal **18**(3): 465-478.

Bronnimann, C., Z. Bodnar, et al. (1994). "Direct Oxidation of L-Sorbose to 2-Keto-L-gulonic Acid with Molecular Oxygen on Platinum- and Palladium-Based Catalysts." Journal of Catalysis **150**(1): 199-211.

Bujalski, W., M. Konno, et al. (1998). Suspension at high solid concentrations in agitated vessels. IChemE Research Event, A Two-Day Symposium, Newcastle upon Tyne, institution of Chemical Engineers,.

Bujalski, W., A. W. Nienow, et al. (1990). "The use of upward pumping 45° pitched blade turbine impellers in three-phase reactors." Chemical Engineering Science **45**(2): 415-421.

Butt, J. B. (1980). Catalyst Deactivation. Amsterdam.

Butt, J. B. (1982). Progress in Catalyst Deactivation. Boston.

Cainelli, G. and G. Cardillo (1984). Chromium Oxidation in Organic Chemistry. Berlin, Springer-Verlag.

Calderbank, P. H. and M. B. Moo-Young (1961). "The continuous phase heat and mass-transfer properties of dispersions." Chemical Engineering Science **16**(1-2): 39-54.

Carey, F. A. and R. J. Sundberg (2007). Advanced Organic Chemistry - Part A: Structure and Mechanisms, Springer - Verlag.

Carrettin, S., P. McMorn, et al. (2003). "Oxidation of glycerol using supported Pt, Pd and Au catalysts." Physical Chemistry Chemical Physics **5**(6): 1329-1336.

Chang, P. and C. R. Wilke (1955). "Some Measurements of Diffusion in Liquids. doi:10.1021/j150529a005." The Journal of Physical Chemistry **59**(7): 592-596.

Chapman, C. M., A. W. Nienow, et al. (1983). "Particle-Gas-Liquid Mixing in stirred vessels Part 1." Chemical Engineering Research & Design **61a**: 71.

Chapman, C. M., A. W. Nienow, et al. (1983). "Particle-Gas-Liquid Mixing in stirred vessels Part 2." Chemical Engineering Research & Design **61a**: 82.

Chaudhari, R. V., R. V. Gholap, et al. (1987). "Gas-Liquid Mass Transfer in "Dead-End" Autoclave Reactors." The Canadian Journal of Chemical Engineering **65**: 744-751.

Chaudhari, R. V. and P. A. Ramachandran (1980). "Three phase slurry reactors." AIChE Journal **26**(2): 177-201.

Cheremisinoff, N., P. Rosenfeld, et al. (2008). Responsible Care - A New Strategy for Pollution Prevention and Waste Reduction through Environmental Management., Gulf Publishing Company.

Christensen, C., J. Betina, et al. (2006). "Formation of Acetic Acid by Aqueous-Phase Oxidation of Ethanol with Air in the Presence of a Heterogeneous Gold Catalyst13." Angewandte Chemie International Edition **45**(28): 4648-4651.

Chuang, K. T., S. Cheng, et al. (1992). "Removal and destruction of benzene, toluene, and xylene from wastewater by air stripping and catalytic oxidation." Ind. Eng. Chem. Res. **31**(11): 2466-2472.

Clark, J. H. and C. N. Rhodes (2000). Clean Synthesis using Porous Inorganic Solid Catalysts and Supported Reagents.

Colmati, F., E. Antolini, et al. (2006). "Effect of temperature on the mechanism of ethanol oxidation on carbon supported Pt, PtRu and Pt3Sn electrocatalysts." Journal of Power Sources **157**(1): 98-103.

Davis, B. H. and W. P. Hettinger (1983). "ACS Symposium Series." ACS **No 222**.

de Lange, M. W., J. G. van Ommen, et al. (2001). "Deoxygenation of benzoic acid on metal oxides: 1. The selective pathway to benzaldehyde." Applied Catalysis A: General **220**(1-2): 41-49.

Dean, J. A. (1999). Lange's Handbook of Chemistry.

Demirel, S., P. Kern, et al. (2007). "Oxidation of mono- and polyalcohols with gold: Comparison of carbon and ceria supported catalysts." Catalysis Today **122**(3-4): 292-300.

DiCosimo, R. and G. M. Whitesides (1989). "Oxidation of 2-propanol to acetone by dioxygen on a platinized electrode under open-circuit conditions." J. Phys. Chem. **93**(2): 768-775.

Dijkgraaf, P. J. M., M. J. M. Rijk, et al. (1988). "Deactivation of platinum catalysts by oxygen : 1. Kinetics of the catalyst deactivation." Journal of Catalysis **112**(2): 329-336.

Dimitratos, N., J. A. Lopez-Sanchez, et al. (2007). "Solvent free liquid phase oxidation of benzyl alcohol using Au supported catalysts prepared using a sol immobilization technique." Catalysis Today **122**(3-4): 317-324.

Dimitratos, N., F. Porta, et al. (2005). "Synergetic effect of platinum or palladium on gold catalyst in the selective oxidation of D-sorbitol." Catalysis Letters **99**(3): 181-185.

Dimitratos, N., A. Villa, et al. (2006). "Pd and Pt catalysts modified by alloying with Au in the selective oxidation of alcohols." Journal of Catalysis **244**(1): 113-121.

Dirkx, J. M. H. and H. S. van der Baan (1981). "The oxidation of glucose with platinum on carbon as catalyst." Journal of Catalysis **67**(1): 1-13.

Donze, C., P. Korovchenko, et al. (2007). "Aerobic selective oxidation of (hetero)aromatic primary alcohols to aldehydes or carboxylic acids over carbon supported platinum." Applied Catalysis B: Environmental **70**(1-4): 621-629.

Doornkamp, C., M. Clement, et al. (1999). "Activity and selectivity patterns in the oxidation of allyl iodide on the period IV metal oxides: The participation of lattice oxygen in selective and total oxidation reactions." Applied Catalysis A: General **188**(1-2): 325-336.

Doornkamp, C. and V. Ponec (2000). "The universal character of the Mars and Van Krevelen mechanism." Journal of Molecular Catalysis A: Chemical **162**(1-2): 19-32.

Ebitani, K., H.-B. Ji, et al. (2004). "Highly active trimetallic Ru/CeO2/CoO(OH) catalyst for oxidation of alcohols in the presence of molecular oxygen." Journal of Molecular Catalysis A: Chemical **212**(1-2): 161-170.

Edwards, J., P. Landon, et al. (2007). "Outstanding Meeting Paper/Review: Nanocrystalline gold and gold–palladium as effective catalysts for selective oxidation." Journal of materials research **22**: 831.

Enache, D. I., D. Barker, et al. (2007). "Solvent-free oxidation of benzyl alcohol using titania-supported gold-palladium catalysts: Effect of Au-Pd ratio on catalytic performance." Catalysis Today **122**(3-4): 407-411.

Enache, D. I., J. K. Edwards, et al. (2006). "Solvent-Free Oxidation of Primary Alcohols to Aldehydes Using Au-Pd/TiO2 Catalysts 10.1126/science.1120560." Science **311**(5759): 362-365.

Enache, D. I., D. W. Knight, et al. (2005). "Solvent-free Oxidation of Primary Alcohols to Aldehydes using Supported Gold Catalysts." Catalysis Letters **103**(1): 43-52.

Farrauto, R. J. and C. H. Bartholemew (1988). Fundamentals of Industrial Catalytic Processes. London.

Fishwick, R. P., J. M. Winterbottom, et al. (2005). "Hydrodynamic Measurements of Up- and Down-Pumping Pitched-Blade Turbines in Gassed, Agitated Vessels, Using Positron Emission Particle Tracking." Ind. Eng. Chem. Res. **44**(16): 6371-6380.

Fogler, H. S. (2001). Elements of Chemical Reaction Engineering.

Froment, G. F. (1980). A Quantitative Approach of Catalyst Deactivation by Coke Formation. Amsterdam.

Fuentes, G. A. (1985). "Catalyst deactivation and steady-state activity: A generalized power-law equation model." Applied Catalysis **15**(1): 33-40.

Gabriele, A., A. W. Nienow, et al. "Use of angle resolved PIV to estimate local specific energy dissipation rates for up- and down-pumping pitched blade agitators in a stirred tank." Chemical Engineering Science **In Press, Corrected Proof**.

Gallezot, P. (1997). "Selective oxidation with air on metal catalysts." Catalysis Today Heterogenous Catalysis in Organic Reactions **37**(4): 405-418.

Gangwal, V. R., J. v. d. Schaaf, et al. (2004). "Catalyst performance for noble metal catalysed alcohol oxidation: reaction-engineering modelling and experiments." Catalysis Today **96**(4): 223-234.

Gangwal, V. R., J. van der Schaaf, et al. (2005). "Influence of pH on noble metal catalysed alcohol oxidation: reaction kinetics and modelling." Journal of Catalysis **229**(2): 389-403.

Gangwal, V. R., J. van der Schaaf, et al. (2005). "Noble-metal-catalysed aqueous alcohol oxidation: reaction start-up and catalyst deactivation and reactivation." Journal of Catalysis **232**(2): 432-443.

Gangwal, V. R., B. G. M. van Wachem, et al. (2002). "Platinum catalysed aqueous alcohol oxidation: model-based investigation of reaction conditions and catalyst design." Chemical Engineering Science **57**(24): 5051-5063.

Golovanov, I. and S. Zhenodarova (2005). "Quantitative Structure-Property Relationship: XXIII. Solubility of Oxygen in Organic Solvents." Russian Journal of General Chemistry **75**(11): 1795-1797.

Grasselli, R. K. (2001). "Genesis of site isolation and phase cooperation in selective oxidation catalysis." Topics in Catalysis **15**(2): 93-101.

Grasselli, R. K. (2002). "Fundamental Principles of Selective Heterogeneous Oxidation Catalysis." Topics in Catalysis **21**(1): 79-88.

Grootendorst, E. J., Y. Verbeek, et al. (1995). "The Role of the Mars and Van Krevelen Mechanism in the Selective Oxidation of Nitrosobenzene and the Deoxygenation of Nitrobenzene on Oxidic Catalysts." Journal of Catalysis **157**(2): 706-712.

Grunberg, L. and A. H. Nissan (1949). "Mixture law for viscosity." Nature **164**: 799.

Hackett, S. F. J., Brydson R.M, et al. (2007). "High-Activity, Single-Site Mesoporous Pd Catalysts for Selective Aerobic Oxidation of Allylic Alcohols13." Angewandte Chemie International Edition **46**(45): 8593-8596.

Hamilton, C. A., S. D. Jackson, et al. (2002). "Competitive reactions in alkyne hydrogenation." Applied Catalysis A: General **237**(1-2): 201-209.

Hardacre, C., E. A. Mullan, et al. (2005). "Use of a rotating disc reactor to investigate the heterogeneously catalysed oxidation of cinnamyl alcohol in toluene and ionic liquids." Journal of Catalysis **232**(2): 355-365.

Hayden, B. E. (1997). "The promotion of CO electro-oxidation on platinum-bismuth as a model for surface mediated oxygen transfer." Catalysis Today
Fuel Cells and Catalysis **38**(4): 473-481.

Heineman, H. (1981). Catalysis, Science and Technology, Springer.

Hills, C. W., M. S. Nashner, et al. (1999). "Carbon Support Effects on Bimetallic Pt-Ru Nanoparticles Formed from Molecular Precursors." Langmuir **15**(3): 690-700.

Hongli, W., Z. Qinghong, et al. (2005). "Solvent-Free Aerobic Oxidation of Alcohols Catalyzed by an Efficient and Recyclable Palladium Heterogeneous Catalyst." Advanced Synthesis & Catalysis **347**(10): 1356-1360.

Hughes, M. D., Y.-J. Xu, et al. (2005). "Tunable gold catalysts for selective hydrocarbon oxidation under mild conditions." **437**(7062): 1132-1135.

Hutchings, G. J. (1985). "Vapor phase hydrochlorination of acetylene: Correlation of catalytic activity of supported metal chloride catalysts." Journal of Catalysis **96**(1): 292-295.

Hutchings, G. J. (2008). "Nanocrystalline gold and gold palladium alloy catalysts for chemical synthesis." Chemical Communications(10): 1148-1164.

Hutchings, G. J. and M. Haruta (2005). "A golden age of catalysis: A perspective." Applied Catalysis A: General
Catalysis by Gold **291**(1-2): 2-5.

Isdale, J. D. (1979). Proceedings of Symposium on Transp. Prop. Fluids and Fluid Mixtures. National Engineering Lab, East Kilbride, Glasgow, Scotland,.

Iwamoto, M., Y. Yoda, et al. (1978). "Study of metal oxide catalysts by temperature programmed desorption. 4. Oxygen adsorption on various metal oxides." J. Phys. Chem. **82**(24): 2564-2570.

Jackson, S. D., C. A. Hamilton, et al. (2001). "The Hydrogenation of c-5 Alkynes over Palladium Catalysts." Reaction Kinetics and Catalysis Letters **73**(1): 77-82.

Jackson, S. D. and A. Monaghan (2007). "Hydrogenation of unsaturated hydrocarbons--40 years on: Hydrogenation of 1,3-pentadiene over Pd/alumina." Catalysis Today Special Issue Dedicated to Mike Winterbottom **128**(1-2): 47-51.

Jia, C.-G., F.-Y. Jing, et al. (1994). "Liquid-phase oxidation of alcohols by dioxygen using oxide-supported platinum catalysts." Journal of Molecular Catalysis **91**(1): 139-147.

Kapteijn, F., G. B. Marin, et al. (1999). "Catalytic reaction engineering." Studies in Surface Science and Catalysis. **123**: 375.

Kawabata, T., Y. Shinozuka, et al. (2005). "Nickel containing Mg-Al hydrotalcite-type anionic clay catalyst for the oxidation of alcohols with molecular oxygen." Journal of Molecular Catalysis A: Chemical **236**(1-2): 206-215.

Kawase, Y., S. K;, et al. (1997). "Gas-Liquid Mass Transfer in Three-Phase Stirred Tank Reactors: Newtonian and Non-Newtonian Fluids." The Canadian Journal of Chemical Engineering **75**: 1159.

Kazakis, N. A., A. A. Mouza, et al. (2008). "Experimental study of bubble formation at metal porous spargers: Effect of liquid properties and sparger characteristics on the initial bubble size distribution." Chemical Engineering Journal **137**(2): 265-281.

Kent, j. A. (2007). Kent and Riegel's Handbook of Industrial Chemistry and Biotechnology.

Keresszegi, C., T. Bürgi, et al. (2002). "On the Role of Oxygen in the Liquid-Phase Aerobic Oxidation of Alcohols on Palladium." Journal of Catalysis **211**(1): 244-251.

Keresszegi, C., D. Ferri, et al. (2005). "On the role of CO formation during the aerobic oxidation of alcohols on Pd/Al2O3: an in situ attenuated total reflection infrared study." Journal of Catalysis **234**(1): 64-75.

Keresszegi, C., J.-D. Grunwaldt, et al. (2004). "In situ EXAFS study on the oxidation state of Pd/Al2O3 and Bi-Pd/Al2O3 during the liquid-phase oxidation of 1-phenylethanol." Journal of Catalysis **222**(1): 268-280.

Keresszegi, C., T. Mallat, et al. (2004). "A simple discrimination of the promoter effect in alcohol oxidation and dehydrogenation over platinum and palladium." Journal of Catalysis **225**(1): 138-146.

Khenkin, A. M. and R. Neumann (2000). "Low-Temperature Activation of Dioxygen and Hydrocarbon Oxidation Catalyzed by a Phosphovanadomolybdate: Evidence for a Mars-van Krevelen Type Mechanism in a Homogeneous Liquid Phase13." Angewandte Chemie **39**(22): 4088-4090.

Kimura, H., A. Kimura, et al. (1993). "Palladium based multi-component catalytic systems for the alcohol to carboxylate oxidation reaction." Applied Catalysis A: General **95**(2): 143-169.

Kimura, H., K. Tsuto, et al. (1993). "Selective oxidation of glycerol on a platinum-bismuth catalyst." Applied Catalysis A: General **96**(2): 217-228.

Kluytmans, J. H. J., A. P. Markusse, et al. (2000). "Engineering aspects of the aqueous noble metal catalysed alcohol oxidation." Catalysis Today **57**(1-2): 143-155.

Korovchenko, P., C. Donze, et al. (2007). "Oxidation of primary alcohols with air on carbon-supported platinum catalysts for the synthesis of aldehydes or acids." Catalysis Today

The Catalytic Approach for the Synthesis of Fine Chemicals: Selected Papers of the 7th CAFC **121**(1-2): 13-21.

Kresta, S. M., Edward PL, et al. (2004). Handbook of Industrial Mixing - Science and Practice, John Wiley & Sons.

Kreutzer, M. T., F. Kapteijn, et al. (2005). "Multiphase monolith reactors: Chemical reaction engineering of segmented flow in microchannels." Chemical Engineering Science
7th International Conference on Gas-Liquid and Gas-Liquid-Solid Reactor Engineering **60**(22): 5895-5916.

Kushalkar, K. B. and V. G. Pangarkar (1994). "Particle-Liquid Mass Transfer in Three-Phase Mechanically Agitated Contactors." Ind. Eng. Chem. Res. **33**(7): 1817-1820.

Landon, P., P. J. Collier, et al. (2002). "Direct formation of hydrogen peroxide from H2/O2 using a gold catalyst." Chemical Communications(18): 2058-2059.

Lee A, F., G. J.J, et al. (2000). "Aspects of allylic alcohol oxidation—a bimetallic heterogeneous selective oxidation catalyst." Green chemistry **2**: 279.

Lemaitre, J., F. Delannay, et al. (1982). "The influence of preparation and doping on the reducibility of hematite by hydrogen." Journal of Materials Science **17**(2): 607-615.

Leung, L. W. H. and M. J. Weaver (1990). "Influence of adsorbed carbon monoxide on electrocatalytic oxidation of simple organic molecules at platinum and palladium electrodes in acidic solution: a survey using real-time FTIR spectroscopy." Langmuir **6**(2): 323-333.

Levenspiel, O. (1972). Chemical Reaction Engineering. New York, Wiley.

Levenspiel, O. (1999). Chemical Reaction Engineering. USA, John Wiley & Sons.

Levins, D. M. and J. R. Glastonbury (1972). "Application of Kolmogorofff's theory to particle--liquid mass transfer in agitated vessels." Chemical Engineering Science **27**(3): 537-543.

Lewis, R. and R. Gomer (1968). "Adsorption of oxygen on platinum." Surface Science **12**(2): 157-176.

Litmans, B. A., I. S. Kukurechenko, et al. (1972). "Investigation of the Liquid Phase Mass Transfer Coefficient in Baffled Apparatus With Mechanical Agitation." Theoretical Foundations of Chemical Engineering **6**: 689-690.

Lu, W.-M., H.-Z. Wu, et al. (1997). "Effects of baffle design on the liquid mixing in an aerated stirred tank with standard Rushton turbine impellers." Chemical Engineering Science
Gas-Liquid-Solid Reactor Engineering **52**(21-22): 3843-3851.

Makwana, V. D., Y.-C. Son, et al. (2002). "The Role of Lattice Oxygen in Selective Benzyl Alcohol Oxidation Using OMS-2 Catalyst: A Kinetic and Isotope-Labeling Study." Journal of Catalysis **210**(1): 46-52.

Mallat, T. and A. Baiker (1994). "Oxidation of alcohols with molecular oxygen on platinum metal catalysts in aqueous solutions." Catalysis Today **19**(2): 247-283.

Mallat, T., Z. Bodnar, et al. (1993). "Preparation of Promoted Platinum Catalysts of Designed Geometry and the Role of Promoters in the Liquid-Phase Oxidation of 1-Methoxy-2-propanol." Journal of Catalysis **142**(1): 237-253.

Mallat, T., Z. Bodnar, et al. (1995). "Selective Oxidation of Cinnamyl Alcohol to Cinnamaldehyde with Air over Bi-Pt/Alumina Catalysts." Journal of Catalysis **153**(1): 131-143.

Markusse, A. P., B. F. M. Kuster, et al. (2001). "Platinum catalysed aqueous methyl [alpha]--glucopyranoside oxidation in a multiphase redox-cycle reactor." Catalysis Today **66**(2-4): 191-197.

Miller, C. and G. Kaibel (2004). "Packings for fixed bed reactors and reactive distillation." Chemical Engineering Science
ISCRE18 **59**(22-23): 5373-5379.

Miller, D. N. (1974). "Scale-up of agitated vessels gas-liquid mass transfer." AIChE Journal **20**(3): 445-453.

Miyahara, T., H. Kanzaki, et al. (2001). "Liquid-phase oxidation of benzene to phenol by CuO-Al2O3 catalysts prepared by co-precipitation method." Journal of Molecular Catalysis A: Chemical **176**(1-2): 141-150.

Mondelli, C., D. Ferri, et al. (2007). "Combined liquid-phase ATR-IR and XAS study of the Bi-promotion in the aerobic oxidation of benzyl alcohol over Pd/Al2O3." Journal of Catalysis **252**(1): 77-87.

Monteiro, A. C. A. (2005). Hydrotreating: Hydrogenation Studies on Ni-Mo and Ni-Ru/Alumina Catalysts for the Hydrogenation of Naphtalene. Catalysis and Reaction Engineering. Birmingham, University of Birmingham.

Muzart, J. (2003). "Palladium-catalysed oxidation of primary and secondary alcohols." Tetrahedron **59**(31): 5789-5816.

Nicoletti, J. W. and G. M. Whitesides (1989). "Liquid-phase oxidation of 2-propanol to acetone by dioxygen using supported platinum catalysts." J. Phys. Chem. **93**(2): 759-767.

Nienow, A. W. (1998). "Hydrodynamics of stirred bioreactors." American Society of Mechanical Engineers **51**(1): 4.

Nienow, A. W. (1998). "Hydrodynamics of stirred bioreactors." Applied Mechanics Review **51**(1): 3.

Nienow, A. W. and W. Bujalski (2002). "Recent Studies on Agitated Three-Phase (Gas-Solid-Liquid) Systems in the Turbulent Regime." Chemical Engineering Research and Design
Fluid Mixing VII **80**(8): 832-838.

Nijhuis, T. A., F. M. Dautzenberg, et al. (2003). "Modeling of monolithic and trickle-bed reactors for the hydrogenation of styrene." Chemical Engineering Science **58**(7): 1113-1124.

Opre, Z., J.-D. Grunwaldt, et al. (2005). "Selective oxidation of alcohols with oxygen on Ru-Co-hydroxyapatite: A mechanistic study." Journal of Molecular Catalysis A: Chemical **242**(1-2): 224-232.

Parsons, R. and T. VanderNoot (1988). "The oxidation of small organic molecules : A survey of recent fuel cell related research." Journal of Electroanalytical Chemistry **257**(1-2): 9-45.

Pastor, E., S. Wasmus, et al. (1993). "Spectroscopic investigations of C3 primary alcohols on platinum electrodes in acid solutions. : Part I. n-propanol." Journal of Electroanalytical Chemistry **350**(1-2): 97-116.

Perry, R. H. (1997). Perry's Chemical Engineers' Handbook.

Petersen, E. E. (1965). "A general criterion for diffusion influenced chemical reactions in porous solids." Chemical Engineering Science **20**(6): 587-591.

Pintar, A. and J. Levec (1992). "Catalytic liquid-phase oxidation of refractory organics in waste water." Chemical Engineering Science **47**(9-11): 2395-2400.

Pintar, A. and J. Levec (1992). "Catalytic oxidation of organics in aqueous solutions : I. Kinetics of phenol oxidation." Journal of Catalysis **135**(2): 345-357.

Pinxt, H. H. C. M., B. F. M. Kuster, et al. (2000). "Promoter effects in the Pt-catalysed oxidation of propylene glycol." Applied Catalysis A: General **191**(1-2): 45-54.

Poling, B. E., J. M. Prausnitz, et al. (2001). Properties of Gases and Liquids, McGraw-Hill.

Popovic, K. D., N. M. Markovic, et al. (1991). "Structural effects in electrocatalysis : Oxidation of D-glucose on single crystal platinum electrodes in alkaline solution." Journal of Electroanalytical Chemistry **313**(1-2): 181-199.

Popovic, K. D., A. V. Tripkovic, et al. (1992). "Oxidation of -glucose on single-crystal platinum electrodes: A mechanistic study." Journal of Electroanalytical Chemistry **339**(1-2): 227-245.

Porta, F. and L. Prati (2004). "Selective oxidation of glycerol to sodium glycerate with gold-on-carbon catalyst: an insight into reaction selectivity." Journal of Catalysis **224**(2): 397-403.

Prati, L. and M. Rossi (1998). "Gold on Carbon as a New Catalyst for Selective Liquid Phase Oxidation of Diols." Journal of Catalysis **176**(2): 552-560.

Prati, L., A. Villa, et al. (2007). "Effect of gold addition on Pt and Pd catalysts in liquid phase oxidations." Topics in Catalysis **44**(1): 319-324.

Prati, L., A. Villa, et al. (2007). "Single-phase gold/palladium catalyst: The nature of synergistic effect." Catalysis Today **122**(3-4): 386-390.

Qu, Z., W. Huang, et al. (2005). "Enhancement of the catalytic performance of supported-metal catalysts by pretreatment of the support." Journal of Catalysis **234**(1): 33-36.

Rajadhyaksha, R. A. and S. L. Karwa (1986). "Solvent effects in catalytic hydrogenation." Chemical Engineering Science **41**(7): 1765-1770.

Ramachandran, P. A. and R. V. Chaudhari (1983). Three-Phase Catalytic Reactors.

Sakata, Y., C. A. van Tol-Koutstaal, et al. (1997). "Selectivity Problems in the Catalytic Deoxygenation of Benzoic Acid." Journal of Catalysis **169**(1): 13-21.

Satterfield, C. N. (1991). Heterogeneous Catalysis in Industrial Practice. Florida.

Schuurman, Y., B. F. M. Kuster, et al. (1992). "Selective oxidation of methyl [alpha]-D-glucoside on carbon supported platinum: II. Assessment of the Arrhenius and Langmuir parameters." Applied Catalysis A: General **89**(1): 31-46.

Schwank, J. (1985). "Gold in Bimetallic Catalysts." Gold Bulletin **18**(1): 2.

Sheng, J., H. Meng, et al. (2000). "A large eddy PIV method for turbulence dissipation rate estimation." Chemical Engineering Science **55**(20): 4423-4434.

Smith, T. R., S. J. Xia, et al. "Effect of Hydrogen Sulfide on the Direct Internal Reforming of Methane in Solid Oxide Fuel Cells." Applied Catalysis A: General **In Press, Accepted Manuscript**.

Souto, R. M., J. L. Rodríguez, et al. (2000). "Electrochemical reactions of benzoic acid on platinum and palladium studied by DEMS. Comparison with benzyl alcohol." Journal of Electroanalytical Chemistry **494**(2): 127-135.

Srinivas, N., V. Radha Rani, et al. (2001). "Liquid phase selective oxidation of alcohols over modified molecular sieves." Journal of Molecular Catalysis A: Chemical **172**(1-2): 187-191.

Teschner, D., E. Vass, et al. (2006). "Alkyne hydrogenation over Pd catalysts: A new paradigm." Journal of Catalysis **242**(1): 26-37.

Tokarev, A. V., E. V. Murzina, et al. (2006). "Kinetic behaviour of electrochemical potential in three-phase heterogeneous catalytic oxidation reactions." Journal of Molecular Catalysis A: Chemical **255**(1-2): 199-208.

Tsujino, T., S. Ohigashi, et al. (1992). "Oxidation of propylene glycol and lactic acid to pyruvic acid in aqueous phase catalyzed by lead-modified palladium-on-carbon and related systems." Journal of Molecular Catalysis **71**(1): 25-35.

Twigg, M. V. and Richardson (2002). "Theory and applications of ceramic foam catalysts." Trans IChemE **80**(A).

Van den Tillaart, J. A. A., B. F. M. Kuster, et al. (1994). "Oxidative dehydrogenation of aqueous ethanol on a carbon supported platinum catalyst." Applied Catalysis A: General **120**(1): 127-145.

Van't Riet, K. (1979). "Review of Measuring Methods and Results in Nonviscous Gas-Liquid Mass Transfer in Stirred Vessels." Ind. Eng. Chem. Proc. Des. Dev. **18**(3): 357-364.

Vayenas, C. G., S. Bebelis, et al. (2001). Electrochemical Activation of Catalysis - Promotion, Electrochemical Promotion, and Metal-Support Interactions., Springer - Verlag.

Vleeming, J. H., B. F. M. Kuster, et al. (1997). "Graphite-Supported Platinum Catalysts: Effects of Gas and Aqueous Phase Treatments." Journal of Catalysis **166**(2): 148-159.

Wang, D., A. Villa, et al. (2008). "Bimetallic Gold/Palladium Catalysts: Correlation between Nanostructure and Synergistic Effects
doi:10.1021/jp800805e." The Journal of Physical Chemistry C **112**(23): 8617-8622.

Waterhouse, G. I. N., G. A. Bowmaker, et al. (2001). "The thermal decomposition of silver (I, III) oxide: A combined XRD, FT-IR and Raman spectroscopic study." Physical Chemistry Chemical Physics **3**(17): 3838-3845.

Weisz, P. B. and C. D. Prater (1954). Interpretation of Measurements in Experimental Catalysis
Advances in Catalysis. V. I. K. a. E. K. R. W.G. Frankenburg, Academic Press**:** 143-196.

Weller, S. (1956). "Analysis of kinetic data for heterogeneous reactions." AIChE Journal **2**(1): 59-62.

Weng, L.-T. and B. Delmon (1992). "Phase cooperation and remote control effects in selective oxidation catalysts." Applied Catalysis A: General **81**(2): 141-213.

Wenkin, M., P. Ruiz, et al. (2002). "The role of bismuth as promoter in Pd-Bi catalysts for the selective oxidation of glucose to gluconate." Journal of Molecular Catalysis A: Chemical **180**(1-2): 141-159.

Wieland, H. (1921). "Mechanism of oxidation processes. IV." Berichte der Deutschen Chemischen Gesellschaft [Abteilung] B: Abhandlungen **54**: 2353.

Winterbottom, J. M. and King (1999). Reactor Design for Chemical Engineers.

Wu, H. and G. K. Patterson (1989). "Laser-Doppler measurements of turbulent-flow parameters in a stirred mixer." Chemical Engineering Science **44**(10): 2207-2221.

Yagi, H. and F. Yoshida (1975). "Gas Absorption by Newtonian and Non-Newtonian Fluids in Sparged Agitated Vessels." Ind. Eng. Chem. Proc. Des. Dev. **14**(4): 488-493.

Yaws, C. L. (2003). Yaws' Handbook of Thermodynamic and Physical Properties of Chemical Compounds., Knovel.

Yei, L. H. E., B. Beden, et al. (1988). "Electrocatalytic oxidation of glucose at platinum in alkaline medium: on the role of temperature." Journal of Electroanalytical Chemistry **246**(2): 349-362.

Zelenay, P. and J. Sobkowski (1984). "The inhibitory effect of some surface active organic compounds on the electrooxidation of strongly adsorbed species derived from HCOOH on polycrystalline platinum." Journal of Electroanalytical Chemistry **176**(1-2): 209-224.

Zeng, X., J. Quaye, et al. (2004). "Partition of hematite in the Triton X-100/Dextran aqueous biphase system." Colloids and Surfaces A: Physicochemical and Engineering Aspects **246**(1-3): 135-145.

Zhou and Kresta (1996). "Impact of tank geometry on the maximum turbulence energy dissipation rate for impellers." AIChE Journal **42**(9): 2476-2490.

Zwietering, T. N. (1958). "Suspending of solid particles in liquid by agitators." Chemical Engineering Science **8**(3-4): 244-253.